AN ABSTRACT OF THE DISSERTATION OF

Tongchate Nakhata for the degree of Doctor of Philosophy in Civil Engineering

presented on May 22, 2002.

Title: Stability Analysis of Nonlinear Coupled Barge Motions

Abstract approved: Redacted for Privacy

Solomon C.S. Yim

The present research investigates nonlinear barge motions through analyses of coupled multi-degree-of-freedom (MDOF) deterministic and stochastic models. Roll-Heave-Sway and other lower-ordered models are developed to predict the nonlinear motions and analyze the stability of a class of ship-to-shore cargo barges. The governing equations of motion contain coupled rigid body Roll-Heave-Sway relations, hydrostatic and hydrodynamic terms. The rigid body relationships are a part of the general six-degree-of-freedom model. Hydrostatic terms include effects of the barge's sharp edge and of relative Roll-Heave states. Hydrodynamic terms are in a "Morison" form. The characteristics of the excitation wave field are based on linear wave theory.

Predictive capabilities of the Roll-Heave-Sway and the Roll-Heave models are investigated. System parameters are calibrated to match experimental test results using several regular wave test cases. Potential theory predictions provide initial

estimates of several key system parameters. With the identified system parameters, numerical predictions obtained from time domain simulations of both models are compared with experimental test results for a random wave case, and compared to each other to investigate the coupling effects of sway on roll and heave motions.

Reliability against capsizing of a barge in random seas is investigated using stochastic analysis techniques. With the Markov process assumption, the barge response density to random waves is derived as a solution to the corresponding Fokker-Planck equation. The path integral solution technique is employed to obtain numerical solutions for the Roll-Heave and the Roll models. A quasi-2DOF model is introduced to improve the accuracy of the 1DOF Roll model. The reliability of a barge in a variety of sea conditions is analyzed as a first passage problem using the quasi-2DOF model. Mean times to reach specified capsizing probabilities for a barge operating in sea states 1 through 9 are obtained.

Stability Analysis of Nonlinear Coupled Barge Motions

by

Tongchate Nakhata

A DISSERTATION

Submitted to

Oregon State University

In partial fulfillment of
The requirements for the
Degree of

Doctor of Philosophy

Presented May 22, 2002
Commencement June 2003

Doctor of Philosophy dissertation of Tongchate Nakhata presented on May 22, 2002.

APPROVED:

Redacted for Privacy

16 JUL 2002

Major Professor, representing Civil Engineering

Redacted for Privacy

7/16/02

Head of the Department of Civil Construction and Environmental Engineering

Redacted for Privacy

Dean of the Graduate School

I understand that my dissertation will become part of the permanent collection of Oregon State University libraries. My signature below authorizes release of my dissertation to any reader upon request.

Redacted for Privacy

Jul 16, 02

Tongchate Nakhata, Author

ACKNOWLEDGMENTS

First of all, thanks to Professor Solomon C.S. Yim, my major professor, for his guidance on the research and for providing me a graduate research assistantship. Thanks to Mr. Warren Bartel and Mr. Shafik Salamor who provided strong foundation for the research. Thanks to Dr. Huan Lin for his advice on many aspects of the research.

Partial support from the Office of Naval Research Grant N00014-92-J-1221 is gratefully acknowledged.

TABLE OF CONTENTS

TABLE OF CONTENTS (Continued)

TABLE OF CONTENTS (Continued)

LIST OF FIGURES

LIST OF FIGURES (Continued)

LIST OF FIGURES (Continued)

LIST OF FIGURES (Continued)

LIST OF FIGURES (Continued)

LIST OF TABLES

LIST OF APPENDIX FIGURES

LIST OF APPENDIX FIGURES (Continued)

NOMENCLATURE

B	beam of barge
C_{22_L}	linear hydrodynamic damping coefficient for sway
C_{22_N}	nonlinear hydrodynamic damping coefficient for sway
C_{33_L}	linear hydrodynamic damping coefficient for heave
C_{33_N}	nonlinear hydrodynamic damping coefficient for heave
C_{44_L}	linear hydrodynamic damping coefficient for roll
C_{44_N}	nonlinear hydrodynamic damping coefficient for roll
D	depth of barge
f	frequency
F_1	applied force in surge direction
F_2	applied force in sway direction
F_3	applied force in heave direction
g	gravity
H	wave height
H_s	significant wave height
I	rigid body inertia
$I_{a_{44}}$	added inertia in roll direction
k	wave number
KG	vertical center of gravity above keel
L	length of barge

NOMENCLATURE (Continued)

LCG	Longitudinal center of gravity
m	mass
$m_{a_{22}}$	added mass in sway direction
$m_{a_{33}}$	added mass in heave direction
M_1	applied moment in roll direction
M_2	applied moment in pitch direction
M_3	applied moment in yaw direction
R_{22}	stiffness in sway direction
R_{33}	stiffness in heave direction
R_{44}	stiffness in roll direction
t	time
T_p	spectral peak period
TCG	transverse center of gravity
v	wave velocity in y direction
$\dot{v}$	wave acceleration in y direction
VCG	vertical center of gravity
w	wave velocity in z direction
$\dot{w}$	wave acceleration in z direction
x	surge displacement

NOMENCLATURE (Continued)

x_g	x position of center of gravity
y	sway displacement
y_g	y position of center of gravity
z	heave displacement
z_g	z position of center of gravity
β	damping coefficient for noise filter
ε	random phase
η	wave free surface elevation
η'	wave slope
ω	wave radian frequency
ϕ	roll angle
Φ	wave velocity potential
ψ	yaw angle
Θ	pitch angle
ξ	white noise
ζ	damping ratio

STABILITY ANALYSIS OF NONLINEAR COUPLED BARGE MOTIONS

CHAPTER 1

General Introduction

1.1 Overview

The stability of a class of ship-to-shore cargo barges is investigated. The U.S. Navy is in the process of redesigning their cargo barges and needs an updated capability to determine the stability of the barges for a range of operational sea conditions. They require the identification of motions and accelerations for design of connector joints and securing of cargos. Information on the sea-keeping characteristics with likelihood of capsizing is of concern as well. The barges operate in many different directional sea states, but the most unstable scenario is if the barge broaches and becomes broadside to the waves in the so called "beam seas", which may incur large amplitude roll, heave and sway motions with a possibility of capsizing. In the case of ship shapes other than barges, the most unstable scenario usually is associated with following or quartering seas. However, for those conditions, the barge has significant restoring moments along the diagonal of the hull form and so it will not be as unstable.

At the present, the Navy uses linear frequency domain ship motion models, nonlinear time domain models, and experimental measurements for their research and development. This information is cost effective and useful under motion design situations. Their frequency domain models provide linear response characteristics for a range of wave periods. For larger motions, their nonlinear time domain ship motion models provide a response for a specified wave input. The nonlinear time domain model is well tested but a limitation is they provide one realization of the response for a given wave case and require discretization of the barge into many finite elements. This provides more accurate response for final design purposes but requires significant computational effort.

This dissertation is presented in the form of two papers (Chapters 2 and 3) that provided self-contain summaries of particular aspect of the overall study. Chapter 1 is the general introduction of the study. Chapter 2 covers the formulation of the equations of motion, parameter identification and calibration with experimental results. Chapter 3 presents stochastic analyses to the models. A quasi-2DOF model is developed. Reliability against capsizing of a barge operating in various sea conditions is obtained. Chapter 4 provides general conclusions to the overall study.

1.2 Background

Ship roll motion has been investigated using several single-degree-of-freedom (SDOF) models. Virgin (1987) modeled the roll motion of a ship as a

SDOF system with nonlinear damping and roll stiffness. Cases of complex behavior prior to capsize were found for deterministic loading. Period doubling routes to chaotic roll response were found. He also utilized his model to study the likelihood of capsizing. Virgin and Bishop (1988) investigated nonlinear behavior in ship roll, and articulated tower and semi submersible motions. They modeled the ship roll as a SDOF system with nonlinear damping and higher order polynomial for roll restoring moment. They showed sensitivity to initial conditions for a ship with steady list and demonstrated the possibility of capsizing. Falzarano and Troesch (1990) investigated the vessel with water on deck situation and analyzed it with modern geometric methods. Modeling the roll motion of a fishing vessel with water-on-deck, damping effects due to bilge keels for various regular waves were analyzed. They located regions of stability for the Patti-B clam dredge. Initial conditions due to transient effects were found to be crucial and to impact safety. Falzarano *et al* (1991) modeled the motion of a ship as SDOF in roll and multi-degree-of-freedom (MDOF) in roll, yaw and sway velocity. They used strip theory models to determine the frequency dependent added mass, damping and hydrodynamic force transfer functions. They were interested in studying the stability of a ship in seas using the ships heading as a bifurcation parameter. The fishing trawler, Patti B, was used as the case study as this vessel capsized twice in operation resulting in the death of six seamen. Falzarano *et al* (1992) studied transient motions of ships subjected to periodic wave excitation. Here, they used the theory of lobe dynamics (Wiggins,

1988) to demonstrate unpredictability of capsizing. A SDOF roll model derived from a 6-DOF model was studied.

The coupling effect of heave on roll motion has also been investigated. Liaw (1993) investigated heave excited roll of a ship in head and following seas and found the quadratic coupling effect of heave with roll should be included in dynamic stability analysis. He found the dynamic stability regions and boundaries depend on the excitation and natural frequencies for both roll and heave. The damping and beam-draft ratios affect the stability region as well. Liaw *et al* (1993) also investigated a 2DOF heave excited roll model. They showed the possibility of chaotic response. The model considered was a free floating rectangular barge subject to head or following seas. One observation is the restoring moment changes character when the location of the center of gravity with respect to the free surface is varied. Donescu and Virgin (1993) studied the nonlinear, coupled roll-heave model of a ship in beam seas. They found cases when periodic waves can lead to resonant conditions in roll with a possibility of capsizing. They mapped regions of stability and instability for different initial conditions in their model. Cases of period doubling and chaotic response were found. They discovered cases that contradict linear theory, namely increasing wave steepness does not always lead to occurrence of capsizing. Their results showed regions of capsizing after a certain amount of cycles.

Pauling (1961) investigated transverse stability for head, following and overtaking swells both theoretically and experimentally. He showed the maximum

righting arm is decreased by 50 percent for the case of a wave amidships compared to still water values and recommended that it should be considered in ship design.

Pauling and Rosenburg (1959) investigated nonlinear motion of a ship with coupling between roll, pitch and heave motions. They showed unstable motions may result if any one of the degrees of freedom is parametrically excited by the other two.

Falzarano and Taz Ul Mulk (1994) investigated nonlinear coupled motion of a ship at large angles for various heading angles. They studied the roll, sway and yaw for a T-AGOS survey vessel. The steady-state amplitude of roll of this vessel was found to be multi-valued and highly coupled to sway and yaw. They explained multi-valuedness comes from the backbone curves and well known "jump".

Other groups of researchers studied the roll motions of ships from a stochastic or probabilistic perspective (Robert (1982a,b), Dahle *et al* (1988), Lin and Yim (1995a), Kwon et al (1993) and Cai *et al* (1993)). The work done by Dahle *et al* (1988) was in the form of a probabilistic model where probability of capsizing under specified sea states was computed. Robert (1982a) modeled the roll motion of a ship by the Fokker-Plank (FP) method to obtain the probability distribution of roll response. He proposed an averaging approximation to reduce the FPK equation from two down to one to simplify the solution. This assumption requires the damping to be light so the roll response is narrow banded. Roberts (1982b) studied effects of linear and nonlinear damping and found for the linear case, there was a critical value,

below which the roll becomes unstable. For nonlinear damping, the roll was stable under all conditions. Lin and Yim (1995a) modeled the roll motion of a ship by the Fokker-Plank equation and studied the effects of noise on deterministic regular wave loads. They showed the ship motion to be governed by two diverse dynamical regions – homoclinic and heteroclinic, where the heteroclinic region relates to capsizing. They examined chaotic response behavior with noise with the aid of probability density functions. Kwon *et al* (1993) modeled the roll motion of a ship subjected to an equivalent white noise model of the ocean waves. They studied mean upcrossing times for a nonlinear model of roll righting moment and nonlinear damping. Cai *et al* (1994) provided a stochastic model of nonlinear roll motion of a ship. They modeled the excitation as a stationary Gaussian random process with non-white broad band spectra. The total energy in their dynamical system is approximated as a Markov process, using a modified version of quasi-conservative averaging. They treated the capsizing of the ship as a first passage problem in stochastic dynamics. Multiplicative excitation and stiffness nonlinearity were found to be important.

1.3 Scope

The objective of this research is to examine the capability of a 3DOF model and lower order models to estimate the stochastic properties of barge response. These simpler low dimension models may capture the important nonlinear characteristics of the response for large angle motions. With fewer degrees of

freedom, the governing equation of motion may be solved quickly. This tool will compliment existing ship motion models for preliminary design.

In research conducted earlier at Oregon State university, a single-degree-of-freedom system (Yim *et al*, 1995) was developed to model pure roll motion of a barge in beam seas. Nonlinearities in the righting moment and the fluid-structure viscous effects were included in the model. The damping included a linear term plus a "Morison" type quadratic term (Chakrabarti, 1994). The righting moment included nonlinear stiffness terms to provide a more accurate restoring moment at larger roll angles. The nonlinear roll stiffness term is necessary to predict extreme roll response and the likelihood of capsizing for a given sea state and duration. This type of SDOF model was beneficial in that it provided fairly good prediction of the roll motions for simple shapes, such as barges, with a reasonable amount of effort. The SDOF model was compared with measured barge motion data and was found capable of reasonable predictions in terms of statistical moments, spectral densities and histograms.

In this study, the SDOF model is extended to the MDOF model for roll, heave and sway to include coupling effects induced by the large angle roll motions. For a symmetric barge in beam seas, these are the dominant transverse motions. The hydrostatic righting moment and restoring force are represented by high order polynomials. Experimental results are utilized to identify system parameters of the models. Predicted barge motions due to random waves by time domain simulations are examined and compared with experimental results. The analysis of barge

response is then extended to the probability domain. The Markov process assumption is employed. Barge response densities are derived by numerically solving the Fokker-Planck equation using the path integral solution technique. The reliability of barges operating in a range of sea conditions is investigated.

References

Abkowitz, M.A. 1969. Stability and Motion Control of Ocean Vehicles. MIT Press, Cambridge, MA.

Cai, G.Q., Yu, S.J. and Lin, Y.K. 1994. Ship Rolling in Random Sea. *Stochastic Dyanamics and Reliability of Nonlinear Ocean Systems*, ASME DE-Vol. 77, 81-88.

Chakrabarti,S.K. 1994. Hydrodynamics of Offshore Structures, *Computational Mechanics* Publications, Southampton Boston.

Dahle, E. AA., Myhaug, D. and Dahl, S.J. 1988. Probability of Capsizing in Steep and High Waves from the Side in Open Sea and Coastal Waters. *Ocean Engineering*, 15(2),139-151.

Donescu, P. and Virgin, L.N. 1993. Nonlinear Coupled Heave and Roll Oscillations of a Ship in Beam Seas, *Nonlinear Dynamics of Marine Vehicles*, ASME, 51, 21-28.

Falzarano,J. and Taz Ul Mulk, M. 1994. Large Amplitude Rolling Motion of an Ocean Survey Vessel. *Marine Technology*, 31(4), 278-285.

Falzarano, J.M., Shaw, S.W., and Troesch, A.W. 1992. Application of Global methods for Analyzing Dynamical Systems to Ship Rolling Motion and Capsizing. *International Journal of Bifurcation and Chaos in Applied Sciences and Engineering*, 2(1), 101-116.

Kwon, S.H., Kim, D.W. and McGregor, R.C. 1993. A Stochastic Roll Response Analysis of Ships in Irregular Waves. *International Journal of Offshore and Polar Engineering*, 3(1), 32-34.

Liaw, C.Y. 1993. Dynamic Instability of a Parametrically Excited Ship Rolling Model. *Proc. of the Third International Offshore and Polar Engineering Conference*, Singapore.

Lin, H. and Yim, S.C.S. 1995a. Chaotic Roll Motion and Capsizing of Ships Under Periodic Excitation with Random Noise. *Applied Ocean Research*, 17(3), 185-204.

Lin, H. and Yim, S.C.S. 1995b. Stochastic Analysis of a Nonlinear Ocean Structural System. Oregon State University Report No. OE-95-04.

Martin, J. P. 1994. Roll Stabilization of Small Ships. *Marine Technology*, 31(4), 286-295.

Newland, D.E. 1993. *An Introduction to Random Vibrations, Spectral & Wavelet Analysis*. Longman Scientific and Technical, Essex England.

Ochi, M.C. 1990. *Applied Probability & Stochastic Processes: in Engineering and Physical Sciences*. New York: John Wiley & son.

Roberts, J.B. 1982a. A Stochastic Theory for Nonlinear Ship Rolling in Irregular Seas. *Journal of Ship Research*, 26(4), 229-245.

Roberts, J.B. 1982b. Effect of Parametric Excitation on Ship Rolling Motion in Random Waves. *Journal of Ship Research*, 26(4), 246-253.

Roberts, J.B.,Dunne J.F., and Debonos A. 1994. Stochastic Estimation Methods for Non-Linear Ship Roll Motion. *Probabilistic Engineering Mechanics* 9, 83-93.

Thompson, J.M.T., Rainey, R.C.T. and Soliman, M.S. 1992. Mechanics of Ship Capsize Under Direct and Parametric Wave Excitation," *Phil. Trans. R. Soc. Lond, A*:338, 471-490.

Thompson, J.M.T., and Stewart, H.B. 1986. *Nonlinear Dynamics and Chaos*. John Wiley & Sons.

Virgin, L.N. 1987. The Nonlinear Rolling Response of a Vessel including Chaotic Motions leading to Capsize in Regular Seas. *Applied Ocean Research*, 9(2), 89-95.

Virgin, L.N. and Bishop, S.R. 1988. Catchment Regions of Multiple Dynamic Responses in Nonlinear Problems of Offshore Mechanics. *Proceedings at 7th International Conference on Offshore Mechanics and Arctic Engineering*, Houston, TX. 15-22.

Virgin, L.N. and Erickson, B.K. 1994. A New Approach to the Overturning Stability of Floating Structures. *Ocean Engineering*, 21(1), 67-80.

Yim, S.C.S., Bartel, W.A., Lin, H. and Huang, E. 1995. Nonlinear Roll Motion and Capsizing of Vessels in Random Seas. Naval Facilities Engineering Service Center, Port Hueneme, CA.

CHAPTER 2

Stability Analysis of Nonlinear Coupled Barge Motions: Part I, Models Development and Experimental Calibration

Abstract

This paper presents a coupled Roll-Heave-Sway model to simulate nonlinear barge motions in random seas. The model features realistic and practical approximations of rigid body motion relations, hydrostatic and hydrodynamic force-moment. The hydrostatic force-moment includes effects of the barge's sharp edge and combined roll-heave states. The hydrodynamic terms are in a "Morison" type quadratic form. System parameters of the model are identified using physical model test results from several regular wave cases. The predictive capability of the model is calibrated using model test results from a random wave case. Two distinct processes are employed to create random wave input for the analytical model, namely, measured random waves from experimental data, and simulated random waves. For the measured random waves, wave properties are derived from measured wave elevation profiles. For the simulated random waves, wave profiles are generated via a filtered white noise process with spectral properties specified by the Bretschneider spectrum. A Roll-Heave model is then derived by uncoupling sway from the roll-heave governing equations of motion. Time domain simulations are conducted using the Roll-Heave model for regular and random wave cases.

Comparisons of numerical predictions from the (3DOF) Roll-Heave-Sway and the (2DOF) Roll-Heave models are examined to determine the significant of sway on barge roll and heave motions.

2.1 Introduction

In the design of ship-to-shore transport cargo barges, it is essential to determine barge stability for a range of operational sea conditions. In general, the barges will operate in a variety of directional sea states. However, the most unstable scenario is if the barges broach and become broadside to the waves in the so called "beam seas" and may incur large amplitude roll, heave and sway motions with the possibility of capsizing.

This paper presents a roll-heave-sway model, and a lower order roll-heave model, to estimate the stochastic properties of barge response. These simple low dimensional models may capture the important nonlinear characteristics of the response for large roll angle motions and will be useful in preliminary design and prediction of responses under operational conditions.

In research conducted earlier at Oregon State University, a single-degree-of-freedom (SDOF) system (Yim *et al*, 1995) was developed to model pure roll motion of a barge in beam seas. Nonlinearities of the model include the righting moment and fluid-structure viscous effects. Hydrodynamic and structural damping effects were approximated by a linear term plus a "Morison" type quadratic term (Chakrabarti, 1994). The righting moment included nonlinear stiffness terms to

provide a more accurate restoring moment at larger roll angles. This SDOF model was compared with measured barge motion data and was found capable of reasonable predictions in terms of statistical moments, spectral densities, and histograms.

In this study, the SDOF roll motion model (Yim *et al*, 1995) is first extended to a multi-degrees-of-freedom (MDOF) model that includes coupling effects on roll motion due to heave and sway. The expanded model is expected to improve the predictive capability at large roll angles since the heave and sway are coupled into the roll through hydrostatics and rigid body kinematics. The equations of motion of the rigid barge including hydrostatics are derived. Waves are applied and terms modeling the hydrodynamic properties are added. Relative motion effects of the barge with respect to the free surface are included. The effects due to hydrostatics are represented with sufficiently high order polynomials in the model. Various order polynomials were examined to identify an optimum fit. Because the edges of the barge are sharp, fairly high order polynomials are required. The coupling effects of sway on roll-heave response prediction are examined using the roll-heave-sway model and a corresponding (2DOF) roll-heave model with similar parameters.

2.2 Equations of Motion

Two mathematical models representative of the physics of the fluid structure interaction for the barge in ocean waves are derived. The motions of a rigid body in air are obtained first and then the barge will be placed in water and the effects due to

hydrostatics and hydrodynamics will be included. Once the complete 3DOF model for the barge motions in beam seas is derived, a reduced set of equations of motion (2DOF model) uncoupling sway from roll and heave are derived.

2.2.1 Model assumptions

The underlying physical assumptions used in this study for the development of the equations of motion are summarized in this section. The waves are assumed two-dimensional and the wavelengths are significantly longer than the beam (thus the wave profile is linear across the barge). Wave forces and moments are derived about the center of gravity based on static and dynamic equilibrium. The effect of water-on-deck is treated statically, being modeled only in the hydrostatic restoring moment. Along with this assumption is no bulwarks are present. Coefficients of added inertia, added mass and damping are assumed constant. The longitudinal center of gravity (LCG) is amidships. This is consistent with the physical model in the experimental test data. The barge is symmetric longitudinally and laterally. Radiation and viscous damping are modeled collectively as a linear and a "Morison" type quadratic term. Barge length, beam, displacement, draft, location of vertical center of gravity (KG), specific weight of water, and roll center are considered variable input parameters. Effects due to a linear mooring stiffness may be switched on or off for sway motions.

2.2.2 Roll-Heave-Sway model

The rigid body dynamic equations of motion for the barge are based on Newton's second law which states the rate of change of linear momentum equals the applied forces and the rate of change of angular momentum equals the applied moments:

$$\frac{d}{dt}(mv)=F \qquad \frac{d}{dt}(I\omega)=M \tag{2.1}$$

An inertial coordinate system is placed at the location of the prescribed body-fixed "roll center" of the barge under static equilibrium. Note the inertial coordinate system coincides with the body-fixed (moving) coordinate system initially. Static roll righting moments and heave buoyant restoring forces are calculated as a function of the position and rotation of the barge about the roll center. Equilibrium of forces and moments are considered about the roll center (the position of which is time dependent with respect to the inertia coordinates) with heave and sway directions respect to the inertial coordinates.

The body-fixed coordinates are defined such that X = Surge, Y = Sway, Z = Heave, ϕ = Roll, Θ = Pitch, and ψ = Yaw (Figure 2.1). For the (body-fixed) coordinate system origin (i.e. the roll center) is at the center of gravity of barge and the coordinate system axes are aligned with the principal axes of inertia, the equations become,

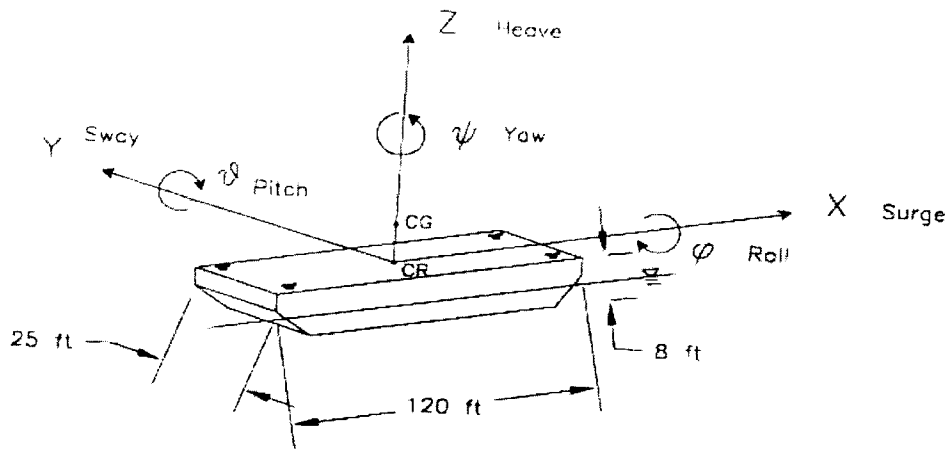

(a)

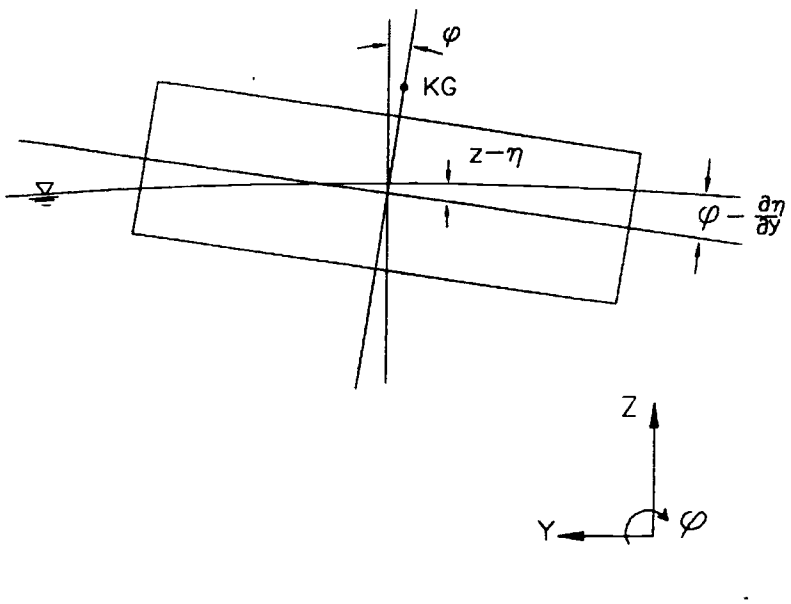

(b)

Figure 2.1 (a) Coordinate system definition, and (b) relative motion system of barge considered.

$$
\begin{aligned}
F_1 &= m(\ddot{x} + \dot{\theta} z - \dot{\psi} y) \\
F_2 &= m(\ddot{y} + \dot{\psi} x - \dot{\phi} z) \\
F_3 &= m(\ddot{z} + \dot{\phi} y - \dot{\theta} x) \\
M_4 &= I_{44} \ddot{\phi} + (I_{66} - I_{55}) \dot{\theta} \dot{\psi} \\
M_5 &= I_{55} \ddot{\theta} + (I_{44} - I_{66}) \dot{\psi} \dot{\phi} \\
M_6 &= I_{66} \ddot{\psi} + (I_{55} - I_{44}) \dot{\phi} \dot{\theta}
\end{aligned}
\tag{2.2}
$$

The coupling terms represent the components of centripetal accelerations on the body arising from the moving (body-fixed) coordinate system and the inertial difference terms represent gyroscopic moments arising from the moving system (Abkowitz, 1969). We place the origin of the moving coordinate system at an assumed "center of rotation". Since this may not coincide with the center of gravity, the equations of motion are modified to become,

$$
\begin{aligned}
F_1 &= m\left[\ddot{x} + \dot{\theta} z - \dot{\psi} y - x_g(\dot{\theta}^2 + \dot{\psi}^2) + y_g(\dot{\phi}\dot{\theta} - \ddot{\psi}) + z_g(\dot{\phi}\dot{\psi} + \ddot{\theta})\right] \\
F_2 &= m\left[\ddot{y} + \dot{\psi} x - \dot{\phi} z - y_g(\dot{\psi}^2 + \dot{\phi}^2) + z_g(\dot{\theta}\dot{\psi} - \ddot{\phi}) + x_g(\dot{\theta}\dot{\phi} + \ddot{\psi})\right] \\
F_3 &= m\left[\ddot{z} + \dot{\phi} y - \dot{\theta} x - z_g(\dot{\phi}^2 + \dot{\theta}^2) + x_g(\dot{\psi}\dot{\phi} - \ddot{\theta}) + y_g(\dot{\psi}\dot{\theta} + \ddot{\phi})\right] \\
M_4 &= I_{44} \ddot{\phi} + (I_{66} - I_{55}) \dot{\theta} \dot{\psi} + m\left[y_g(\ddot{z} + \dot{\phi} y - \dot{\theta} x) - z_g(\ddot{y} + \dot{\psi} x - \dot{\phi} z)\right] \\
M_5 &= I_{55} \ddot{\theta} + (I_{44} - I_{66}) \dot{\psi} \dot{\phi} + m\left[z_g(\ddot{x} + \dot{\theta} z - \dot{\psi} y) - x_g(\ddot{z} + \dot{\phi} y - \dot{\theta} x)\right] \\
M_6 &= I_{66} \ddot{\psi} + (I_{55} - I_{44}) \dot{\phi} \dot{\theta} + m\left[x_g(\ddot{y} + \dot{\psi} x - \dot{\phi} z) - y_g(\ddot{x} + \dot{\theta} z - \dot{\psi} y)\right]
\end{aligned}
\tag{2.3}
$$

Here, the extra terms represent centrifugal forces acting at the origin due to eccentricity of the center of gravity about the origin and inertial reaction forces, and moments about the origin induced by the acceleration of the center of gravity relative to the origin.

Up to now, we have the rigid body equations of motion for all 6-DOF without addition of the fluid forces and fluid moments. One of the main objectives in this study is to extend the equations of motion for a SDOF system in roll to a MDOF system. For a symmetric barge in beam seas, the dominant response will be in sway, heave and roll. The surge, pitch and yaw motions become negligible (Donescu and Virgin, 1993). Equation 2.3 now becomes,

$$
\begin{aligned}
F_2 &= m\left[\ddot{y} - \dot{\phi}\dot{z} - z_g\ddot{\phi}\right] \\
F_3 &= m\left[\ddot{z} + \dot{\phi}\dot{y} - z_g\dot{\phi}^2\right] \\
M_4 &= I_{44}\ddot{\phi} - m\left[z_g(\ddot{y} - \dot{\phi}\dot{z}\right]
\end{aligned}
\tag{2.4}
$$

These equations show the kinematic coupling in the heave and sway equations with extra terms due to the vertical location of the center of gravity not coinciding with the origin of the coordinate system. The longitudinal and lateral centers of gravity coincide with the origin for the barge under study (NFESC, 1996), (i.e. X_g and Y_g are zero) and so those terms do not appear in the equations.

Placing the barge in water will add terms due to the hydrostatic "Archimedes" buoyant restoring forces and moments. As the barge heaves up and down, the available

righting energy of the barge in roll changes. Exact expressions relating the effects of heave on the righting moment were derived from analytical geometry. The analytical geometric method for calculation of the righting moment and buoyant heave force begins with the complete arrangement of possible configurations of the barge in water. These cases may be subdivided into combinations of four main states (Figure 2.2). As the barge is rotated through the roll angles at a value of heave, the method determines which state the underwater portion falls within and subdivides it into triangular sections. From these triangles, the center of buoyancy may be obtained by averaging all the centroids of each triangle.

The initial position of the barge is prescribed by a "roll center" with respect to the inertial coordinates. Righting moments are computed over the preset range of roll and heave. This produces a set of righting moment curves for incremental discrete value of heave. The heave range is typically set at maximum value of the barge being totally out of the water at zero roll. The maximum and minimum roll values are determined by sample calculations to see that angle at which the righting moment becomes zero. Analytical expressions of roll righting moment and heave restoring force are graphically shown in Figure 2.3.

The matrices of analytical roll restoring moment and heave restoring force are approximated with sufficiently high order polynomials. Various high and low order polynomials were tried to determine the optimum fit. The ones which produce errors less than 3 percent at any combined roll-heave positions are selected. Figure 2.3 shows the analytical roll restoring moment and heave restoring force surface.

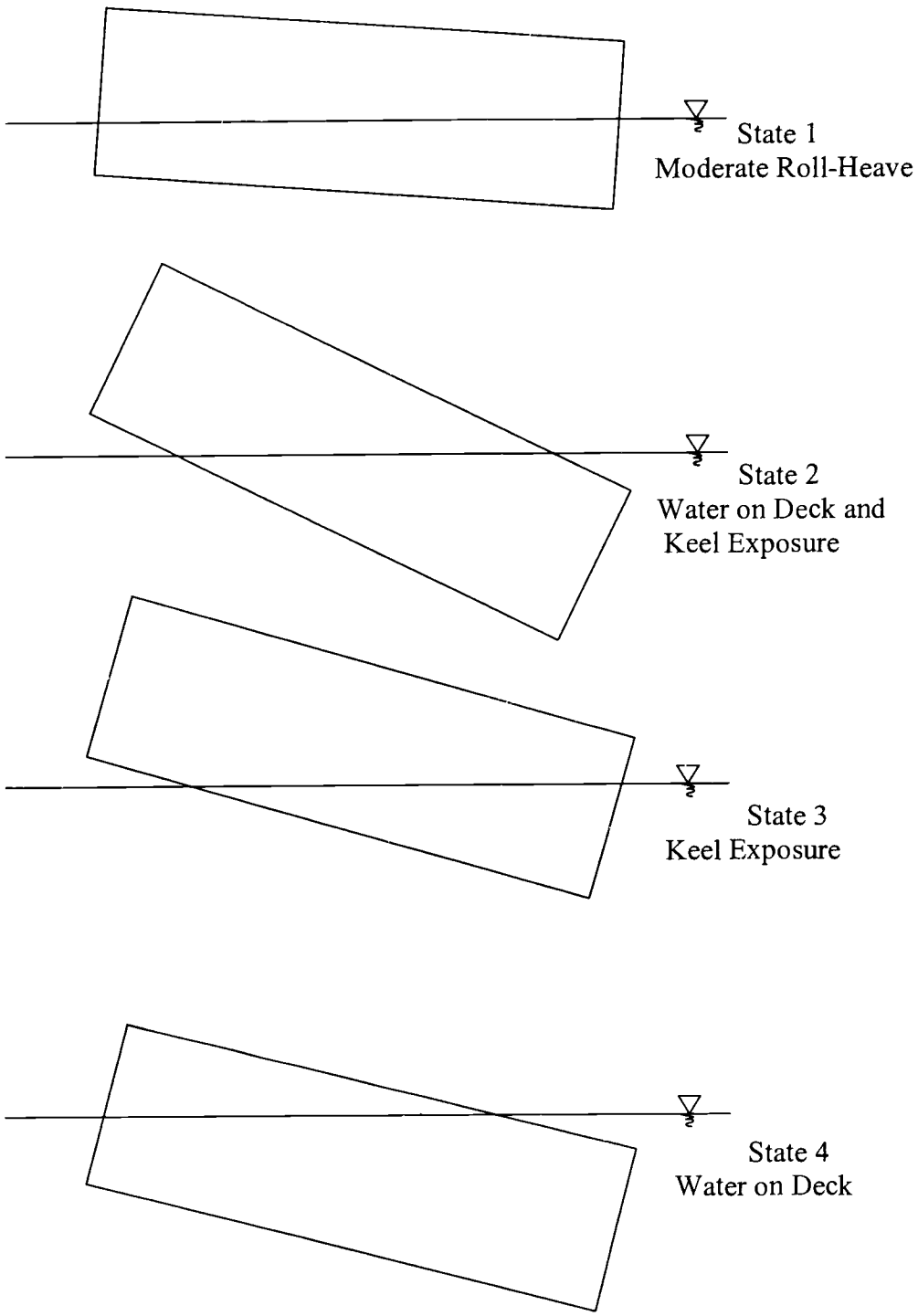

Figure 2.2 Four main states of combined Roll-Heave position of barge motion.

a)

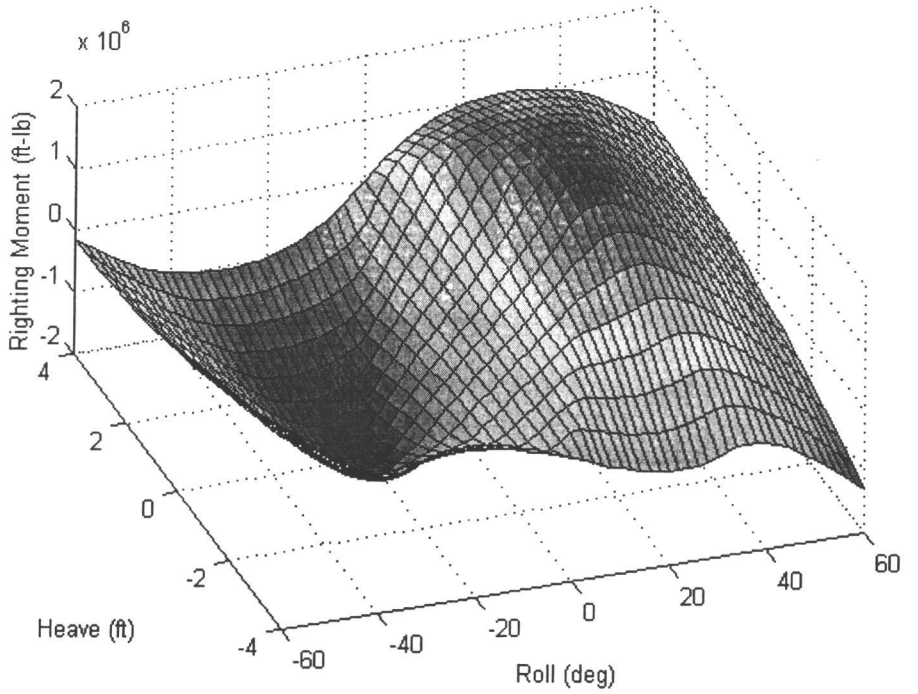

b)

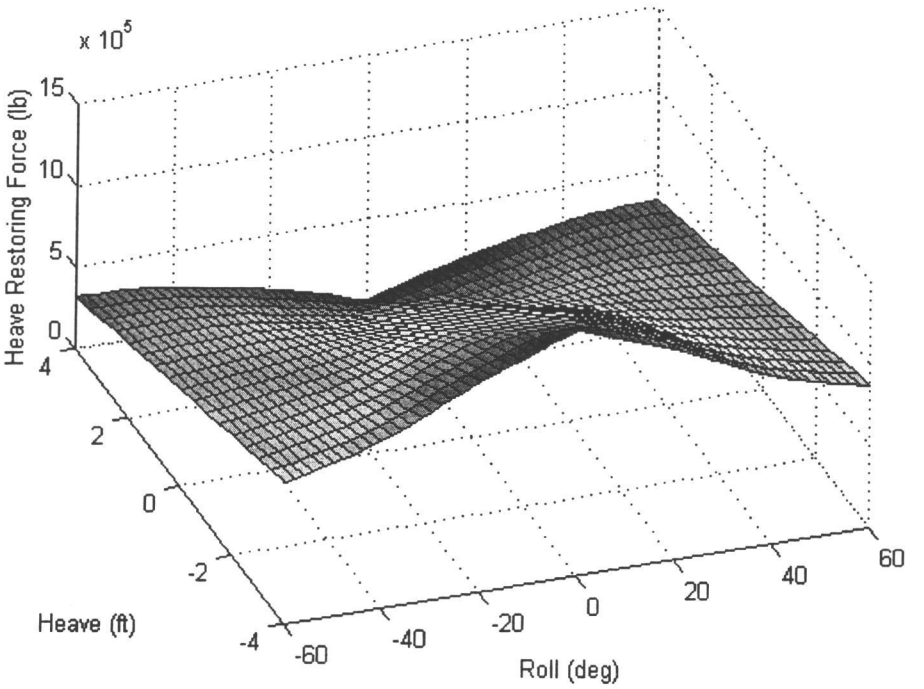

Figure 2.3 Analytical surface of (a) roll righting moment, and (b) heave restoring force (L = 120 ft, b = 25 ft, D = 8 ft, draft = 4 ft and KG = 9.23 ft.)

A 13th order polynomial in roll and 12th order polynomial in heave were found to be sufficient to qualify the general character of the coupled roll-heave restoring moment-forces. The polynomial fitted roll-righting moment and heave restoring force surfaces are graphically shown in Figure 2.4. The accuracy of the polynomial expressions is determined by examining the differences between the "exact" analytical expressions and the least square fit. The polynomial fit for heave restoring force results in Equation 2.5.

$$
\begin{aligned}
R_{33}(z,\phi,\eta,\frac{\partial\eta}{\partial y}) = \\
&\left[A_{1_1}(z-\eta)^5 + A_{1_2}(z-\eta)^4 + A_{1_3}(z-\eta)^3 + A_{1_4}(z-\eta)^2 + A_{1_5}(z-\eta) + A_{1_6}\right](\phi - \frac{\partial\eta}{\partial y})^{12} \\
+ &\left[A_{3_1}(z-\eta)^5 + A_{3_2}(z-\eta)^4 + A_{3_3}(z-\eta)^3 + A_{3_4}(z-\eta)^2 + A_{3_5}(z-\eta) + A_{3_6}\right](\phi - \frac{\partial\eta}{\partial y})^{10} \\
+ &\left[A_{5_1}(z-\eta)^5 + A_{5_2}(z-\eta)^4 + A_{5_3}(z-\eta)^3 + A_{5_4}(z-\eta)^2 + A_{5_5}(z-\eta) + A_{5_6}\right](\phi - \frac{\partial\eta}{\partial y})^{8} \\
+ &\left[A_{7_1}(z-\eta)^5 + A_{7_2}(z-\eta)^4 + A_{7_3}(z-\eta)^3 + A_{7_4}(z-\eta)^2 + A_{7_5}(z-\eta) + A_{7_6}\right](\phi - \frac{\partial\eta}{\partial y})^{6} \quad (2.5) \\
+ &\left[A_{9_1}(z-\eta)^5 + A_{9_2}(z-\eta)^4 + A_{9_3}(z-\eta)^3 + A_{9_4}(z-\eta)^2 + A_{9_5}(z-\eta) + A_{9_6}\right](\phi - \frac{\partial\eta}{\partial y})^{4} \\
+ &\left[A_{11_1}(z-\eta)^5 + A_{11_2}(z-\eta)^4 + A_{11_3}(z-\eta)^3 + A_{11_4}(z-\eta)^2 + A_{115}(z-\eta) + A_{11_6}\right](\phi - \frac{\partial\eta}{\partial y})^{2} \\
+ &\left[A_{13_1}(z-\eta)^5 + A_{13_2}(z-\eta)^4 + A_{13_3}(z-\eta)^3 + A_{13_4}(z-\eta)^2 + A_{13_5}(z-\eta) + A_{13_6}\right]
\end{aligned}
$$

Similarly, the polynomial expression for the roll restoring moment becomes equation 2.6

a)

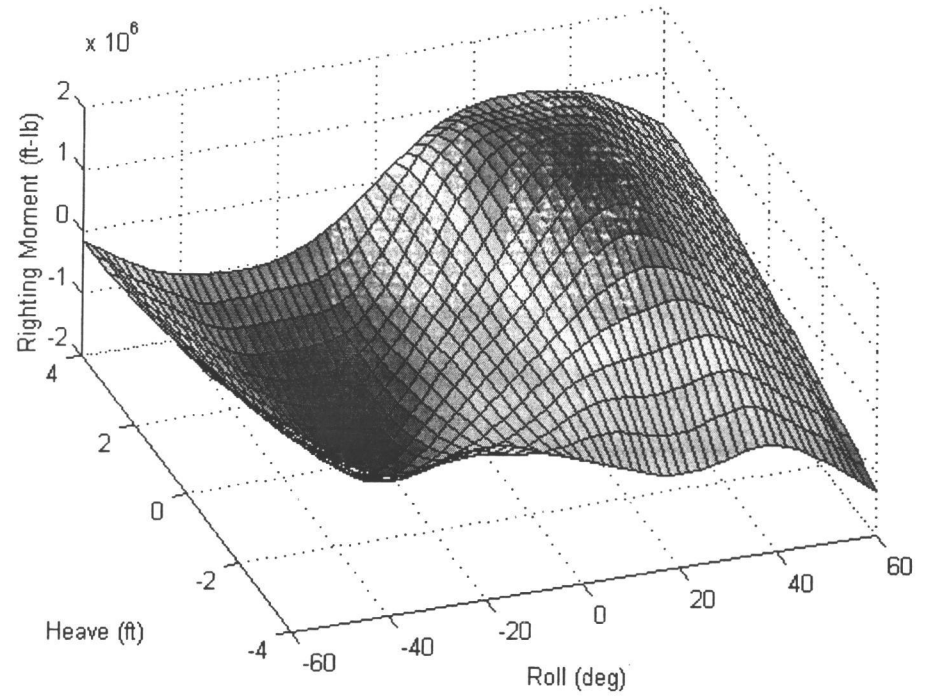

b)

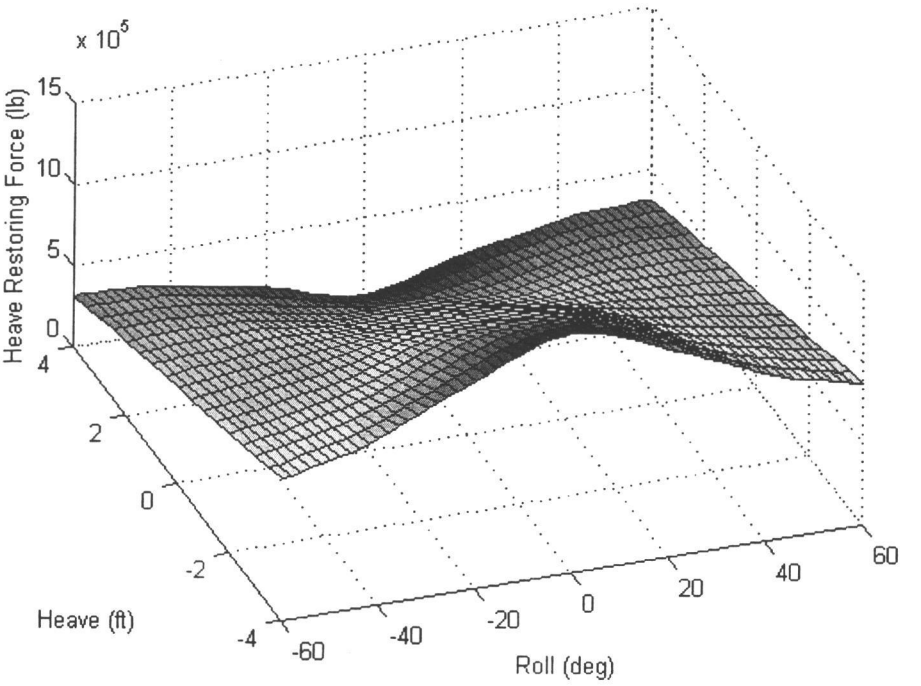

Figure 2.4 Polynomial approximation of (a) roll righting moment, and (b) heave restoring force as a function of roll and heave (L = 120 ft, b = 25 ft, D = 8 ft, draft = 4 ft and KG = 9.23 ft.)

$$
\begin{aligned}
R_{44}(\phi, z, \eta, \frac{\partial \eta}{\partial y}) = \\
&\left[B_{1_1}(z-\eta)^4 + B_{1_2}(z-\eta)^3 + B_{1_3}(z-\eta)^2 + B_{1_4}(z-\eta) + B_{1_5}\right]\left(\phi - \frac{\partial \eta}{\partial y}\right)^{13} \\
&+ \left[B_{3_1}(z-\eta)^4 + B_{3_2}(z-\eta)^3 + B_{3_3}(z-\eta)^2 + B_{3_4}(z-\eta) + B_{3_5}\right]\left(\phi - \frac{\partial \eta}{\partial y}\right)^{11} \\
&+ \left[B_{5_1}(z-\eta)^4 + B_{5_2}(z-\eta)^3 + B_{5_3}(z-\eta)^2 + B_{5_4}(z-\eta) + B_{5_5}\right]\left(\phi - \frac{\partial \eta}{\partial y}\right)^{9} \\
&+ \left[B_{7_1}(z-\eta)^4 + B_{7_2}(z-\eta)^3 + B_{7_3}(z-\eta)^2 + B_{7_4}(z-\eta) + B_{7_5}\right]\left(\phi - \frac{\partial \eta}{\partial y}\right)^{7} \qquad (2.6) \\
&+ \left[B_{9_1}(z-\eta)^4 + B_{9_2}(z-\eta)^3 + B_{9_3}(z-\eta)^2 + B_{9_4}(z-\eta) + B_{9_5}\right]\left(\phi - \frac{\partial \eta}{\partial y}\right)^{5} \\
&+ \left[B_{11_1}(z-\eta)^4 + B_{11_2}(z-\eta)^3 + B_{11_3}(z-\eta)^2 + B_{11_4}(z-\eta) + B_{11_5}\right]\left(\phi - \frac{\partial \eta}{\partial y}\right)^{3} \\
&+ \left[B_{13_1}(z-\eta)^4 + B_{13_2}(z-\eta)^3 + B_{13_3}(z-\eta)^2 + B_{13_4}(z-\eta) + B_{13_5}\right]\left(\phi - \frac{\partial \eta}{\partial y}\right)
\end{aligned}
$$

These stiffness terms include relative motions between the moving barge and the wave free surface elevation and wave slope changes.

Placing the barge in still water and adding ocean wave excitation introduces terms that represent added mass and added inertia due to relative motion accelerations of the barge and the wave. To take into account energy dissipation effects due to radiation of waves from the barge and flow separation around the hull, the hydrodynamic damping may be modeled as relative motion linear and nonlinear terms. The viscous damping for roll is relative to the time rate of change of wave slope, where the slope is relative to the sway direction (for beam sea conditions).

These additional hydrostatic and hydrodynamic force and moment terms are added to the equations of motions that become

$$
\begin{aligned}
&m\ddot{y}+m_{a_{22}}\cos(\frac{\partial\eta}{\partial y})(\ddot{y}-\dot{v})+m_{a_{33}}\sin(\left|\frac{\partial\eta}{\partial y}\right|)(\dot{y}-v)+C_{22_L}\dot{y}+C_{22_N}\dot{y}\left|\dot{y}\right|-m\dot{\phi}\dot{z}\\
&-m(z_g\cos\phi)\ddot{\phi}+R_{33}(\phi,z,\eta,\frac{\partial\eta}{\partial y})\sin(\frac{\partial\eta}{\partial y})+K_{moor}y \quad = \quad 0\\
&m\ddot{z}+m_{a_{33}}\cos(\frac{\partial\eta}{\partial y})(\ddot{z}-\dot{w})+m_{a_{22}}\sin(\left|\frac{\partial\eta}{\partial y}\right|)(\dot{z}-w)+C_{33_L}\dot{z}+C_{33_N}\dot{z}\left|\dot{z}\right|+m\dot{\phi}\dot{y} \qquad (2.7)\\
&-m(z_g\cos\phi)\dot{\phi}^2+mg+R_{33}(\phi,z,\eta,\frac{\partial\eta}{\partial y})\cos(\frac{\partial\eta}{\partial y}) \quad = \quad 0\\
&I_{44}\ddot{\phi}+I_{a_{44}}(\ddot{\phi}-\frac{\partial\ddot{\eta}}{\partial y})+C_{44_L}(\dot{\phi}-\frac{\partial\dot{\eta}}{\partial y})+C_{44_N}(\dot{\phi}-\frac{\partial\dot{\eta}}{\partial y})\left|\dot{\phi}-\frac{\partial\dot{\eta}}{\partial y}\right|+m(z_g\cos\phi)\dot{\phi}\dot{z}\\
&-m(z_g\cos\phi)\ddot{y}+R_{44}(\phi,z,\eta,\frac{\partial\eta}{\partial y})\cos(\frac{\partial\eta}{\partial y})-mgz_g\sin\phi \quad = \quad 0
\end{aligned}
$$

2.2.3 Roll-Heave model

By assuming the influences of sway motion on roll and heave are negligible, the governing equations of motion (the 3DOF model, Equation 2.7) may be reduced to a 2DOF model in roll and heave only.

$$m\ddot{z}+m_{a_{33}}(\ddot{z}-\ddot{w})+C_{33_L}\dot{z}+C_{33_N}\dot{z}|\dot{z}|-m(z_g\cos\phi)\dot{\phi}^2+mg+R_{33}(z,\phi,\eta,\frac{\partial\eta}{\partial y}) = 0$$

$$I_{44}\ddot{\phi}+I_{a_{44}}(\ddot{\phi}-\frac{\partial\ddot{\eta}}{\partial y})+C_{44_L}(\dot{\phi}-\frac{\partial\dot{\eta}}{\partial y})|\dot{\phi}-\frac{\partial\dot{\eta}}{\partial y}|+C_{44_N}(\dot{\phi}-\frac{\partial\dot{\eta}}{\partial y})|\dot{\phi}-\frac{\partial\dot{\eta}}{\partial y}|+m(z_g\cos\phi)\dot{\phi}\dot{z} \quad (2.8)$$

$$+R_{44}(\phi,z,\eta,\frac{\partial\eta}{\partial y})-mgz_g\sin\phi = 0$$

2.3 Numerical Solution Procedure

To obtain barge motion responses in the time domain based on the Roll-Heave-Sway and the Roll-Heave models, Equation 2.7 and 2.8, respectively, are reduced to systems of first order ordinary differential equations and integrated by standard numerical methods. A 4th order Runge-Kutta method is selected to solve the equations of motion (Press et al, 1986).

2.3.1 Regular waves

A description of the ocean wave field is provided by linear wave theory. The barges considered in this study operate from relatively deep to shallow water. However, the condition of deep water in general produces higher coupling effects of heave on roll due to larger vertical wave velocity. To be conservative in our analysis, therefore, deep-water condition is assumed. For linear regular waves with

the assumption of deep water and consideration of water particle kinematics at mean water line (MWL), wave expressions are defined as

$$
\begin{aligned}
k &= \frac{\omega^2}{g} \\
\eta &= A\sin(ky - \omega t) \\
\dot{\eta} &= -\omega A\cos(ky - \omega t) \\
\ddot{\eta} &= -\omega^2 \eta \\
v &= \omega\eta \\
\dot{v} &= \omega\dot{\eta} \\
w &= \eta \\
\dot{w} &= -\omega^2\eta \\
\frac{\partial\eta}{\partial y} &= -\frac{\omega}{g}\dot{\eta} \\
\frac{\partial\dot{\eta}}{\partial y} &= \frac{\omega^3}{g}\eta \\
\frac{\partial\ddot{\eta}}{\partial y} &= \frac{\omega^3}{g}\dot{\eta}
\end{aligned}
\qquad (2.9)
$$

2.3.2 Measured random waves

If measured waves are input to the model, the wave properties as in Equation 2.9 are calculated by central difference method. The second order and forth order accurate formulas are

$$f'(x_i)=\frac{f(x_{i+1})-f(x_i)}{2h}$$
$$f''(x_i)=\frac{f(x_{i+1})-2f(x_i)+f(x_{i-1})}{h^2}$$
$$f'(x_i)=\frac{-f(x_{i+2})+8f(x_{i+1})-8f(x_{i-1})+f(x_{i-2})}{12h} \qquad (2.10)$$
$$f''(x_i)=\frac{-f(x_{i+2})+16f(x_{i+1})-30f(x_i)+16f(x_{i-1})-f(x_{i-2})}{12h^2}$$

Using Equation 2.10, the water particle kinematics may be calculated from the measured wave profile.

2.3.3 Filtered white noise random waves

To simulate barge motion in operational sea conditions, a filtered white noise process is employed to create random wave profiles. The linear filter is defined as

$$\ddot{\eta}+\beta_n\dot{\eta}+(2\pi f_0)^2\eta=\xi \qquad (2.11)$$

where ξ is a Gaussian white noise, which is obtained by using a pseudo random number generator. The transfer function and the spectral density function of the output of the filtered white noise (Lin and Yim, 1995b) are

$$|H(f)|=\frac{1}{[-(2\pi f)^2+(2\pi f_0)^2]^2+(2\pi\beta_n)^2}$$

$$S_\eta(f)=\frac{S_0}{[-(2\pi f)^2+(2\pi f_0)^2]^2+(2\pi\beta_n)^2} \tag{2.12}$$

The present research utilizes the Bretschneider spectrum (Chakrabarti, 1994) to represent ocean wave spectral. It is expressed as

$$S(\omega)=0.1687H_s^2\frac{\omega_s^4}{\omega^5}e^{-0.675(\omega_s/\omega)^4} \tag{2.13}$$

The coefficients in Equation 2.12 are set to satisfy the variance and peak period of the Bretschneider spectrum (Lin and Yim, 1995b). Equation 2.11 is then reduced to a set of first order ordinary differential equations and combined with the equations of motion. This produces eight first order differential equations of motion for the 3DOF model and six equations for the 2DOF model.

2.4 Experimental Results

The Naval Facilities Engineering Service Center (NFESC), Port Hueneme, California, conducted several measurements of a moored and a partially constrained barge in regular and random seas (NFESC, 1995). Under collaboration with the U.S. Navy, we were provided with a set of measured physical model test data for U.S. Navy model barges, which consists of motions of a 1/16-scale barge in regular and random seas. Free vibration tests of the barge in roll, heave and sway were also

conducted to provide estimates of the viscous damping and linear natural periods. The results indicate that 5.25, 4.00 and 27.14 seconds are the natural periods of roll, heave and sway motion respectively. Table 2.1 summarizes the parameters of a sample of physical model test cases employed in this study.

Test results from regular wave cases are used to identify system coefficient for both Roll-Heave-Sway and Roll-Heave models. Time domain simulations of varied system coefficients are compared with the test results to determine the best match. The results from random wave case, SB25, are used to calibrate the accuracy of model predictions.

Table 2.1. Physical Model Test Cases

Test Case	**Wave Type**	**H (ft) or Hs(ft)**	**T (sec) or Tp (sec)**
SB25	Random	4.7	8.2
SB26	Regular	6.0	5.0
SB27	Regular	6.0	6.0
SB28	Regular	6.0	7.0
SB29	Regular	7.0	8.0
SB30	Regular	6.0	10.0
SB31	Regular	10.0	10.0

2.5 Identification of System Parameters

The constant parameters including added mass, added inertia and radiation damping (see Table 2.2) in the governing equations of motion for roll, sway and heave are identified using test results of regular waves of heights from 6 to 10 ft and wave periods of 5 - 10 seconds (test cases SB26 to SB31). Initial approximate values of all system parameters are obtained from a linear potential theory ship motion program developed by Paulling (1995) based on potential theory. These estimates are then fine-tuned to match the predicted response time series and phase plots with measured results. The resulting identified system parameters are then used as input to the model in the next section to calibrate the accuracy of model prediction for the random wave case (SB25). Because the parameters identified are obtained from the 1:16-scaled model test results and not from full–scale prototype tests, these identified parameters are theoretically suitable for only the scale test model. Higher Reynolds numbers in the full-scale prototype may affect the values of the nonlinear damping coefficients. However, based on our experience, the nonlinear damping effects do not significantly affect the predicted barge motion responses. Therefore, we believe that the identified parameters in this section may also be suitable for analysis of the full-scale prototype.

Sample comparison of time histories of the measured versus numerical responses (corresponding to test cases SB27, 29 and 30) are shown in Figures 2.5-2.7. It is observed that practically all the parameters estimated by potential theory, are sufficiently accurate for the Roll-Heave-Sway model. Only minor adjustments in

Table 2.2 Summary of system parameters used in the model

Parameter	**Regular Wave** H from 6 to 10 ft T from 5 to 10 sec	**Measured Random Wave** H_s = 4.7 ft T_p = 8.2 sec	**Simulated Random Wave** H_s = 4.7 ft T_p = 8.2 sec
I_{44} (slugs-ft^2)	2.161E+06	2.161E+06	2.161E+06
$I_{a_{44}}$ (slugs-ft^2)	1.30E+06	1.00E+06	1.00E+06
ζ_{L44}	0.05	0.08	0.03
ζ_{N44}	0.008	0.008	0.008
m (slugs)	2.325E+04	2.325E+04	2.325E+04
$m_{a_{33}}$ (slugs)	1.00E+05	1.00E+05	1.00E+05
ζ_{L33}	0.35	0.35	0.35
ζ_{N33}	0.5	0.5	0.5
m (slugs)	2.325E+04	2.325E+04	2.325E+04
$m_{a_{22}}$ (slugs)	2.00E+04	2.00E+04	1.50E+04
ζ_{L22}	0.5	0.5	0.5
ζ_{N22}	5.0	3.0	3.0

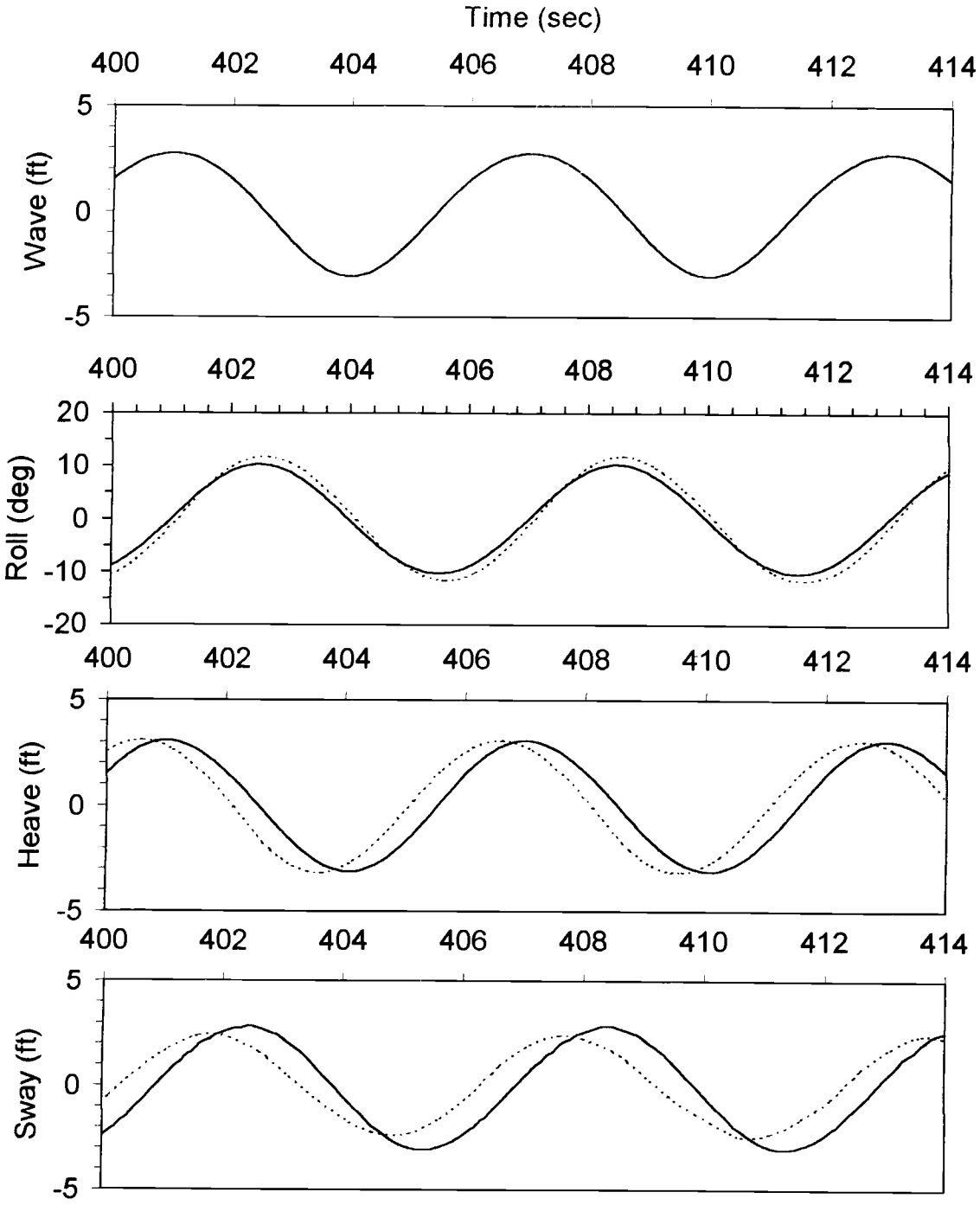

Figure 2.5 Barge roll, heave and sway response time histories to regular waves with H = 6 ft and T = 6 seconds (Case SB27). (solid line = numerical results, dotted line = experimental results)

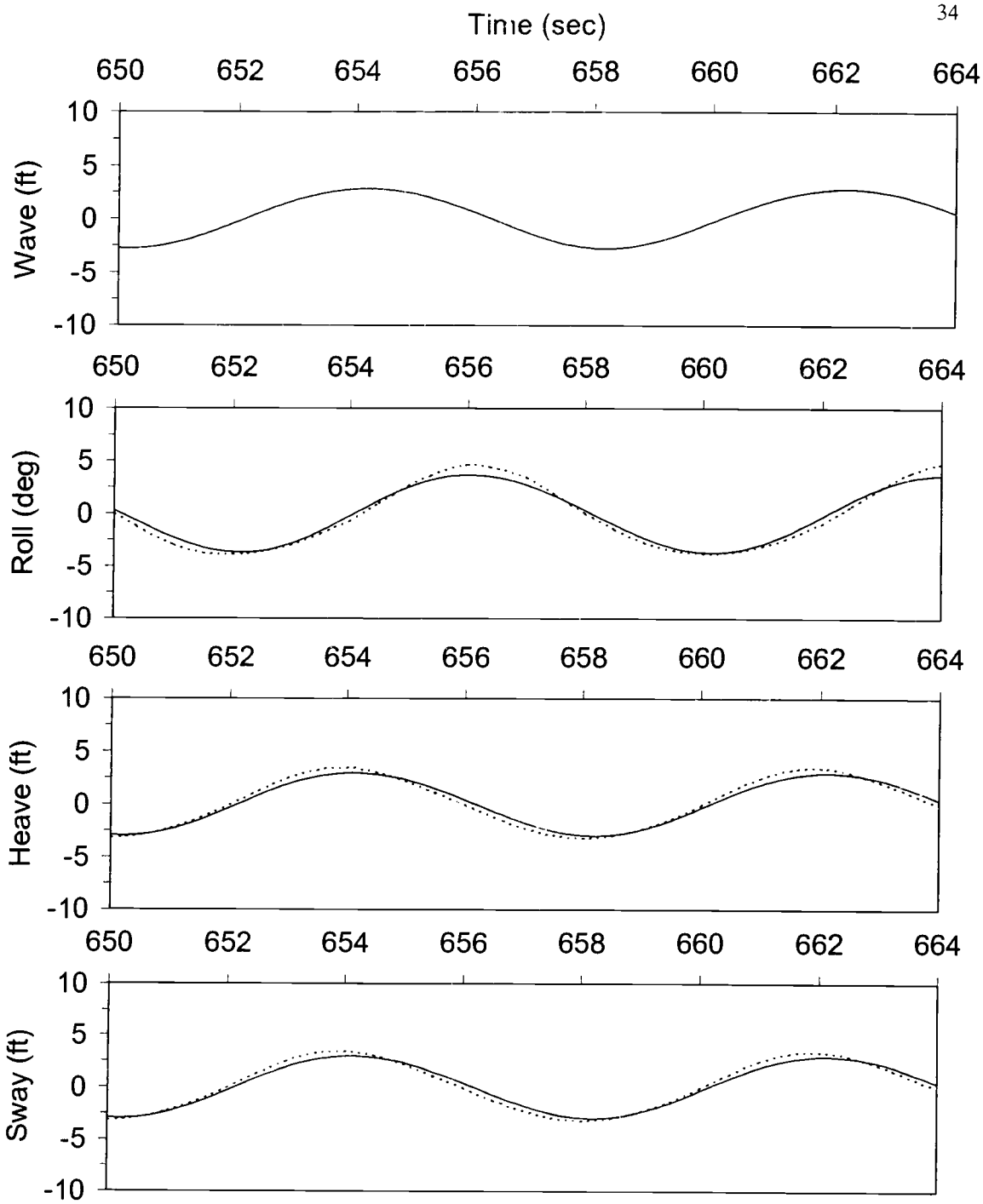

Figure 2.6 Barge roll, heave and sway response time histories to regular waves with H = 7 ft and T = 8 seconds (Case SB29). (solid line = numerical results, dotted line = experimental results)

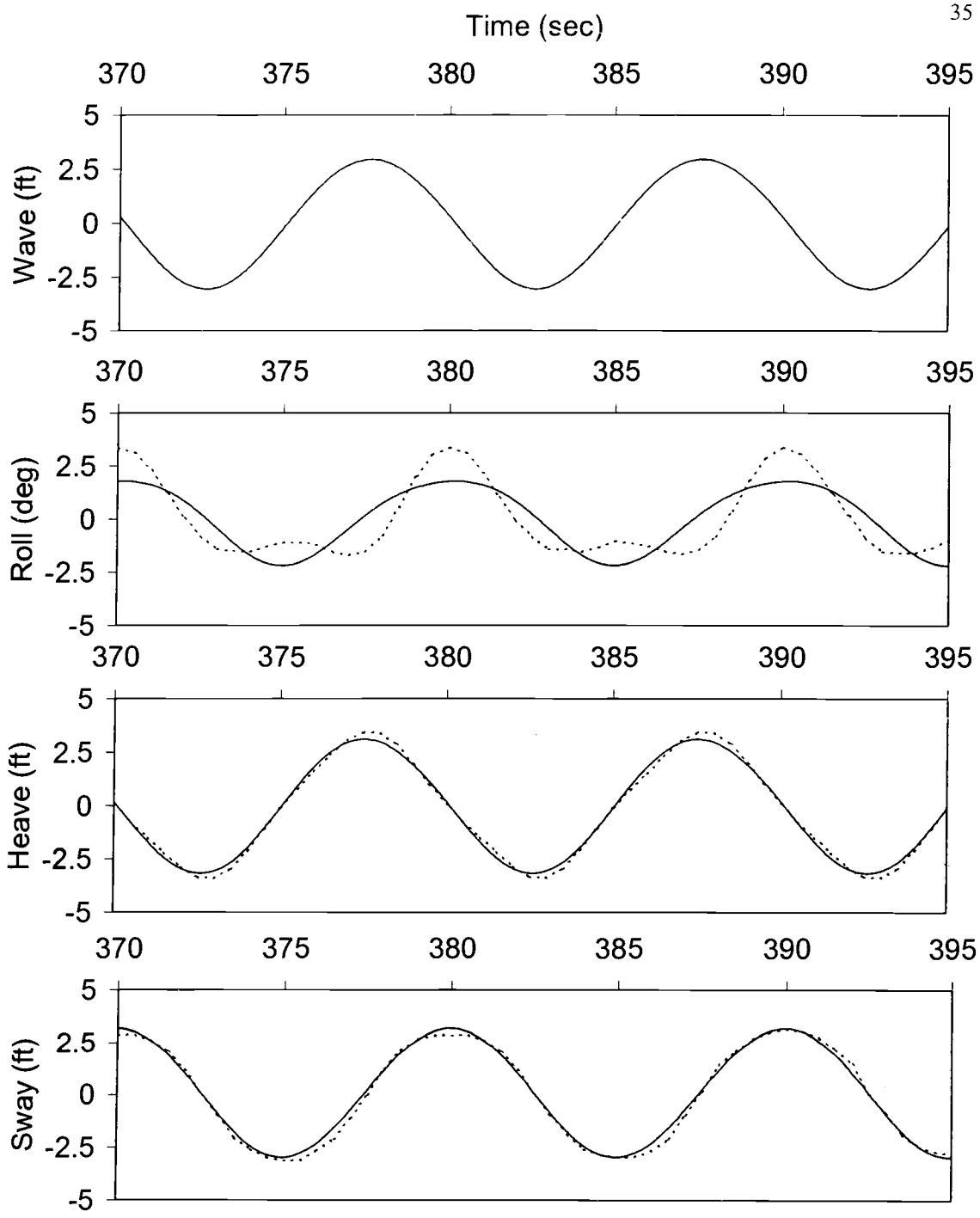

Figure 2.7 Barge roll, heave and sway response time histories to regular waves with H = 6 ft and T = 10 seconds (Case SB30). (solid line = numerical results, dotted line = experimental results)

the roll added inertia and linear roll damping coefficients are needed to match the measured response well for the all test cases. In addition, for the ranges of wave heights and wave periods considered (SB26 to SB31), the identified parameters are practically constant. A summary of the averaged values of the system parameters for regular wave excitations is shown in the second column Table 2.2. Due to wave drift, the steady-state mean position of the barge motions is down stream of the quiescent, static equilibrium position of the moored barge in the experimental set up, where wave elevation was measured. This leads to a time shift (or lag) between the measured wave excitation and barge responses. The wave drift is a function of the wave height and wave period, with larger wave drift magnitude corresponding to larger wave heights. The wave drift also induced tension in the cables used to prevent the barge from drifting down the wave basin. For large wave amplitude excitations (such as SB30, shown in Figure 2.7), the almost taut mooring cables induced a small super harmonic component in the roll response.

Figures 2.5 and 2.6 show that roll is approximately in-phase with sway and heave is in-phase with wave for all regular wave cases. Case SB27 produces the largest roll motions because the wave period (6 seconds) is close to the barge roll natural period of 5.25 seconds, resulting in near resonance.

It is observed that sway is more difficult to match than roll and heave. This is due to the difficulty in modeling the nonlinear mooring cable stiffness, which directly affects the sway motion. Although the model selected in this study represents sway resistant force by a linear spring which that does not reflect the

highly nonlinear features, it is deemed acceptable for the purpose of this study, which focuses primarily on the roll motion. In the open sea, the barge is not moored. Mooring in the experiment is introduced to prevent the model barge from drifting out of the instrumentation area.

2.6 Calibration of Model Prediction Capability

The Roll-Heave-Sway prediction capability of barge motions under random wave excitations of the 3DOF model is investigated in this section. (A detailed study of the 2DOF model will be presented later.) The averaged identified system parameters of the 3DOF model obtained in the above section, with minor adjustments, are used for model predictions for the random wave test case. Measured random waves and simulated random waves (filtered white noise) are both used as input excitations to the model. Comparisons between model predictions and experimental test results are examined. The accuracy of the model predictions of the barge motions due to random waves is demonstrated using a random wave test case SB25 ($H_s = 4.7$ ft., $T_p = 8.2$ s).

2.6.1 Measured random waves

We used the measured random wave profile and numerically derived the wave properties for input to the analytical model. The measured wave was filtered with a low pass tangent Butterworth filter (The Mathworks, 1993) to remove all high frequency wave components above 0.25 Hz (T = 4 sec.) to minimize numerical errors in obtaining derivatives and to adhere to the modeling assumptions that the

wavelength is significantly larger than the beam of the barge. We employed the parameters obtained in above section for regular waves. A minor adjustment in the roll linear coefficient from 5% to 8% was found to provide most accurate predictions.

Time histories of the Roll-Heave-Sway model predictions versus measured results are shown in Figure 2.8. Observe that the model provides good estimations for both roll and heave motion. It also predicts sway reasonably well. As observed in the regular wave cases, roll is in-phase with sway while heave is in-phase with waves. The spectral densities of measured results versus the Roll-Heave-Sway model predictions are shown in Figure 2.9. Overall, the predictions of spectral densities match the measured results well. The sharp peak around the frequency of 0.03 Hz of the measured sway spectral density reflects the nonlinear influence of the mooring cables that is not modeled in this study.

2.6.2 Filtered white noise simulated random waves

Gaussian random waves with a significant wave height, H_s = 4.7 ft, and spectral peak period, T_p = 8.2 seconds, are simulated by the filtered white noise process and used as input into the simulation model. The parameters of the filter are selected to duplicate the statistical and spectral properties of the wave profile specified by the Bretschneider spectrum.

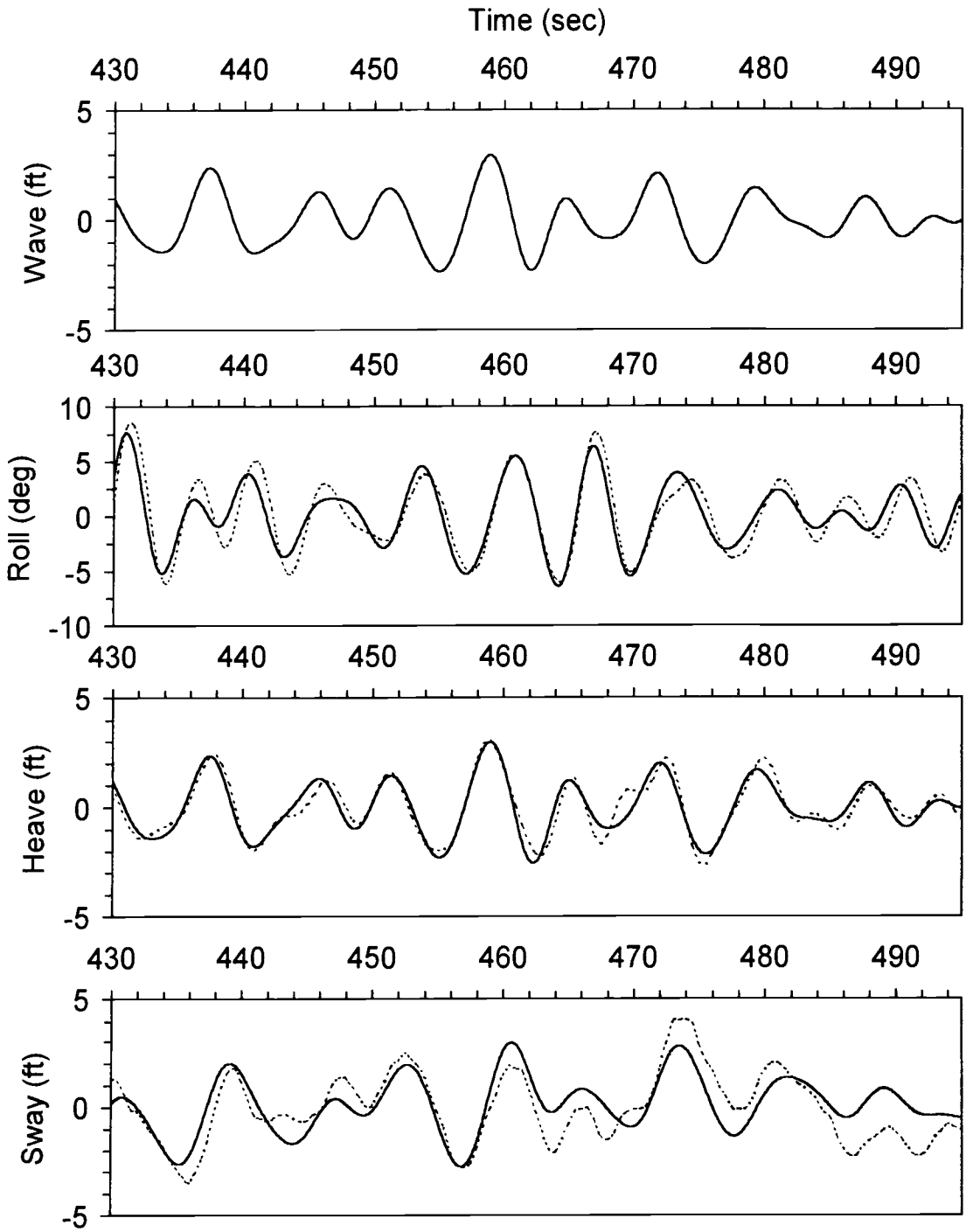

Figure 2.8 Comparison of barge motion response time histories between 3DOF model predictions and experimental results under random wave excitation with H_s = 4.7 ft and T_p = 8.2 seconds (Case SB25). Measured waves are used as model input excitation. (solid line = numerical results, dotted line = experimental results)

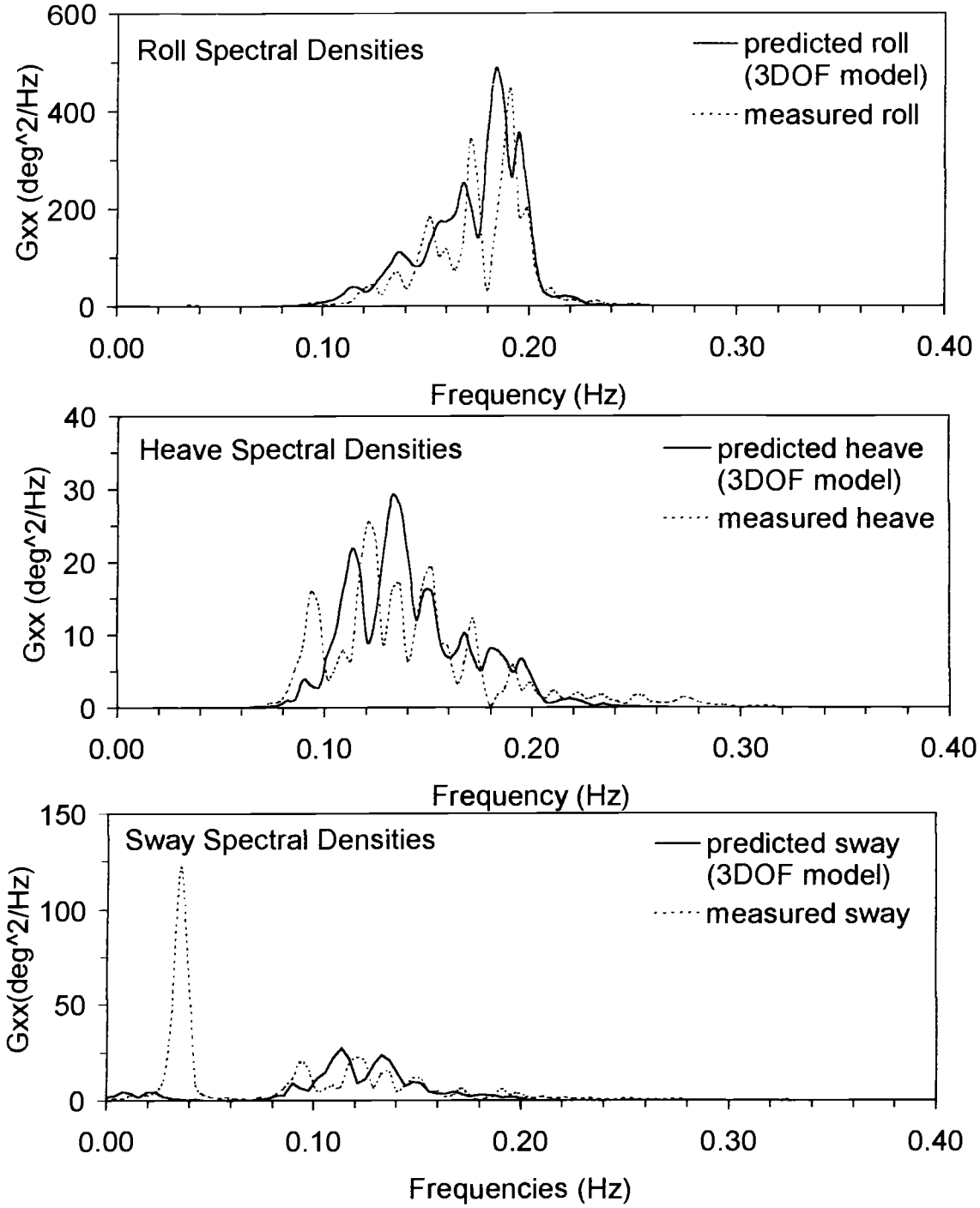

Figure 2.9 Comparison of barge motion response spectral densities between 3DOF model predictions and experimental results under random wave excitation with H_s = 4.7 ft and T_p = 8.2 seconds (Case SB25). Measured waves are used as model input excitation.

Figure 2.10 shows predictions by the Roll-Heave-Sway model match the measured result well, with a slight adjustment in the linear roll-damping ratio from 5 to 3%. The spectral densities of the predicted responses matched reasonably well with the experimental results as shown in Figure 2.11. The model prediction in sway is not as accurate as for roll and heave because of nonlinear characteristics of the mooring cables, which we do not model. The distribution of the predicted roll response to measured and simulated random waves also matched well with the experimental results, as shown in Figure 2.12.

2.7 Coupling Effects of Sway on Roll and Heave Motions

The coupling effects of sway on barge roll and heave motions is examined in this section by comparing numerical results of the 3DOF and the 2DOF models using the same analytical procedure conducted in the above sections. Identical system parameters are employed in both models (when applicable). Responses to regular and random waves are examined. Figures 2.13 shows the time histories of barge responses to regular waves with H = 6 ft and T = 6 seconds (Case SB27) while Figure 2.14 shows the time histories of barge responses to measured random waves with H_s = 4.7 ft and T_p = 8.2 seconds, respectively. Figure 2.15 shows the spectral densities of barge responses based on the 3DOF and the 2DOF models subjected to simulated random waves. Observe that both models provide comparable predictions for both regular and random waves. However, the 2DOF model appears to produce slightly larger roll amplitude than those of the 3DOF model.

a)

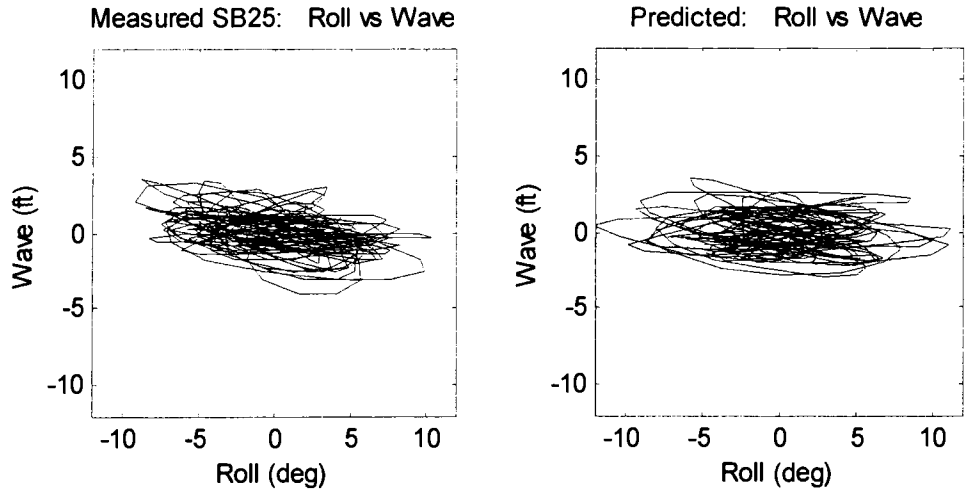

b)

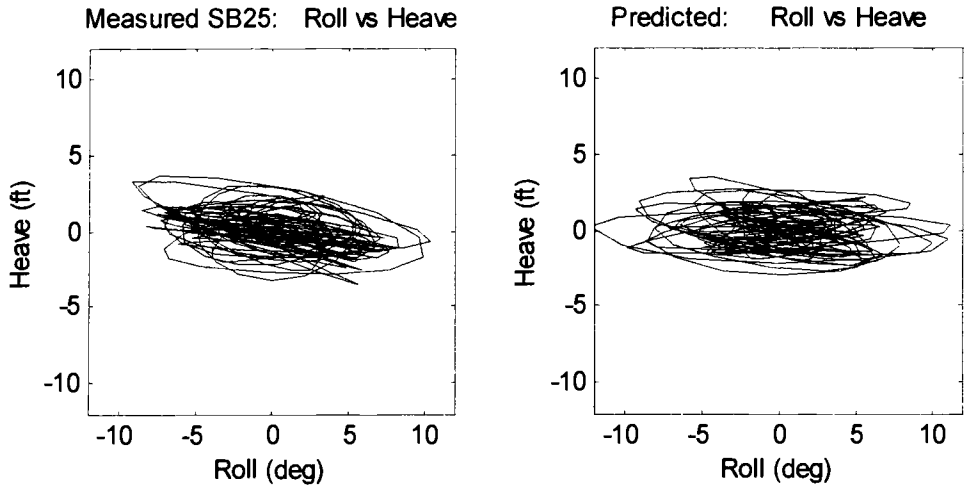

Figure 2.10 Comparison of barge motion phase diagram between 3DOF model predictions and experimental results under random wave excitation with H_s = 4.7 ft and T_p = 8.2 seconds (Case SB25), (a) roll and wave, (b) roll and heave, (c) roll and sway, and (d) heave and sway. Random waves are generated from filtered white noise process. (continued)

c)

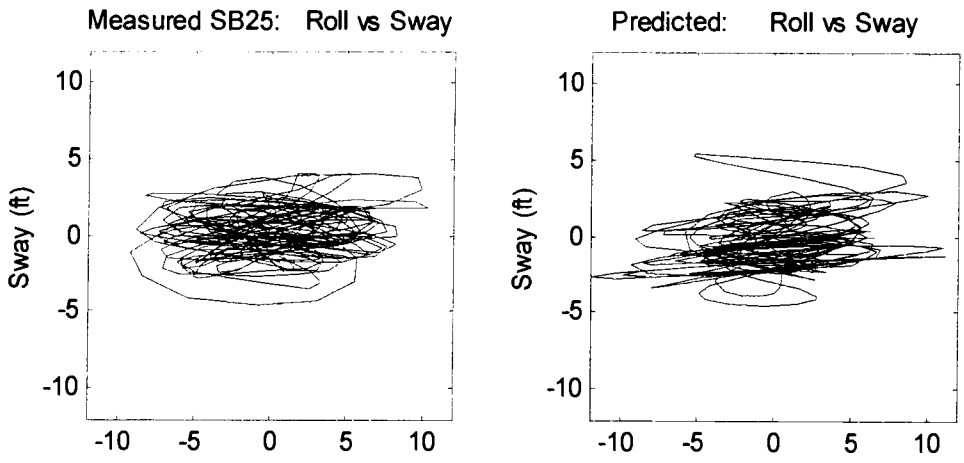

d)

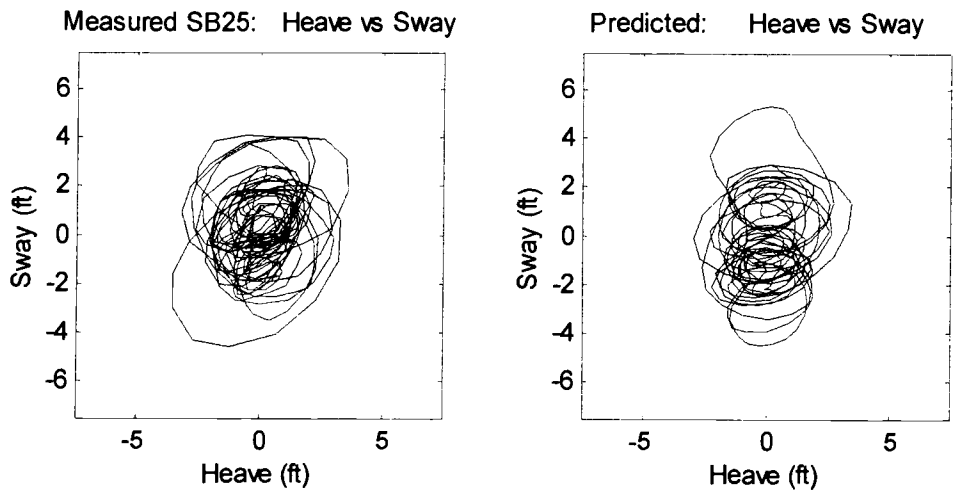

Figure 2.10 Comparison of barge motion phase diagram between 3DOF model predictions and experimental results under random wave excitation with $H_s = 4.7$ ft and $T_p = 8.2$ seconds (Case SB25), (a) roll and wave, (b) roll and heave, (c) roll and sway, and (d) heave and sway. Random waves are generated from filtered white noise process.

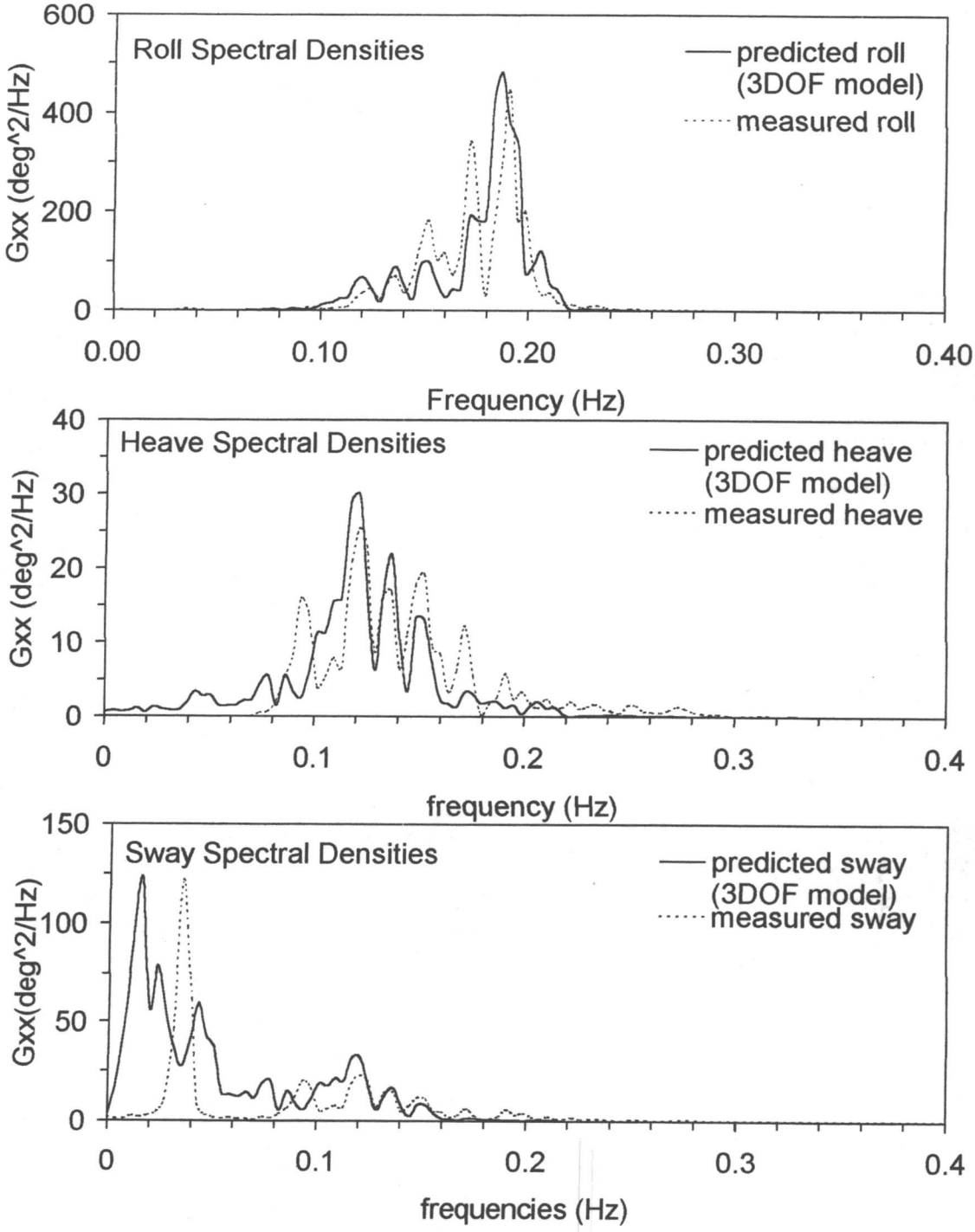

Figure 2.11 Comparison of barge motion spectral densities between 3DOF model predictions and experimental results under random wave excitation with $H_s = 4.7$ ft and $T_p = 8.2$ seconds (Case SB25), (a) roll and wave, (b) roll and heave, (c) roll and sway, and (d) heave and sway. Random waves are generated from filtered white noise process.

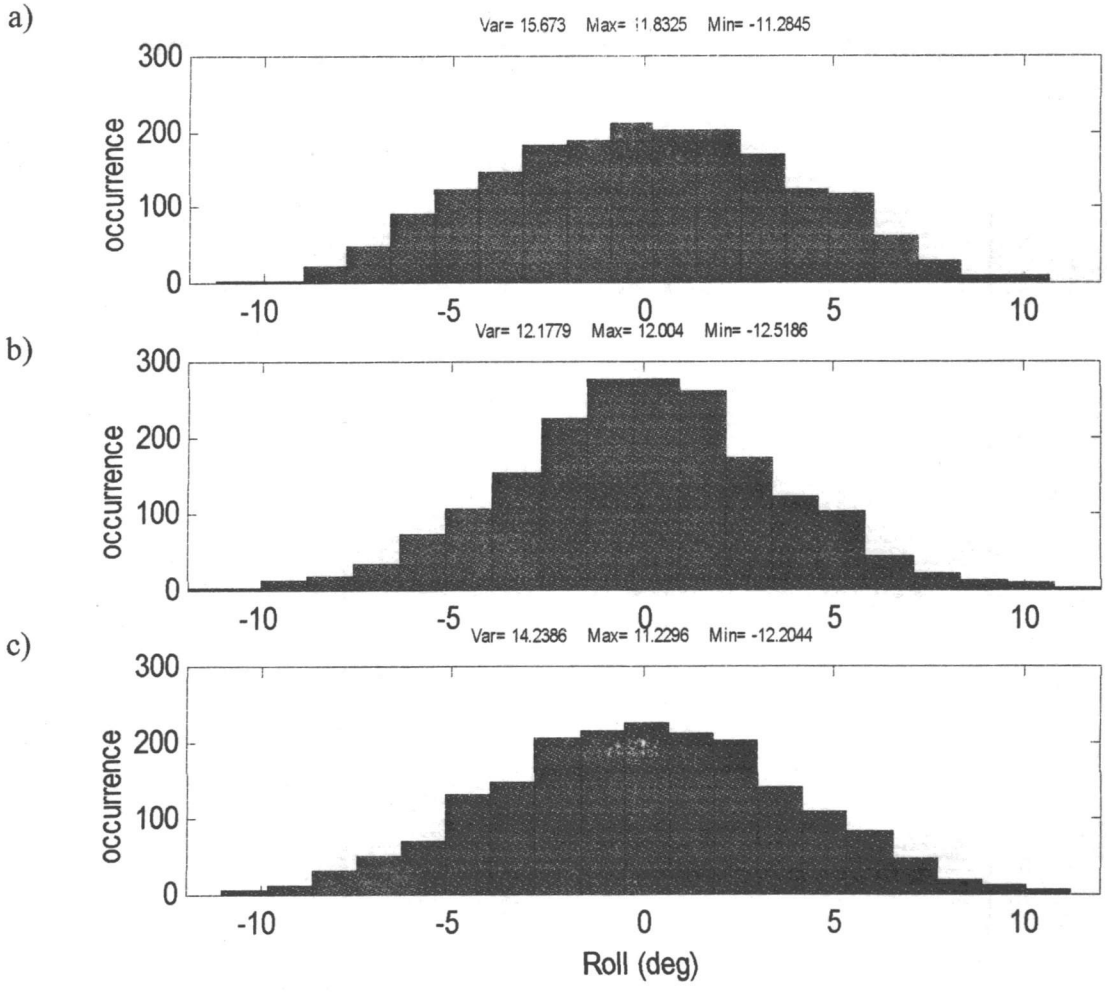

Figure 2.12 Histograms of barge roll response to random wave excitation with H_s = 4.7 ft and T_p = 8.2 seconds (Case SB25), (a) experimental results, (b) 3DOF model under measured random waves, (c) 3DOF model under simulated random waves (sampling rate = 0.5 second, sampling period = 1000 seconds).

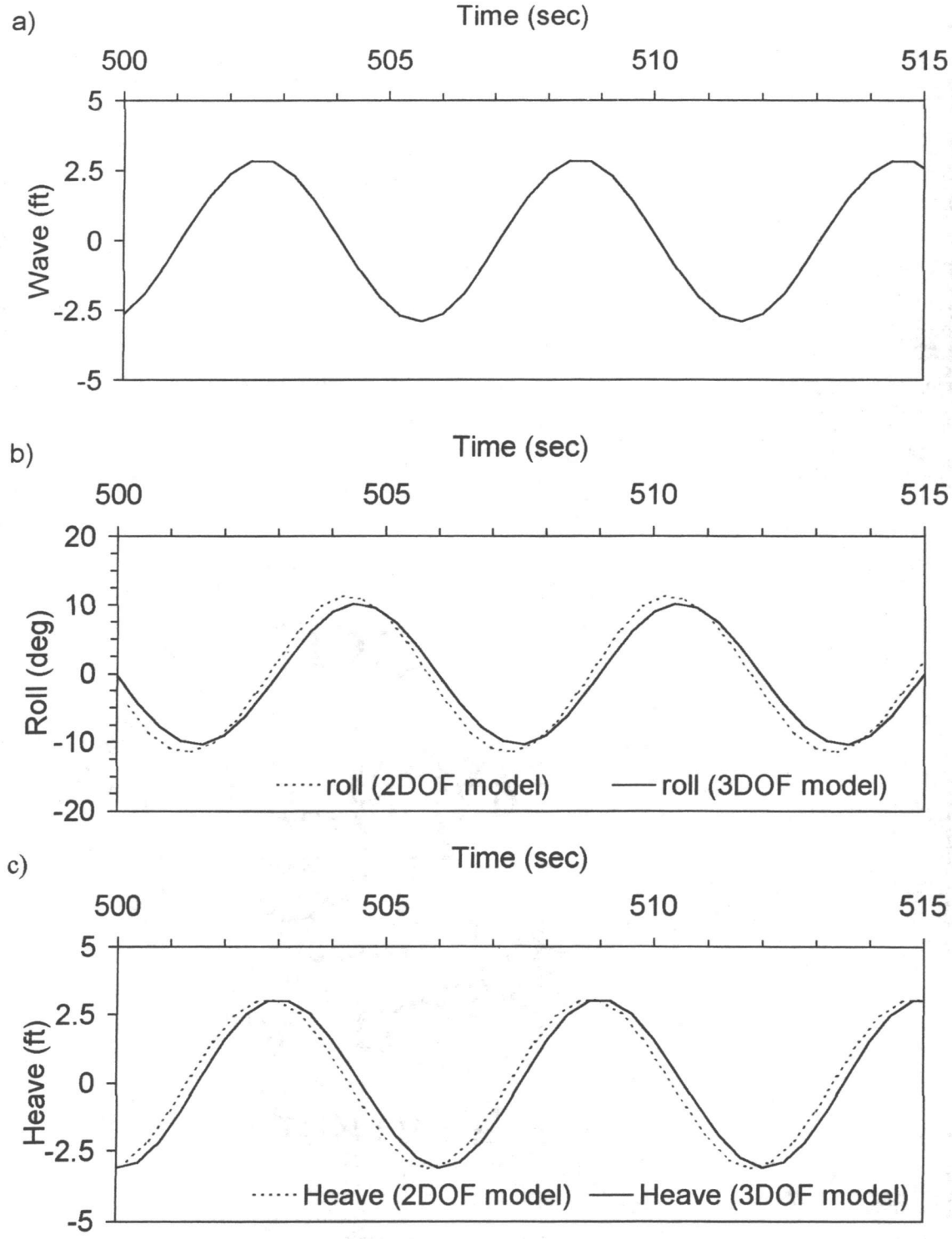

Figure 2.13 Comparison of 3DOF and 2DOF model predictions of time histories of roll and heave barge responses under regular wave excitation with H = 6 ft and T = 6 seconds (Case SB27).

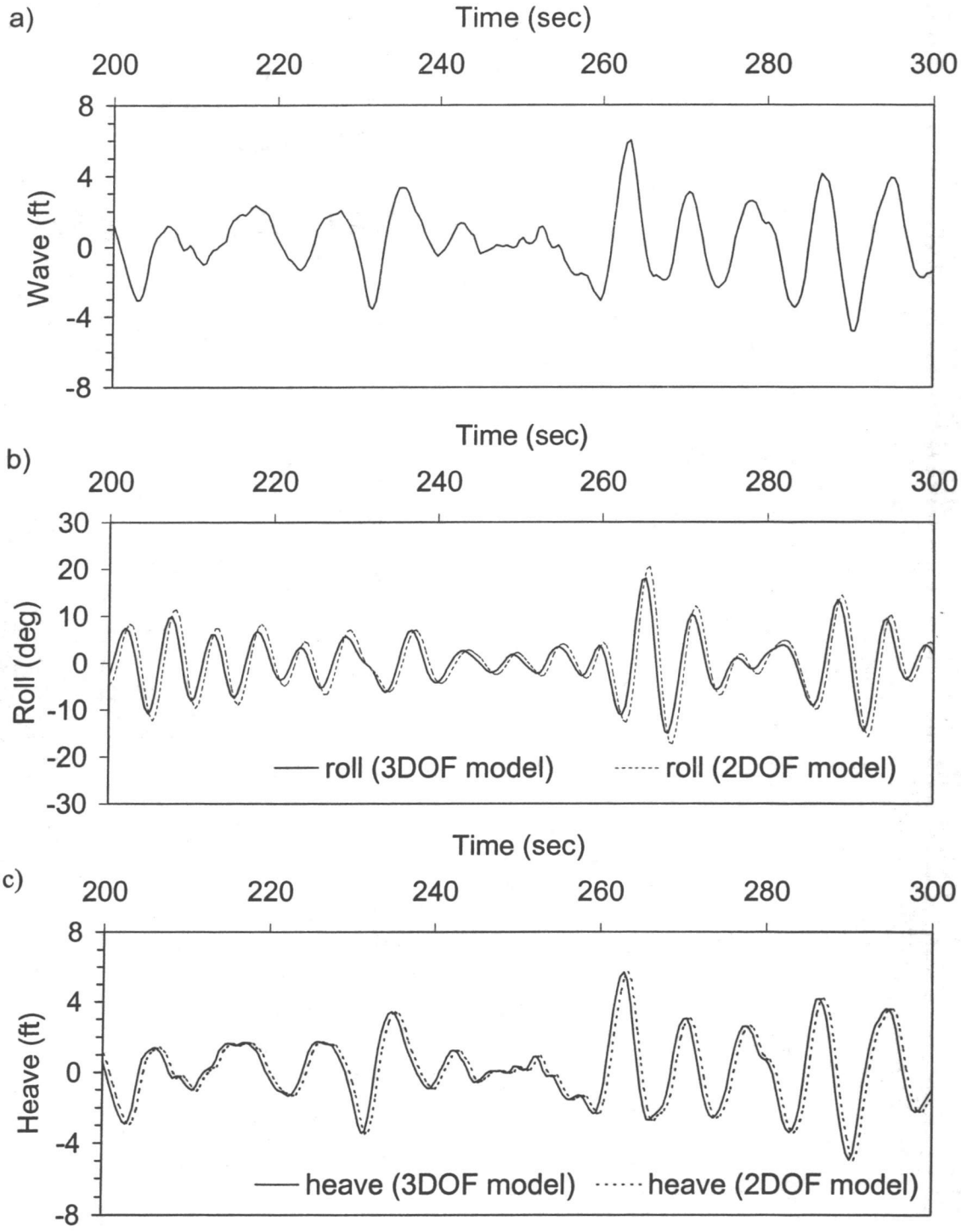

Figure 2.14 Comparison of 3DOF and 2DOF model predictions of time histories of roll and heave barge responses under measured random waves with $H_s = 4.7$ ft and $T_p = 8.2$ seconds (Case SB25).

a)

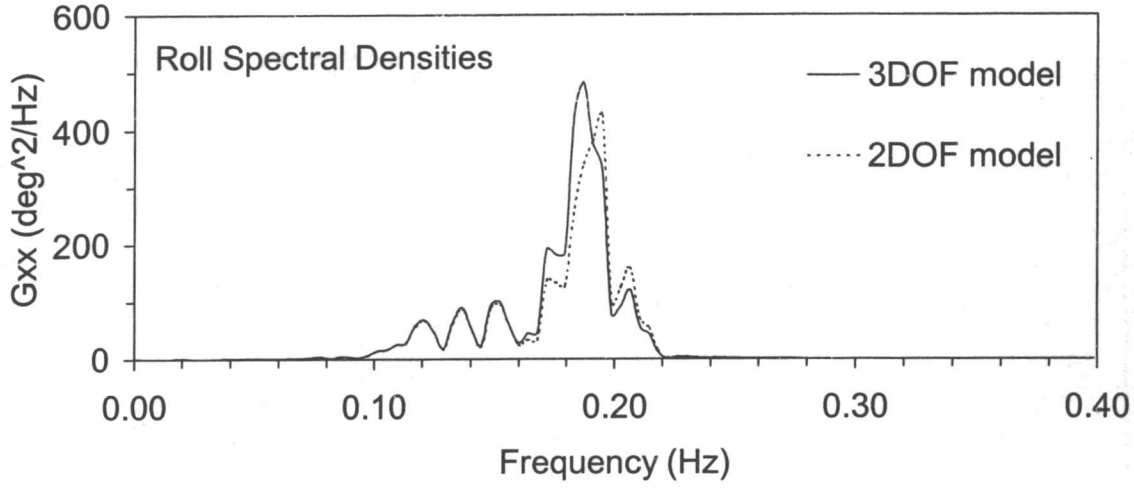

b)

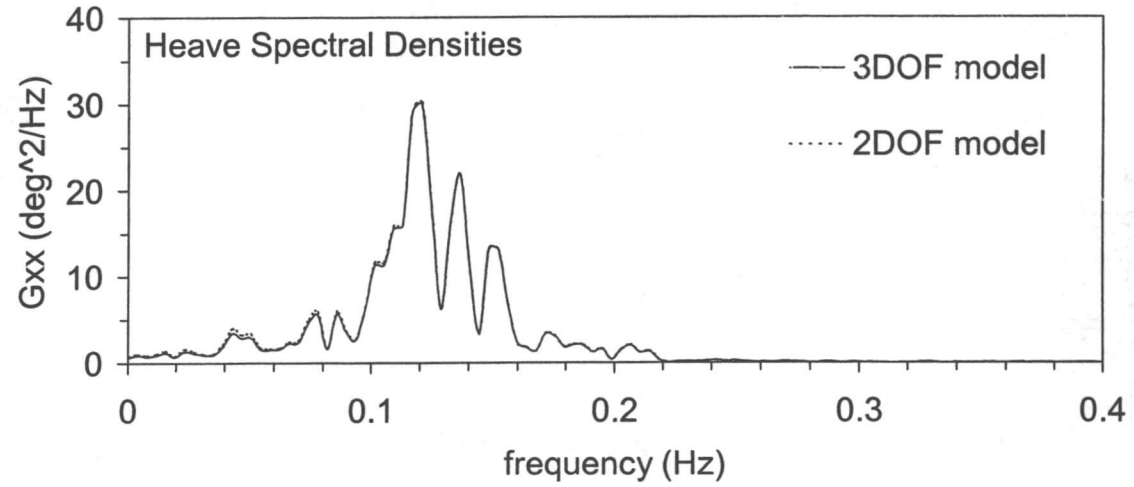

Figure 2.15 Comparison of 3DOF and 2DOF model predictions of (a) roll, and (b) heave spectral densities of barge responses under simulated random waves with H_s = 4.7 ft and T_p = 8.2 seconds (Case SB25).

A preliminary sensitivity study on barge response to regular wave excitation is conducted using both 3DOF and 2DOF models. Barge responses due to several regular waves with various wave heights and wave period are examined. Figure 2.16 shows amplitudes of periodic roll responses for the barge subjected to regular waves with fixed wave height of 6 and 8 ft., varying the wave period between 6 and 9 seconds. Roll amplitude decreases with increasing wave period because the natural frequency for roll motion is 5.25 seconds. The 3DOF model usually produces slightly lower roll response amplitude than the 2DOF model. These results indicate that the effects of moored sway on roll motion could be considered as additional energy dissipation (damping). However, under operations conditions in the open sea, with no mooring, this effect may be negligible. It is observed that sway does not produce noticeable effect on heave motion.

2.8 Conclusions

The equations of motion for roll, heave and sway of a barge in random beam seas have been derived. The model was developed based on rigid body dynamics, coupled with relative motion hydrostatic and hydrodynamic terms. The analytical expressions of the relative motion hydrostatic terms are derived based on the four main states for combined roll-heave positions. The relative motion hydrodynamic terms are in a "Morison" type quadratic form. The relative motion hydrostatic terms, roll righting moment and heave restoring force, are fitted with sufficiently high order polynomials. A 13^{th} -order polynomial in roll and a 12^{th}-order polynomial in heave

a)

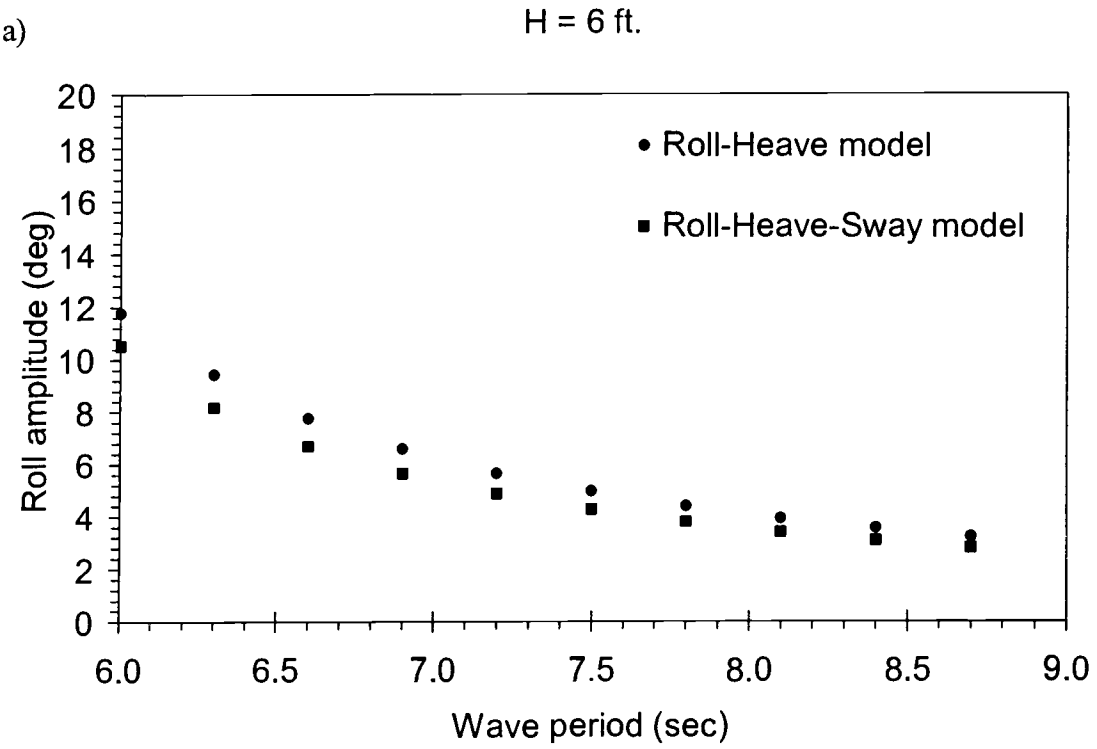

b)

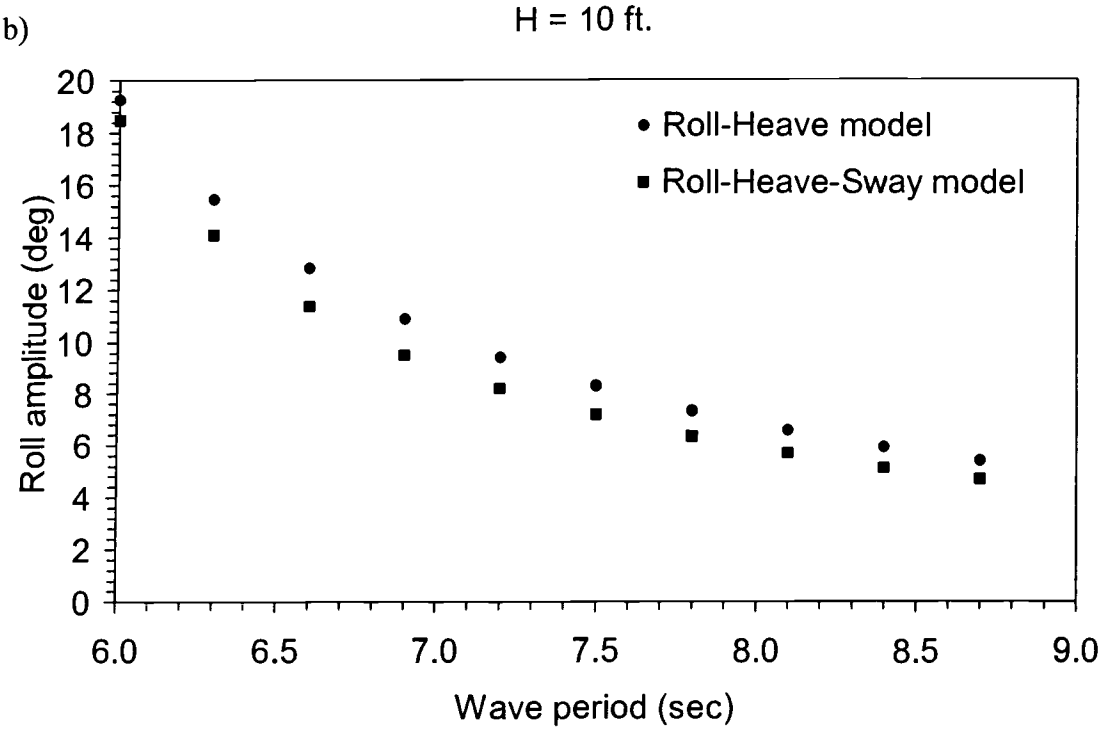

Figure 2.16 Predicted periodic roll response amplitude as a function of regular wave period, with wave height (a) H = 6 ft., and (b) H = 10 ft.

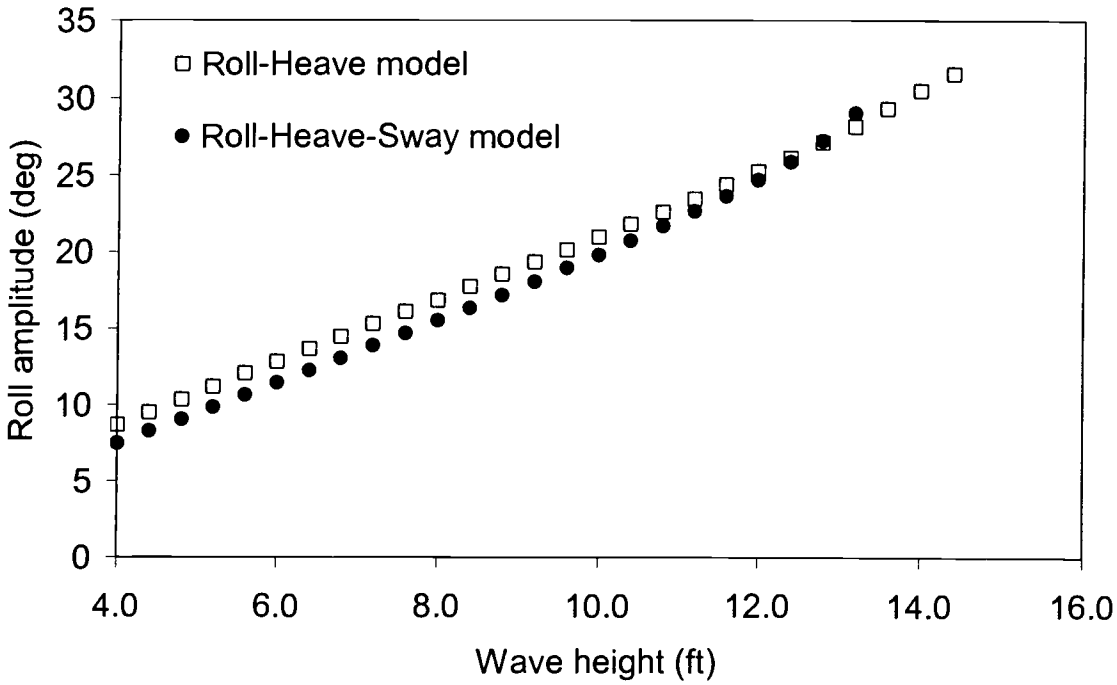

Figure 2.17 Predicted periodic roll response amplitude as a function of regular wave height using 3DOF and 2DOF models under fixed wave period T = 6 seconds.

are sufficient to qualify the general character of the coupled roll-heave restoring moment-forces.

System parameters for the model are identified by matching numerical predictions in the time domain with experimental results of six regular wave test cases, with initial approximate values of the system parameters obtained based on the potential theory. Only minor adjustments to these estimates are needed to obtain optimal match with experimental results. The same set of system parameters is applicable for all the regular-wave cases considered, which ranges in wave period from 6 to 10 seconds.

With the identified system parameters from the regular wave cases, it is found that the 3DOF model provides efficient predictions of barge responses to random waves. Two distinctive processes are used to generate random waves for the models. In the first case, the exact measured random wave data is used as input to the numerical models with other wave properties derived numerically. In the second case, a white noise filter is used to simulate the wave profiles and associated properties. Results from both cases were compared with experimental data. All comparisons indicate close agreement with the model predictions.

The coupling effects of sway on roll and heave barge motions are examined by comparing numerical results from the 3DOF and the 2DOF models employing identical system parameters. Results indicate that the two models provide comparable roll and heave predictions for both regular and random wave cases. It is

observed that the coupling effects of sway on barge roll and heave motions are negligible for the range of system and excitation parameters considered.

References

Abkowitz, M.A. 1969. Stability and Motion Control of Ocean Vehicles. MIT Press, Cambridge, MA.

Bartel, W.A. 1996. *Modelling, Validation and Simulation of Multi-Degree-of Freedom Nonlinear stochastic barge Motions.* A Thesis submitted to Oregon State University.

Cai, G.Q., Yu, S.J. and Lin, Y.K. 1994. Ship Rolling in Random Sea. *Stochastic Dyanamics and Reliability of Nonlinear Ocean Systems*, ASME DE-Vol. 77: 81-88.

Chakrabarti,S.K. 1994. Hydrodynamics of Offshore Structures, *Computational Mechanics* Publications, Southampton Boston.

Dahle, E. AA., Myhaug, D. and Dahl, S.J. 1988. Probability of Capsizing in Steep and High Waves from the Side in Open Sea and Coastal Waters. *Ocean Engineering*, 15:2:139-151.

Donescu, P. and Virgin, L.N. 1993. Nonlinear Coupled Heave and Roll Oscillations of a Ship in Beam Seas, *Nonlinear Dynamics of Marine Vehicles*, ASME, 51: 21-28.

Falzarano,J. and Taz Ul Mulk, M. 1994. Large Amplitude Rolling Motion of an Ocean Survey Vessel. *Marine Technology*, 31:4:278-285.

Falzarano, J.M., Shaw, S.W., and Troesch, A.W. 1992. Application of Global methods for Analyzing Dynamical Systems to Ship Rolling Motion and Capsizing. *International Journal of Bifurcation and Chaos in Applied Sciences and Engineering*, 2:1:101-116.

Liaw, C.Y., Bishop, S.R. and Thompson, J.M.T. 1993. Heave-Excited Rolling Motion of a Rectangular Vessel in Head Seas. *International Journal of Offshore and Polar Engineering*, 3:1:26-31.

Liaw, C.Y. 1993. Dynamic Instability of a Parametrically Excited Ship Rolling Model. *Proc. of the Third International Offshore and Polar Engineering Conference*, Singapore.

Lin, H. and Yim, S.C.S. 1995a. Chaotic Roll Motion and Capsizing of Ships Under Periodic Excitation with Random Noise. *Applied Ocean Research*, 17:3:185-204.

Lin, H. and Yim, S.C.S. 1995b. Stochastic Analysis of a Nonlinear Ocean Structural System. Oregon State University Report No. OE-95-04.

Martin, J. P. 1994. Roll Stabilization of Small Ships. *Marine Technology*, 31:4:286-295.

Naess, A., and Johnsen, J.M., Statistics of Nonlinear Dynamic Systems by path integrations. *Nonlinear Stochastic Mechanics*: 401-409.

Naess, A. and Johnsen, J.M., 1993. Response Statistic of Nonlinear, Compliant Offshore Structures by the Path Integral Solution Method. *Probabilistic Engineering Mechanics*, 8:91-106.

Naess, A. 1995. Prediction of Extreme Response of Nonlinear Structures by Extended Stochastic Linearization. *Probabilistic Engineering Mechanics*, 10:153-160.

Nayfeh, A.H., and Mook, D.T. 1979. Nonlinear Oscillations. New York: John Wiley & son.

Newland, D.E. 1993. *An Introduction to Random Vibrations, Spectral & Wavelet Analysis*. Longman Scientific and Technical, Essex England.

Ochi, M.C. 1990. *Applied Probability & Stochastic Processes: in Engineering and Physical Sciences*. New York: John Wiley & son.

Paulling, J.R. 1990. Inclusion of Theoretical Achievements in the Field of Stability in the Ship Design Process. *STAB '90, Fourth International Conference on Stability of Ships and Ocean Vehicles*, Naples, Italy.

Paulling, J.R. 1961. The Transverse Stability of a Ship in a Longitudinal Seaway. *Journal of Ship Research*. March:37-49.

Paulling, J.R. and Rosenberg, R.M. 1959. On Unstable Ship Motions Resulting From Nonlinear Coupling. *Journal of Ship Research*, 3:pp 36.

Press W.H., Flannery, B.P, Teukolsky, S.A. and Vetterling, W.T. 1986. *Numerical Recipes*, Cambridge University Press.

Roberts, J.B. 1982a. A Stochastic Theory for Nonlinear Ship Rolling in Irregular Seas. *Journal of Ship Research*, 26:4:229-245.

Roberts, J.B. 1982b. Effect of Parametric Excitation on Ship Rolling Motion in Random Waves. *Journal of Ship Research*, 26:4:246-253.

Robert, J.B.,Dunne J.F., and Debonos A. 1994. Stochastic Estimation Methods for Non-Linear Ship Roll Motion. *Probabilistic Engineering Mechanics* 9:83-93.

Thompson, J.M.T., and Stewart, H.B. 1986. *Nonlinear Dynamics and Chaos*. John Wiley & Sons.

Virgin, L.N. and Bishop, S.R. 1988. Catchment Regions of Multiple Dynamic Responses in Nonlinear Problems of Offshore Mechanics. *Proceedings at 7th International Conference on Offshore Mechanics and Arctic Engineering*, Houston, TX. 15-22.

Virgin, L.N. and Erickson, B.K. 1994. A New Approach to the Overturning Stability of Floating Structures. *Ocean Engineering*, 21:1:67-80.

Yim, S.C.S., Bartel, W.A., Lin, H. and Huang, E. 1995. Nonlinear Roll Motion and Capsizing of Vessels in Random Seas. Naval Facilities Engineering Service Center, Port Hueneme, CA.

CHAPTER 3

Stability Analysis of Nonlinear Coupled Barge Motions: Part II, Stochastic Models and Reliability Study

Abstract

This paper presents a stochastic study of the coupled roll and heave barge motions. With the Markov process assumption, roll and heave barge response probability densities are obtained via the Fokker-Planck equation formulation and the path integral solution technique. Numerical results derived from the Roll-Heave (2DOF) and the Roll (1DOF) models are compared in both time domain and probability domain to observe coupling effects of heave on roll motion. A quasi-2DOF model is developed to take advantage of the heave and wave elevation relationship by introducing an additional term to the 1DOF model. Reliability against capsizing of the barge under various sea conditions is analyzed as a first passage time problem using this quasi-2DOF model.

3.1 Introduction

The reliability of ship-to-shore cargo barges under various sea conditions is investigated. While waves excite a barge in many direction sea conditions, the most unstable scenario leading to capsizing is when the barge becomes broadside to the waves, i.e., beam-sea condition. This paper models the barge motions under the

beam-sea condition as a coupled Roll-Heave (2DOF) model and a pure Roll (1DOF) model. A stochastic analysis is conducted to examine barge motions in random beam seas. The path integral solution is employed to numerically obtain barge response probability densities as a solution to the corresponding Fokker-Planck equation. The importance of the coupling effects of heave on roll motion is examined by comparing numerical results obtained from the 2DOF model and the 1DOF model in both time and probability domains. A quasi-2DOF model is then developed to take advantage of the heave and wave elevation relation in modeling the roll-heave coupling effects while keeping the number of governing equations to one. Reliability against capsizing of a barge operating under sea states 1 through 9 is analyzed as a first passage time problem using the quasi-2DOF model.

A significant number of researchers have examined the roll motion of ships from a stochastic perspective (Robert (1982a,b), Dahle *et al* (1988), Lin and Yim (1995a), Kwon *et al* (1993) and Cai *et al* (1993)). The work done by Dahle *et al* (1988) was in the form of a probabilistic model where probability of capsizing under specified sea states were computed. Robert (1982a) modeled the roll motion of a ship by the Fokker-Planck (FP) method to obtain the probability distribution of roll response. He proposed an averaging approximation to reduce the FP equations from two down to one to allow for ease of solution. Lin and Yim (1995a) modeled the roll motion of a ship by the FP equation and studied the effects of noise on deterministic regular wave loads. They showed the ship motion to be governed by two diverse dynamical regions – homoclinic and heteroclinic, where the heteroclinic region

relates to capsizing. They examined chaotic response behavior with noise with the aid of probability density functions. Kwon *et al* (1993) modeled the roll motion of a ship subjected to an equivalent white noise model of ocean waves. They studied mean upcrossing times for a nonlinear model of roll righting moment and nonlinear damping. Cai *et al* (1994) provided a stochastic model of nonlinear roll motion of a ship. They modeled the excitation as a stationary Gaussian random process with non-white broadband spectra. The total energy in their dynamical system is approximated as a Markov process, using a modified version of quasi-conservative averaging. They treated the capsizing of the ship as a first passage problem in stochastic dynamics. (A first passage problem evaluates the reliability of a system by deriving the mean-time that the probability mass exits a prescribed safe domain.) Multiplicative excitation and stiffness nonlinearity were found to be important.

3.2 Equations of Motion

A mathematical model representative of the fluid-structure interaction of the barge in ocean waves is derived. The coupled rigid body relation of the barge in the air is first obtained by considering the roll and heave part of the six degree of freedom rigid body relation (Abkowitz, 1969). The hydrostatics and hydrodynamics terms are then included when placing the barge in water. Hydrostatic terms are in the form of a high order polynomial to represent the characteristics of restoring force and moment. Hydrodynamic terms are in a "Morison" type quadratic form (Chakrabarti, 1994). Once the Roll-Heave (2DOF) model for the barge motions in beam-sea condition is

derived, the equations of motion are then uncoupled to obtain a 1DOF Roll model. The resulting equations of motion for Roll-Heave motion are

$$m\ddot{z}+m_{a_{33}}(\ddot{z}-\ddot{w})+C_{33_L}\dot{z}+C_{33_N}\dot{z}|\dot{z}|-m(z_g\cos\phi)\dot{\phi}^2+mg+R_{33}(z,\phi,\eta,\frac{\partial\eta}{\partial y}) = 0$$

$$I_{44}\ddot{\phi}+I_{a_{44}}(\ddot{\phi}-\frac{\partial\ddot{\eta}}{\partial y})+C_{44_L}(\dot{\phi}-\frac{\partial\dot{\eta}}{\partial y})+C_{44_N}(\dot{\phi}-\frac{\partial\dot{\eta}}{\partial y})|\dot{\phi}-\frac{\partial\dot{\eta}}{\partial y}|+m(z_g\cos\phi)\dot{\phi}\dot{z} \qquad (3.1)$$
$$+R_{44}(\phi,z,\eta,\frac{\partial\eta}{\partial y})-mgz_g\sin\phi = 0$$

Assuming the effects of heave are negligible, the corresponding Roll only (1DOF) model is

$$I_{44}\ddot{\phi}+I_{a_{44}}(\ddot{\phi}-\frac{\partial\ddot{\eta}}{\partial y})+C_{44_L}(\dot{\phi}-\frac{\partial\dot{\eta}}{\partial y})+C_{44_N}(\dot{\phi}-\frac{\partial\dot{\eta}}{\partial y})|\dot{\phi}-\frac{\partial\dot{\eta}}{\partial y}| \qquad (3.2)$$
$$+R_{44}(\phi,\frac{\partial\eta}{\partial y})-mgz_g\sin\phi = 0$$

The physical assumptions of the models are as follow. The wave free surface elevation is assumed linear across the beam of the barge (i.e., wavelength is significantly longer than the barge beam). Wave forces and moments act at the center of gravity and are based on momentum theory. The effect of water on deck is treated statically, being modeled only in the hydrostatic restoring moment. Coefficients of added inertia, added mass and damping are assumed constant. The

longitudinal center of gravity (LCG) is amidships. The barge is symmetric longitudinally and laterally.

3.2.1 Regular wave excitation

Regular waves are used as input to the time domain simulation. The characteristics of the excitation wave field are based on linear wave theory. For linear regular waves with the assumption of deep water and consideration of water particle kinematics at mean water line (MWL), wave expressions are defined as

$$
\begin{aligned}
k &= \frac{\omega^2}{g} \\
\eta &= A\sin(ky - \omega t) \\
\dot{\eta} &= -\omega A\cos(ky - \omega t) \\
\ddot{\eta} &= -\omega^2 \eta \\
v &= \omega\eta \\
\dot{v} &= \omega\dot{\eta} \\
w &= \dot{\eta} \\
\dot{w} &= -\omega^2\eta \\
\frac{\partial\eta}{\partial y} &= -\frac{\omega}{g}\dot{\eta} \\
\frac{\partial\dot{\eta}}{\partial y} &= \frac{\omega^3}{g}\eta \\
\frac{\partial\ddot{\eta}}{\partial y} &= \frac{\omega^3}{g}\dot{\eta}
\end{aligned}
\qquad (3.3)
$$

Barges operate from relatively deep to shallow water. However, the deep-water condition in general produces higher coupling effects of heave on roll due to larger vertical wave velocity. Therefore, for conservatism of the analysis, the deep-water condition is assumed.

3.2.2 Random wave excitation

For random waves, the wave free surface elevation is represented as sum of regular waves (Chakrabarti, 1994) by

$$\eta = \sum_{i=1}^{N} \frac{H_i}{2} \sin(k_i y - \omega_i t + \varepsilon_i) \tag{3.4}$$

which adheres to an ocean wave spectral model such as that of Bretschneider (Chakrabarti, 1994) represented by

$$S(\omega) = 0.1687 H_s^2 \frac{\omega_s^4}{\omega^5} e^{-0.675(\omega_s/\omega)^4} \tag{3.5}$$

The present research utilizes filtered white noise to create a random free surface elevation. The linear filter is defined as

$$\ddot{\eta} + \beta_n \dot{\eta} + (2\pi f_0)^2 \eta = \xi \tag{3.6}$$

where ξ is Gaussian white noise, which is obtained by using a pseudo random number generator. The transfer function and the spectral density function of the output of the filtered white noise (Lin and Yim, 1995b) are

$$|H(f)| = \frac{1}{[-(2\pi f)^2 + (2\pi f_0)^2]^2 + (2\pi\beta_n)^2}$$
$$S_\eta(f) = \frac{S_0}{[-(2\pi f)^2 + (2\pi f_0)^2]^2 + (2\pi\beta_n)^2} \tag{3.7}$$

The coefficients in Equation 3.6 are set to satisfy the variance and peak period of the Bretschneider spectrum (Lin and Yim, 1995b).

3.3 Time Domain Predictions

To obtain barge responses in the time domain, equations of motion are reduced to a system of first order ordinary differential equations and solved by standard numerical procedure. For the random wave case, linear filtered white noise is added to the system. A 4th order Runge-Kutta method (Press et al, 1986) is employed for numerical integration. A Gaussian distributed random number generator used in the filtered white noise model in this study is based on Press *et al* (1986).

3.4 Probability Domain Predictions

By assuming the stochastic response is a function of only the most recent probability states, a Markov process assumption can be applied. Barge response probability density is numerically derived as a solution to the associated Fokker-Planck equation (FPE) by the path integral solution (Wissel, 1979). A general nonlinear stochastic system can be written as

$$\dot{X} = F(X) + G(X)\eta(t) \tag{3.8}$$

where

$$X = [x_1\ x_2 \ldots x_N]^T,\ F(X,t) = [F_1\ F_2 \ldots F_N]^T,\ G(X) = [G_1\ G_2 \ldots G_N]^T \tag{3.9}$$

For Equation 3.8 the associated FPE is

$$\frac{\partial f(X,t)}{\partial t} = Lf(X,t) \tag{3.10}$$

where the operator

$$L = \frac{1}{2}\frac{\partial^2}{\partial x_\nu \partial x_\mu} Q_{\nu\mu}(X) - \frac{\partial}{\partial x_\nu} K_\nu(X,t);\ \nu,\mu = 1,2,\ldots N \tag{3.11}$$

and

$$K_\nu = F_\nu(X); \quad Q_{\nu\mu} = \kappa G_\nu G_\mu \tag{3.12}$$

With f(X,t) representing the PDF, K_ν's (ν = 1,2,...N) are the entries in the drift vector K, and $Q_{\nu\mu}$ are the entries of the N x N diffusion matrix Q.

The path-integral solution has been developed by Graham (1978), Haken (1976), and Wissel (1979) to solve the FPE. It can be represented by a (discrete) Riemann sum (Wissel, 1979)

$$f(X_n,t_n)=\lim_{\substack{n\to\infty \\ n\tau=t-t_0}}\prod_{i=0}^{n-1}(\mu_i dx_i)\exp\left(-\tau\sum_{j=0}^{n-1}L^*(X_{j+1},X_j,\tau\right)f(X_{j+1},X_j,\tau)f(X_0,t_0) \quad (3.13)$$

where $\mu_i dx_i$ is the (Wiener) measure in the functional space, and L^* is the Lagrangian. A short transition can be obtained analytically using a first order approximation to Equation 3.13.

With specified drift vector and diffusion tensor for the FPE, the associated short time propagator (Green's function) is given by (Wissel, 1979)

$$P_{t,\tau}(X'\mid X)=(2\pi\tau)^{\frac{-n}{2}}Q^{\frac{-1}{2}}\exp\left\{\begin{array}{l}-\frac{\tau}{2}[Q_{\nu\lambda}^{(\lambda)}+K_\nu-\frac{x'_\nu-x_\nu}{\tau}]Q_{\nu\mu}^{-1} \\ [Q_{\mu\rho}^{(\rho)}+K_\mu-\frac{x'_\mu-x_\mu}{\tau}]+\tau K_\nu^{(\nu)}+\frac{\tau}{2}Q_{\nu\mu}^{(\nu\mu)}\end{array}\right\} \quad (3.14)$$

Using a multi-dimensional histogram representation of the PDF, the path sum (Equation 3.13) can be implemented numerically. The probability domain at time t is discretized into a finite number of elements represented by function π.

$$P(X,t)=\sum_{i=1}^{I}\pi(x_1-x_{1i})\pi(x_2-x_{2i})...\pi(x_N-x_{Ni})f(X,t) \quad (3.15)$$

where

$$\pi(x_n - x_{ni}) = \begin{cases} 1 & for\ x_n - \dfrac{\Delta x_{n(i-1)}}{2} \le x \le x_{n(i)} + \dfrac{\Delta x_{n(i)}}{2} \\ 0 & otherwise \end{cases} \tag{3.16}$$

with n = 1,2, ... N. The short-time propagator is also discretized into a short-time transition tensor $T_{kl}(\tau)$. Subscripts k and l represent the discretized probability domain at the pre and post state respectively. The short time propagation can be numerically implemented by determining the most probable position in the phase space and the local random response following a Gaussian distribution. The most probable phase position after a short-time propagation for each element is deterministically computed by the drift coefficients. The PDF at time $t + \tau$ can be obtained by summing all the probability mass propagated from time t (and normalizing afterward)

$$P_k(t+\tau) = T_{kl}(\tau)P_l(t) \tag{3.17}$$

where the transition tensor is given by

$$T_{kl}(\tau) = \frac{2^N}{(\Delta x_{kl(i-1)} + \Delta x_{kl(i)})...(\Delta x_{kn(j-1)} + \Delta x_{kN(j)})} \int_{x_{kl(i)}-\frac{\Delta x_{kl(i-1)}}{2}}^{x_{kl(i)}+\frac{\Delta x_{kl(i)}}{2}} dx_{k1} ... \int_{x_{kN(i)}-\frac{\Delta x_{kN(i-1)}}{2}}^{x_{kn(i)}+\frac{\Delta x_{kN(i)}}{2}} dx_{kN}$$

$$\int_{x_{Ll(i)}-\frac{\Delta x_{Ll(i-1)}}{2}}^{x_{Ll(i)}+\frac{\Delta x_{Ll(i)}}{2}} dx_{l1} ... \int_{x_{LN(i)}-\frac{\Delta x_{LN(i-1)}}{2}}^{x_{LN(i)}+\frac{\Delta x_{LN(i)}}{2}} dx_{lN} \; P_{t,\tau}(X_k \mid X_l) \qquad (3.18)$$

The PDF at a desired time can be obtained by applying the short time transition in Equation 3.18 iteratively.

To obtain numerical results, the initial conditions are assumed deterministic, represented by the product of two Dirac delta functions

$$P(X,t_0) = \delta(x_1 - x_{10})\delta(x_2 - x_{20}) \qquad (3.19)$$

which is represented by a point with area virtually zero in the phase space. For accuracy, the grid size of the discretized probability domain has to be sufficiently small. Moreover, the time step (τ) has to be compatible with the associated grid size. For a given grid size, too small a time step results in no propagation of the probability mass. However, too large a time step is not theoretically appropriate and would lead to inaccurate results. Therefore, the selected time step (τ) in this study is the smallest one that produces propagation of probability mass for a given grid size.

The path integral solution is a first order Euler approximation (Wissel, 1979), and one possible numerical evaluation based on lattice representation (path sum) (Wehner and Wolfer, 1983) can be applied to implement the solution numerically. Using this standard numerical procedure, the results can demonstrate the evolution of the response density. A 4th order Runge-Kutta integration procedure is employed to compute the deterministic response trajectory.

3.4.1 2DOF stochastic model

Bretschneider random waves are approximated by a linear filtered white noise process. With the addition of wave variables, the 2DOF model could be defined as

$$\frac{d}{dt}\begin{bmatrix} X_1 \\ X_2 \\ \eta_1 \\ \eta_2 \end{bmatrix} = \begin{bmatrix} X_2 \\ \dot{X}_2 \\ X_4 \\ \dot{X}_4 \\ \eta_2 \\ \dot{\eta}_2 \end{bmatrix} + \begin{bmatrix} 0 \\ 0 \\ 0 \\ \xi \end{bmatrix} \tag{3.20}$$

The Fokker-Planck equation is given by

$$\partial P(X_1, X_2, X_3, X_4, \eta_1, \eta_2, t) = -\frac{\partial[X_2 P]}{\partial X_1} - \frac{\partial\left[\dot{X}_2 P\right]}{\partial X_2} - \frac{\partial[X_4 P]}{\partial X_3} - \frac{\partial\left[\dot{X}_4 P\right]}{\partial X_4}$$
$$- \frac{\partial[\eta_2 P]}{\partial \eta_1} - \frac{\partial\left[\dot{\eta}_2\right]}{\partial \eta_2} + \frac{\kappa}{2}\frac{\partial^2 P}{\partial \eta_2^2} \tag{3.21}$$

where

$$\dot{X}_2 = \frac{\left[I_{a_{44}} \frac{\partial \ddot{\eta}}{\partial y} - C_{44_L}(X_2 - \frac{\partial \dot{\eta}}{\partial y}) - C_{44_N}(X_2 - \frac{\partial \dot{\eta}}{\partial y})\left|X_2 - \frac{\partial \dot{\eta}}{\partial y}\right| - R_{44}(X_1, \frac{\partial \eta}{\partial y}) + mgz_g \sin(X_1) \right]}{(I_{44} + I_{a_{44}})}$$

$$\dot{X}_4 = \frac{\left[m_{a_{33}} \omega^2 \eta_1 - C_{33_L} X_4 - C_{33_N} X_4 |X_4| + mz_g \cos(X_1) X_2^2 - mg - R_{33}(X_1, X_3, \eta_1, \frac{\partial \eta}{\partial y}) \right]}{m + m_{a_{33}}}$$

$$\dot{\eta}_2 = -\beta_n \eta_2 - (2\pi f_0)^2 \eta_1$$

The corresponding short-time propagator is given by

$$\begin{aligned} G(X_1', X_2', X_3', X_4', \eta_1', \eta_2', X_1, X_2, \eta_1, \eta_2, t; \tau) \\ = (2\pi\tau)^{-4} \kappa^{-1/2} \exp(\frac{-\tau}{2\kappa}(\sigma^2 \eta_2 + \Omega_f^2 \eta_1 + \frac{\eta_2' - \eta_2}{\tau})^2) \\ \delta(\dot{X}_2 - \frac{\eta_2' - \eta_2}{\tau}) \delta(X_2 - \frac{X_1' - X_1}{\tau}) \delta(\eta_2 - \frac{\eta_1' - \eta_1}{\tau}) \\ \delta(\dot{X}_4 - \frac{\eta_2' - \eta_2}{\tau}) \delta(X_4 - \frac{X_3' - X_3}{\tau}) \end{aligned} \qquad (3.22)$$

3.4.2 1DOF stochastic model

Bretschneider random waves are approximated by a linear filtered white noise process. With the addition of wave variables, the 1DOF model could be defined as

$$\frac{d}{dt}\begin{bmatrix} X_1 \\ X_2 \\ \eta_1 \\ \eta_2 \end{bmatrix} = \begin{bmatrix} X_2 \\ \dot{X}_2 \\ \eta_2 \\ \dot{\eta}_2 \end{bmatrix} + \begin{bmatrix} 0 \\ 0 \\ 0 \\ \xi \end{bmatrix} \tag{3.23}$$

The Fokker-Planck equation is given by

$$\partial P(X_1, X_2, \eta_1, \eta_2, t) = -\frac{\partial[X_2 P]}{\partial X_1} - \frac{\partial\left[\dot{X}_2 P\right]}{\partial X_2} - \frac{\partial[\eta_2 P]}{\partial \eta_1} - \frac{\partial\left[\dot{\eta}_2\right]}{\partial \eta_2} + \frac{\kappa}{2}\frac{\partial^2 P}{\partial \eta_2^2} \tag{3.24}$$

where

$$\dot{X}_2 = \frac{\left[I_{a_{44}} \frac{\partial \ddot{\eta}}{\partial y} - C_{44_L}(X_2 - \frac{\partial \dot{\eta}}{\partial y}) - C_{44_N}(X_2 - \frac{\partial \dot{\eta}}{\partial y})\left|X_2 - \frac{\partial \dot{\eta}}{\partial y}\right| - R_{44}(X_1, \frac{\partial \eta}{\partial y}) + mgz_g \sin(X_1) \right]}{(I_{44} + I_{a_{44}})}$$

$$\dot{\eta}_2 = -\beta_n \eta_2 - (2\pi f_0)^2 \eta_1$$

The corresponding short-time propagator is given by

$$G(X_1^{'},X_2^{'},\eta_1^{'},\eta_2^{'},X_1,X_2,\eta_1,\eta_2,t;\tau)=(2\pi\tau)^{-4}\kappa^{-1/2}\exp(\frac{-\tau}{2\kappa}(\sigma^2\eta_2+\Omega_f^2\eta_1+\frac{\eta_2^{'}-\eta_2}{\tau})^2)$$
$$\delta(\dot{X}_2-\frac{\eta_2^{'}-\eta_2}{\tau})\delta(X_2-\frac{X_1^{'}-X_1}{\tau})\delta(\eta_2-\frac{\eta_1^{'}-\eta_1}{\tau}) \quad (3.25)$$

3.5 System Parameters

Table 3.1 summarizes the parameters of a sample of physical model test cases employed in this study. The parameters shown are identified by matching numerical predictions with experimental results in the time domain for six regular wave cases, SB26 to SB31. Initial values for the parameters are base on the potential theory results predicted by Paulling (1995). Then, they are fine-tuned to obtain the best fit. Table 3.2 provides the identified parameters that are applied to all models.

Table 3.1. Physical Model Test Cases

Test Case	Wave Type	H (ft) or H_s(ft)	T (sec) or T_p (sec)
SB25	Random	4.7	8.2
SB26	Regular	6.0	5.0
SB27	Regular	6.0	6.0
SB28	Regular	6.0	7.0
SB29	Regular	7.0	8.0
SB30	Regular	6.0	10.0
SB31	Regular	10.0	10.0

Table 3.2 Summary of System Coefficients Used in the Model

Parameter	**Regular Wave H from 6 to 10 ft T from 5 to 10 sec**
I_{44} (slugs-ft^2)	2.161E+06
$I_{a_{44}}$ (slugs-ft^2)	1.30E+06
ζ_{L44}	0.05
ζ_{N44}	0.008
m (slugs)	2.325E+04
$m_{a_{33}}$ (slugs)	1.00E+05
ζ_{L33}	0.35
ζ_{N33}	0.5
m (slugs)	2.325E+04
$m_{a_{22}}$ (slugs)	2.00E+04
ζ_{L22}	0.5
ζ_{N22}	5.0

3.6 Coupling Effects of Heave on Roll Barge Motion

Barge roll responses derived from the 2DOF and the 1DOF model in the time domain simulation are examined. Several regular and random waves are used as excitations. Figure 3.2a shows barge roll responses to regular waves with H = 6 ft and T = 8 seconds, while Figure 3.2b shows the barge response to random wave with H_s = 4.7 ft and T_p = 8.2 seconds. These numerical results indicate good agreement between the 2DOF and the 1DOF models. The 2DOF model produces slightly larger roll amplitude. However, the differences increase significantly in those cases with larger roll responses as shown in Figure 3.3. Numerical results from the probability domain simulation also indicate the same behavior. Resulting roll response densities by the 2DOF and 1DOF models after 5 minutes of exposure time in random waves are compared. Figure 3.4 shows roll response density due to random waves with H_s = 4.7 ft and T_p = 8.2 seconds. Figure 3.5 shows roll response density due to random waves with H_s = 5.5 ft and T_p = 5.5 seconds. The corresponding marginal densities of roll motion by both models are compared in Figure 3.6. Results show that the 2DOF model produces greater density at larger roll amplitude at the same exposure time. These differences become more significant for cases with larger roll motion.

The governing equations of motion indicate that the coupling effect of heave on roll is presented in two distinctive mechanisms. First, the relative heave motion to wave elevation impact the hydrostatic roll righting moment. Second, the heave velocity creates inertia moment caused by eccentricity of the roll center and KG.

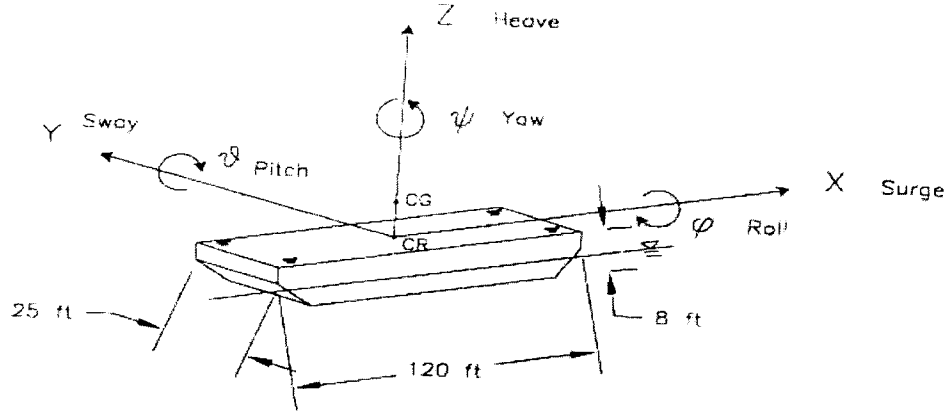

(a)

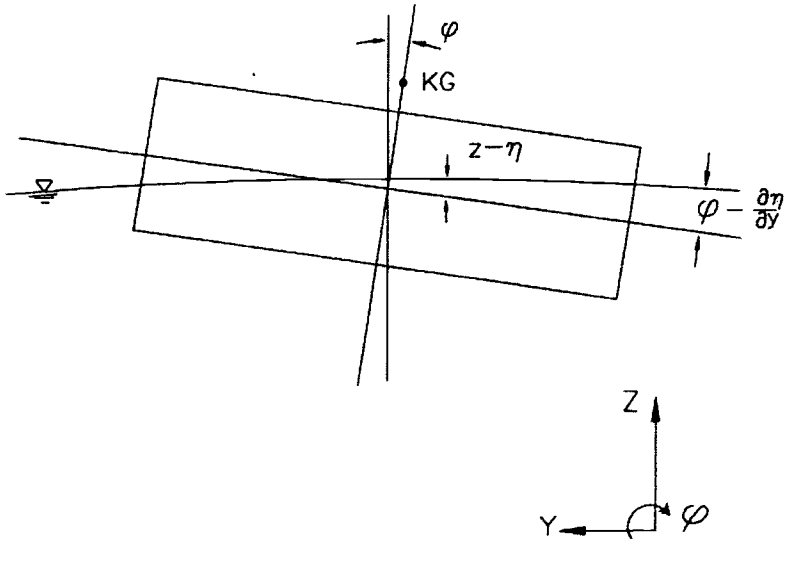

(b)

Figure 3.1 (a) Coordinate system definition and (b) Relative motion system of barge considered.

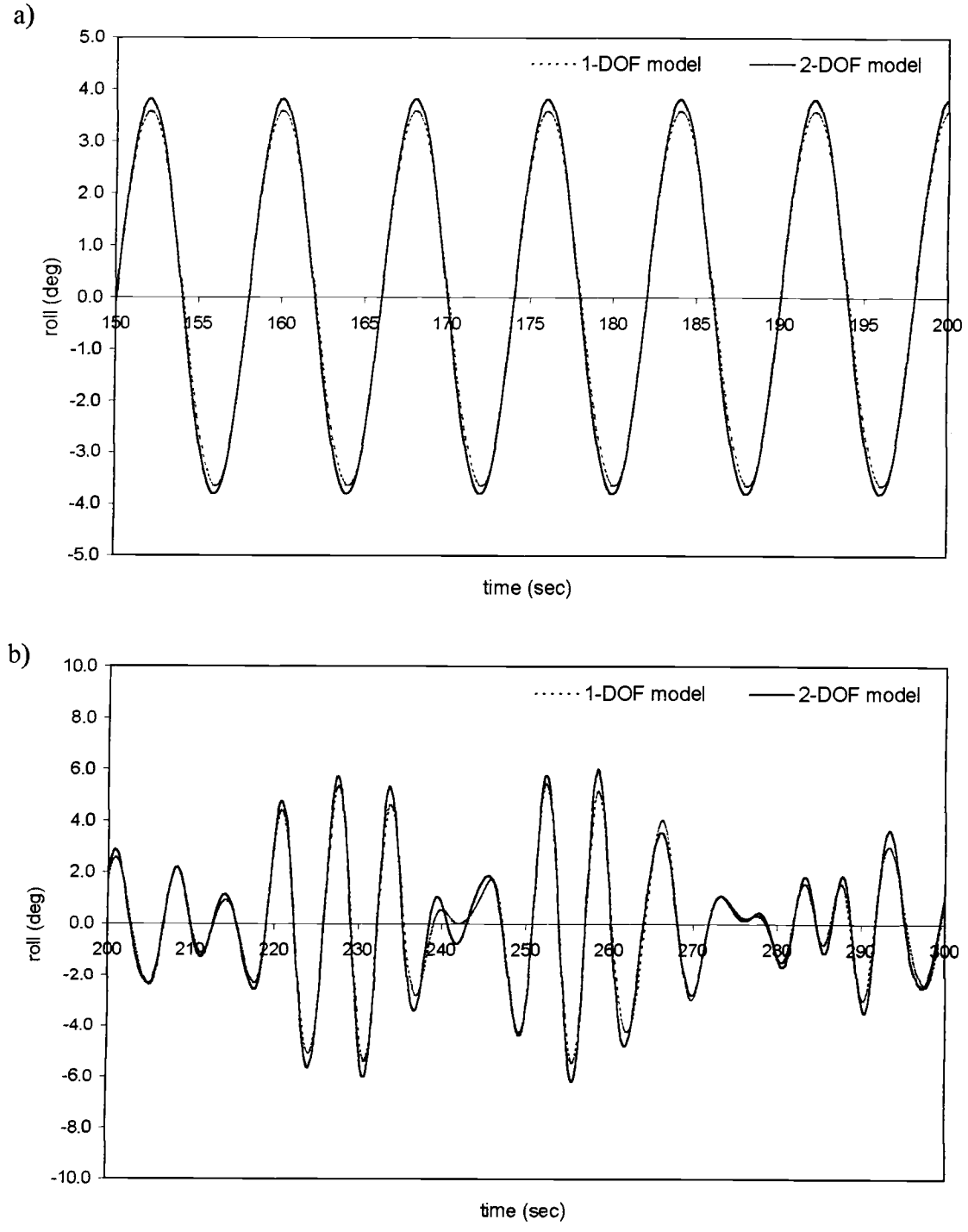

Figure 3.2 Comparison of barge roll response time histories predicted by 2DOF and 1DOF models under (a) regular waves with H = 6 ft and T = 8 seconds, and (b) random waves with H_s = 4.7 ft and T_p = 8.2 seconds.

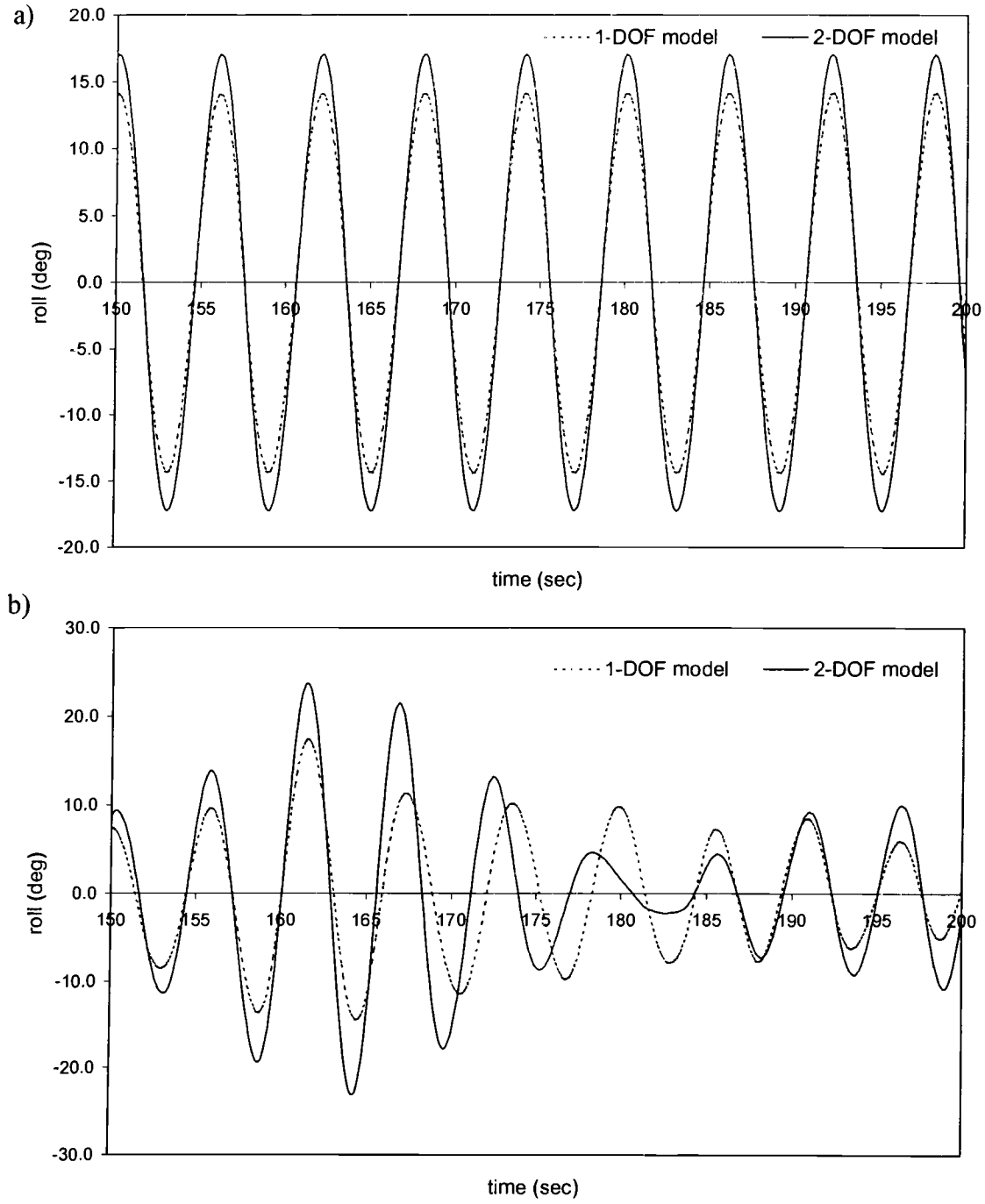

Figure 3.3 Comparison of barge roll response time histories predicted by 2DOF and 1DOF models under (a) regular waves with H = 6.5 ft and T = 6 seconds, and (b) random waves with H_s = 5.5 ft and T_p = 6.0 seconds.

a)

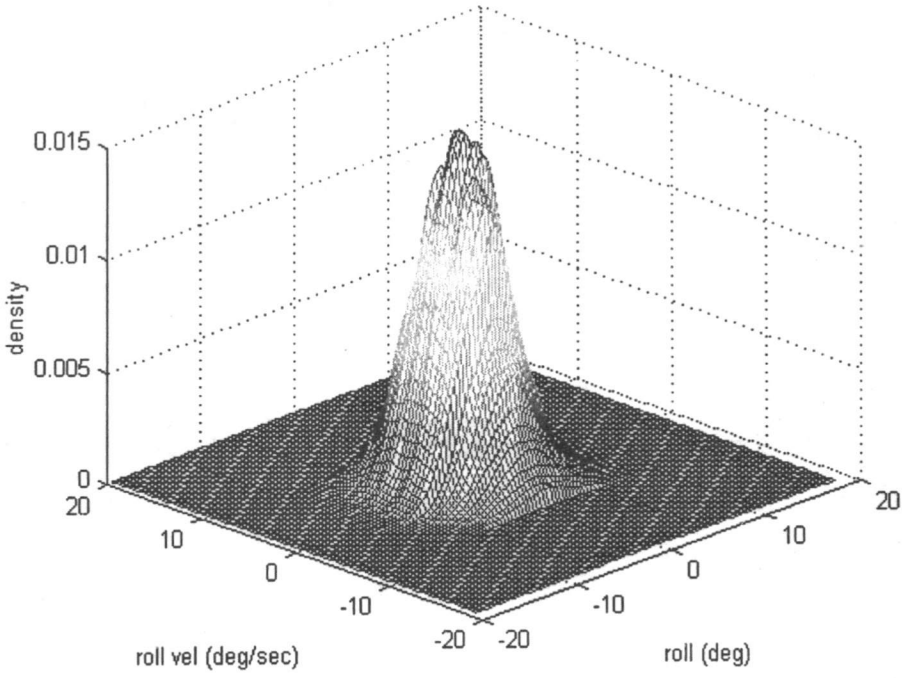

b)

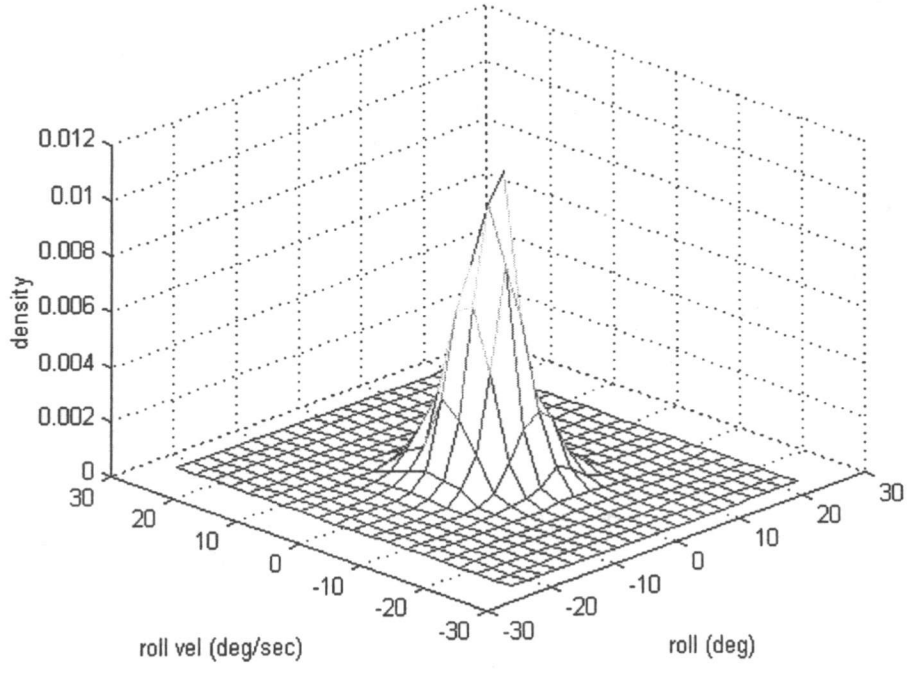

Figure 3.4 (a) 1DOF model, and (b) 2DOF model path integral solution prediction of probability density of roll response under random waves with $H_s = 4.7$ ft and $T_p = 8.2$ seconds at time t = 5 minutes.

a)

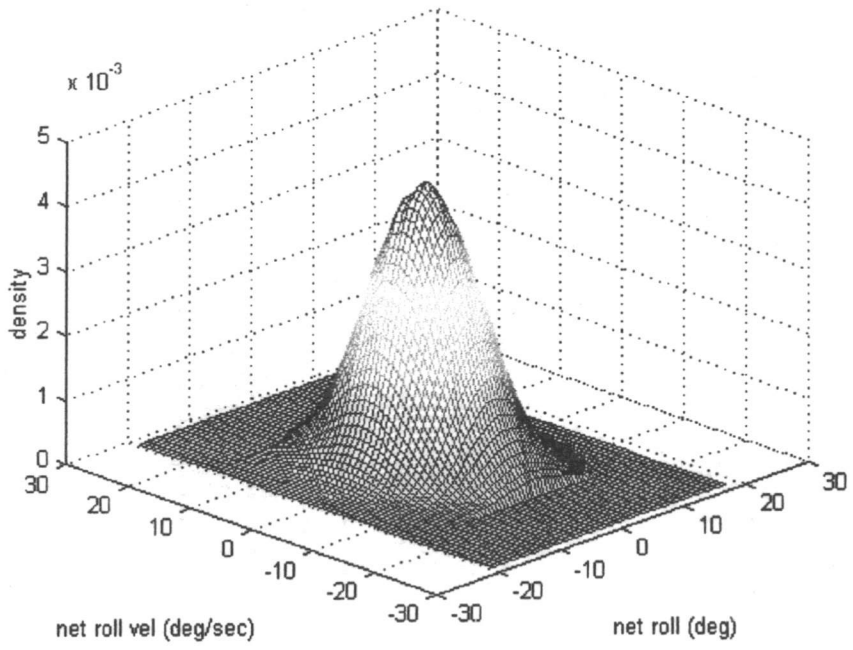

b)

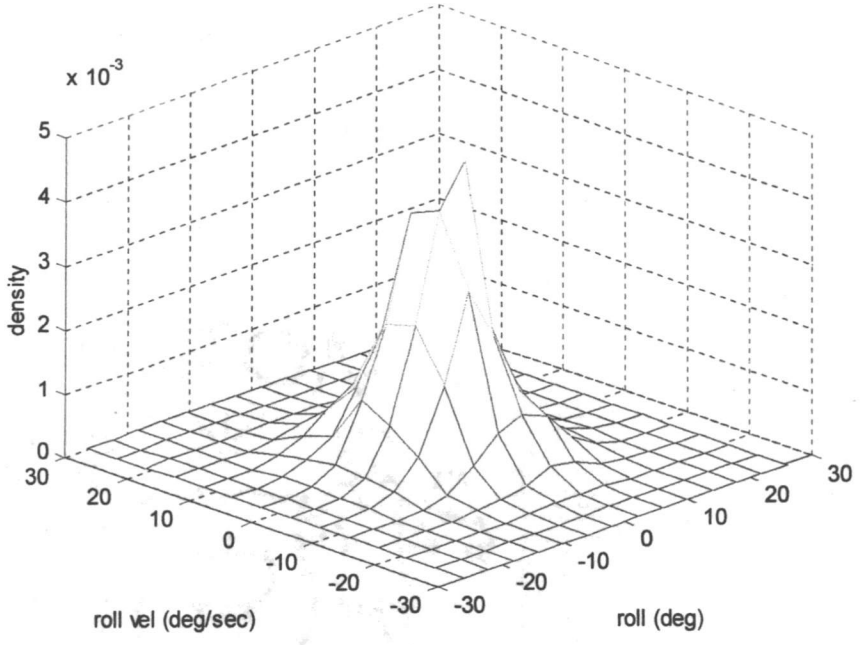

Figure 3.5 (a) 1DOF model, and (b) 2DOF model path integral solution prediction of probability density of roll response under random waves with H_s = 5.5 ft and T_p = 5.5 seconds at time t = 5 minutes.

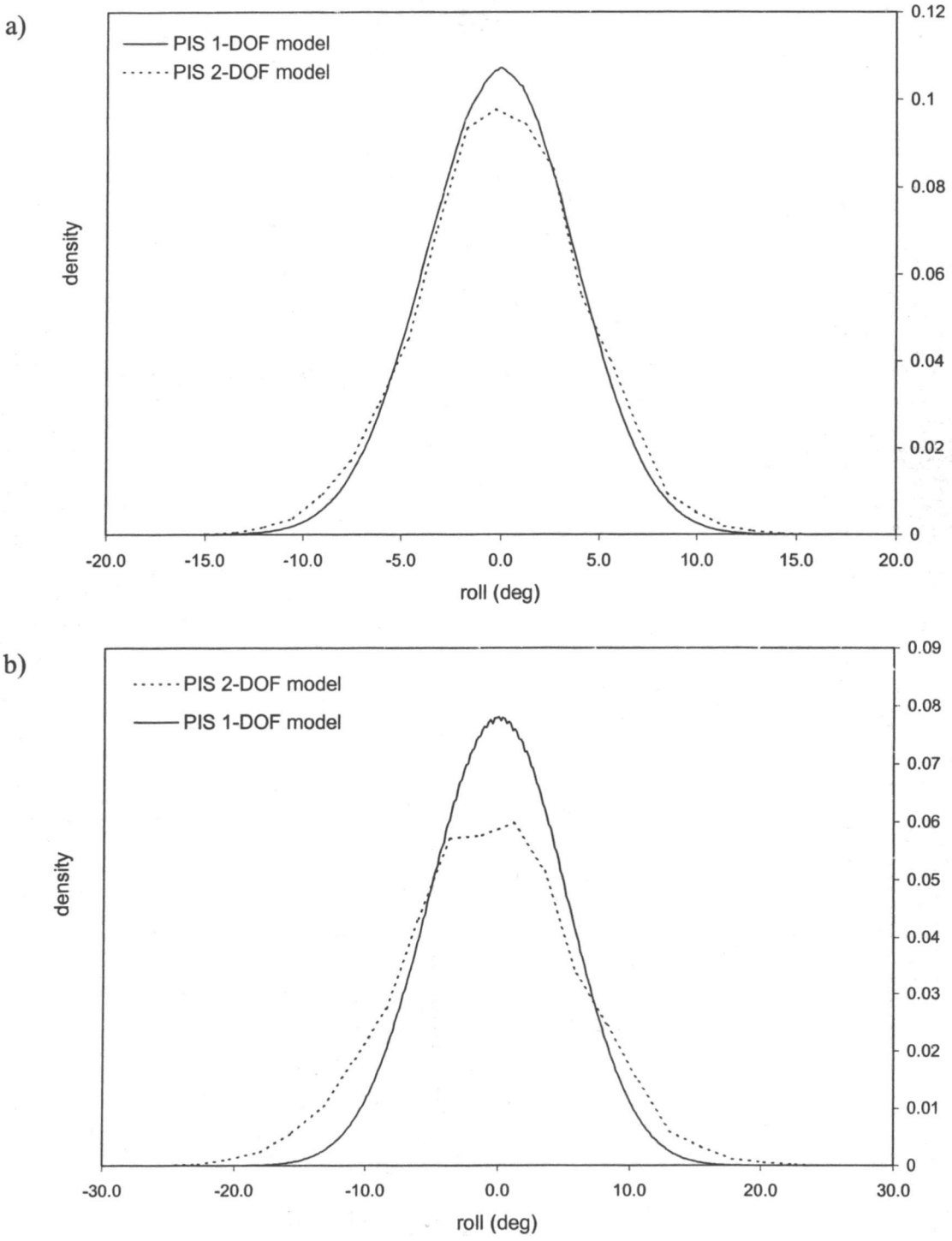

Figure 3.6 Comparison of roll response marginal probability density between numerical predictions of 2DOF and 1DOF models at time t = 5 minutes under random wave with (a) H_s = 4.7 ft and T_p = 8.2 seconds, and (b) H_s = 5.5 ft and T_p = 5.5 seconds.

3.7 QUASI-2DOF MODEL

Time histories of barge heave responses to regular and random waves based on experimental results are shown in Figure 3.7. It is observed that the relative motions between heave and wave elevation are small. A quasi-2DOF model is developed here with the assumption that relative motion between heave and wave is insignificant, in fact, the heave motion can be approximated by the wave elevation. Thus, the hydrostatic roll restoring moment is not affected by heave. The coupling effects of heave and roll are presented via the inertia moment caused by eccentricity of roll center and KG.

The quasi-2DOF model is developed by adding an additional term to the equation of motion of the 1DOF model that represents heave-induced inertia moment due to eccentricity of roll center and KG. Heave velocity is approximated by the vertical wave velocity. The resulting equation of motion of the quasi-2DOF model is

$$I_{44}\ddot{\phi} + I_{a_{44}}(\ddot{\phi} - \frac{\partial \ddot{\eta}}{\partial y}) + C_{44_L}(\dot{\phi} - \frac{\partial \dot{\eta}}{\partial y}) + C_{44_N}(\dot{\phi} - \frac{\partial \dot{\eta}}{\partial y})\left|\dot{\phi} - \frac{\partial \dot{\eta}}{\partial y}\right| + m(z_g \cos\phi)\dot{\phi} w \quad (3.26)$$

$$+ R_{44}(\phi, z, \eta, \frac{\partial \eta}{\partial y}) - mgz_g \sin\phi \quad = \quad 0$$

The advantage of the quasi-2DOF model is that it retains a majority of the coupling effects of heave effect on roll motion while keeping the DOF of the model at unity. While the path integral solution of the FPE for the 2DOF model requires a much greater computational effort than that of the corresponding 1DOF model, the

a)

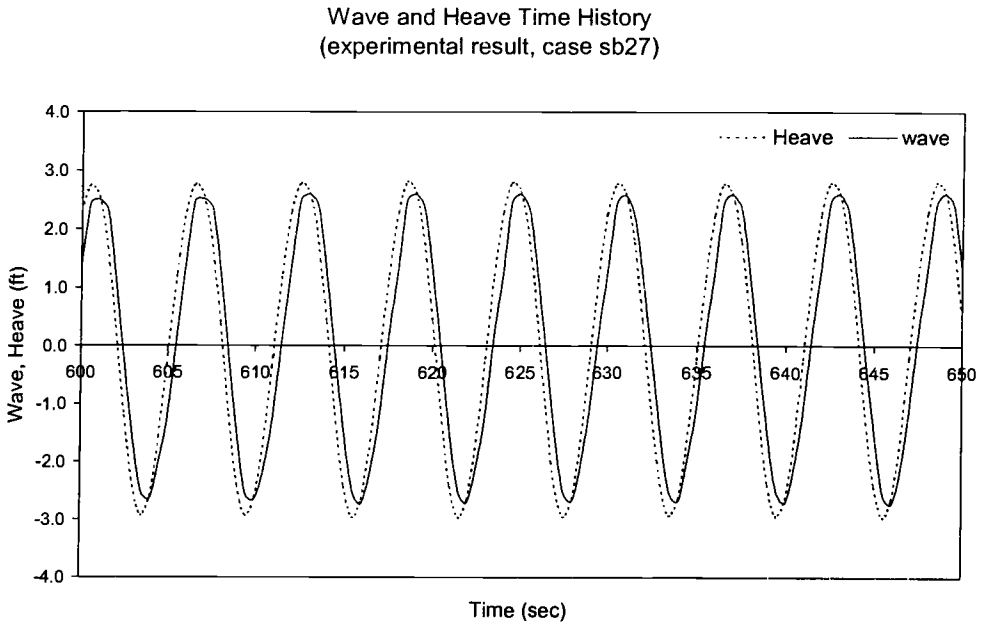

b)

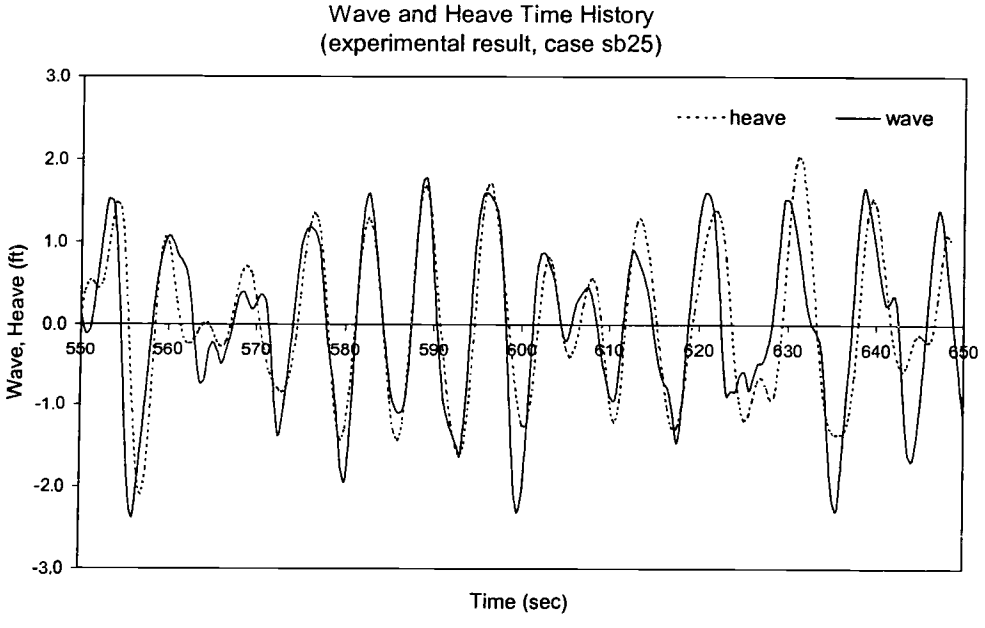

Figure 3.7 Comparison of measured experimental heave and wave time histories under (a) regular wave with H = 6 ft and T = 6 seconds, and (b) random wave with H_s = 4.7 ft and T_p = 8.2 seconds.

quasi-2DOF model solution takes the same order of computation effort as that of the 1DOF. Time domain and probability domain simulations of the quasi-2DOF model using regular and random waves as excitation are conducted to examine the accuracy of the simplified model. Results indicate a significant improvement of the quasi-2DOF model over the 1DOF model when compared with results from the 2DOF model as shown in Figure 3.8 and 3.9.

3.8 Reliability against Capsizing

Reliability of the roll motion of a barge in a variety sea conditions is analyzed here as a first passage time problem. As the barge rolls in random seas, the net roll response density propagates with time and eventually exits the safe domain. Here, net roll is defined as the difference between roll angle and wave slope. Hydrostatic roll restoring moment indicates a zero value once net roll exceeds 58 degrees for the ship-to-shore cargo barge as shown in Figure 3.10. Reliability against capsizing of the barge is defined as the cumulative net roll response density, which lies within the safe domain. At a given time t, reliability is

$$Wo(t) = \int_{\tilde{\phi}=-58}^{\tilde{\phi}=58} P(\tilde{\phi}, \dot{\tilde{\phi}}) d\tilde{\phi} \tag{3.27}$$

The path integral solution of the FPE of the quasi-2DOF model provides the evolution of the net roll response density. Considering the evolution of the roll

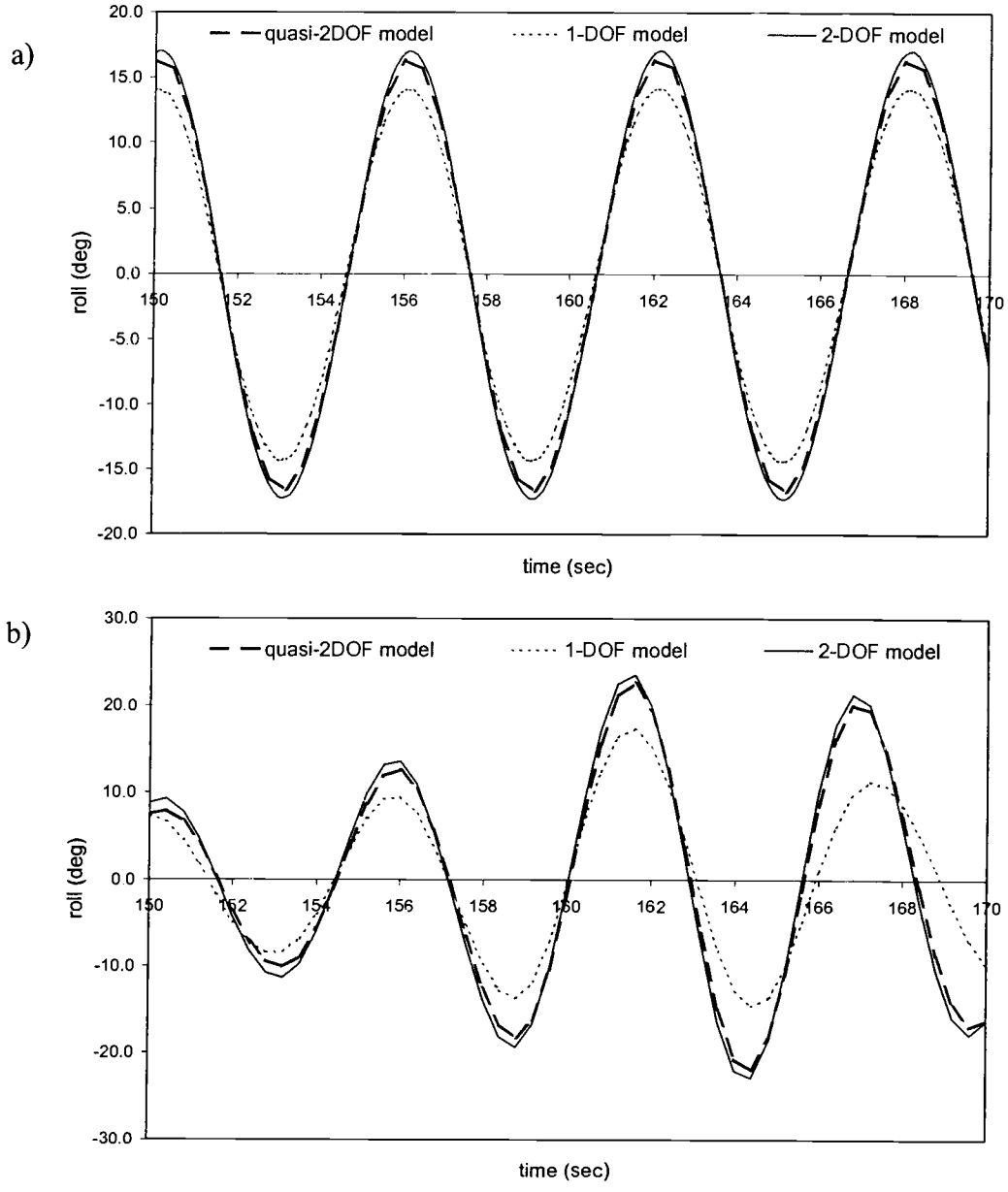

Figure 3.8 Comparison of predicted barge roll response time histories predicted by 2DOF, 1DOF, and quasi-2DOF models, (a) regular waves with H = 6.5 ft and T = 6 seconds, and (b) random waves with H_s = 5.5 ft and T_p = 6.0 seconds.

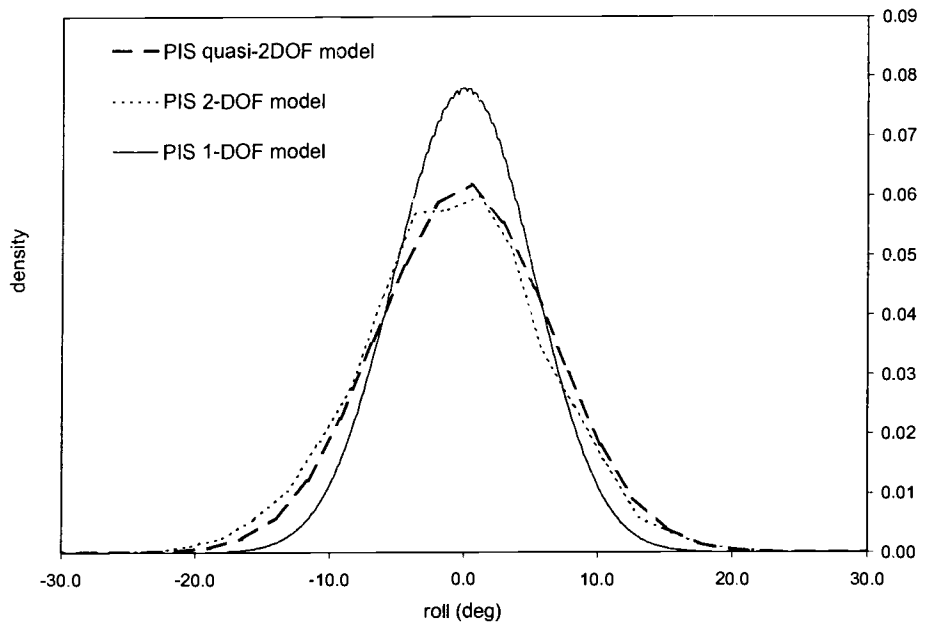

Figure 3.9 Comparison of roll response marginal density at 5 minutes predicted by 2DOF, 1 DOF, and quasi-2DOF models under random wave excitation with $H_s = 5.5$ ft and $T_p = 5.5$ second.

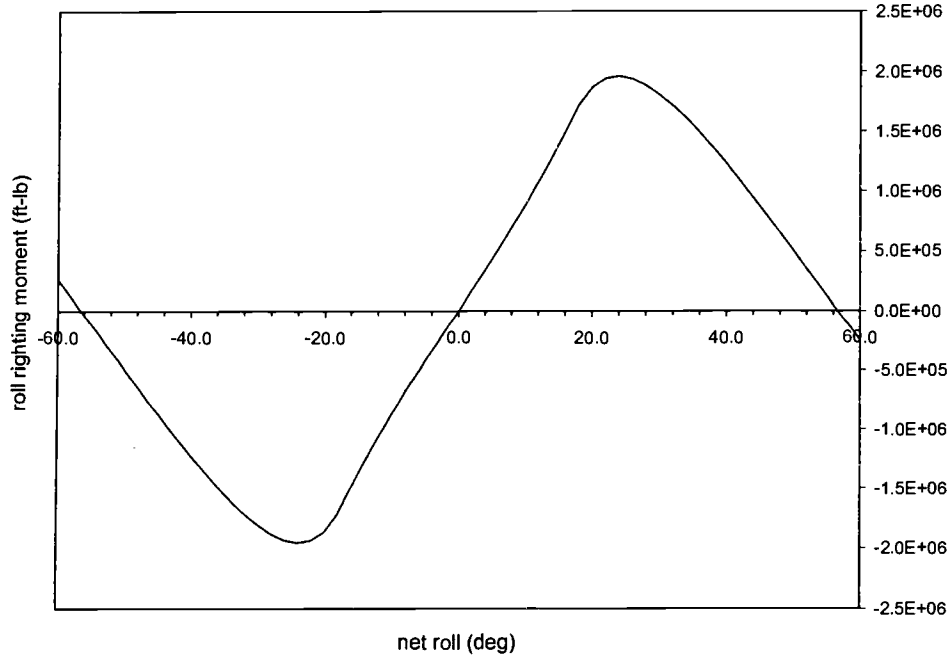

Figure 3.10 Analytical roll righting moment of barge considered.

response density, the reliability of the barge at a specified exposure time is the probability mass of net roll response density in the prescribed safe domain. Sea states 1 through 9 are represented by their average significant wave height, H_s, and spectral peak periods, T_p, as shown in Table 3.3. Excitations according to each sea state are applied to the quasi-2DOF stochastic model. The evolution of the net roll response density and reliability for sea states 1 through 9 are shown in Figures 3.11 through 3.19. The numerical results indicate no likelihood of capsizing for barges operating under sea states 1 and 2 in 10 hours of exposure time. It takes approximately 1 to 3 hours for barges operating in sea state 3 through 6 to attain 1% probability of capsizing. Barges exposed to sea state 7 and more severe sea states have a significantly larger probability of capsizing in a short period of time. This information is presented in a more succinct manner (time to reach 1, 2, 5 and 10 percent probability of capsizing for barge operation in sea state 3 through 9) in Figure 3.20.

a)

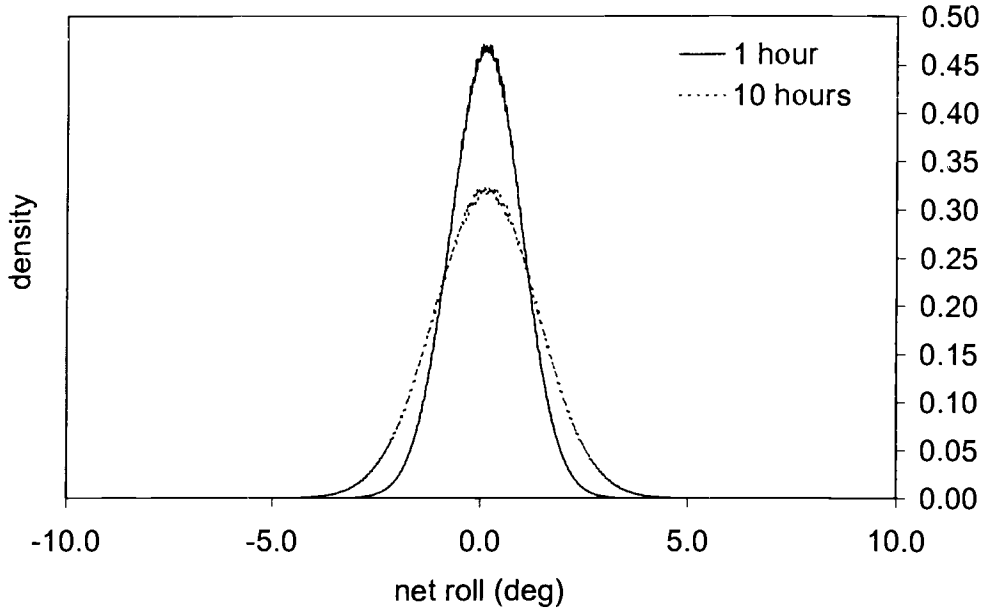

b)

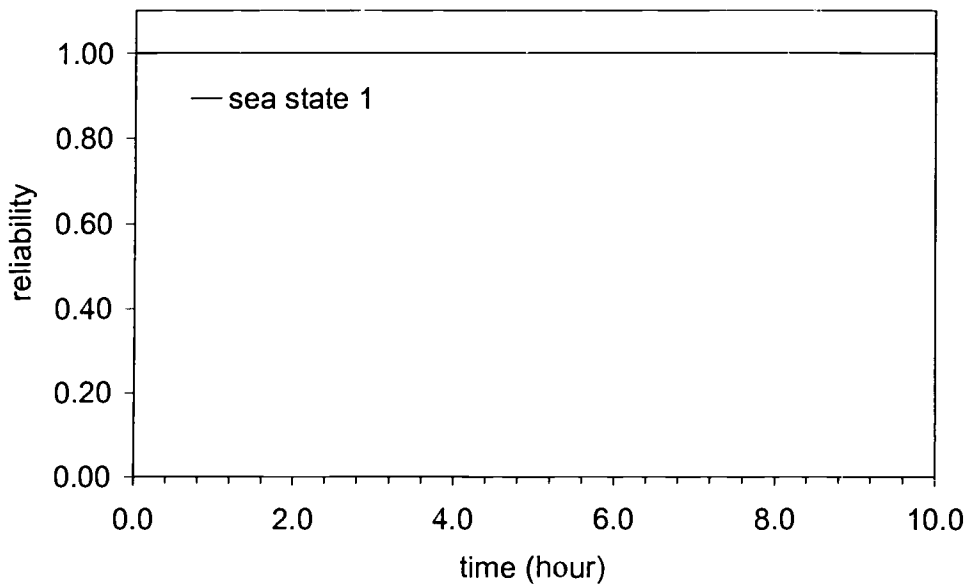

Figure 3.11 (a) Probability density, and (b) reliability against capsizing of barge roll response to sea state 1 random waves.

a)

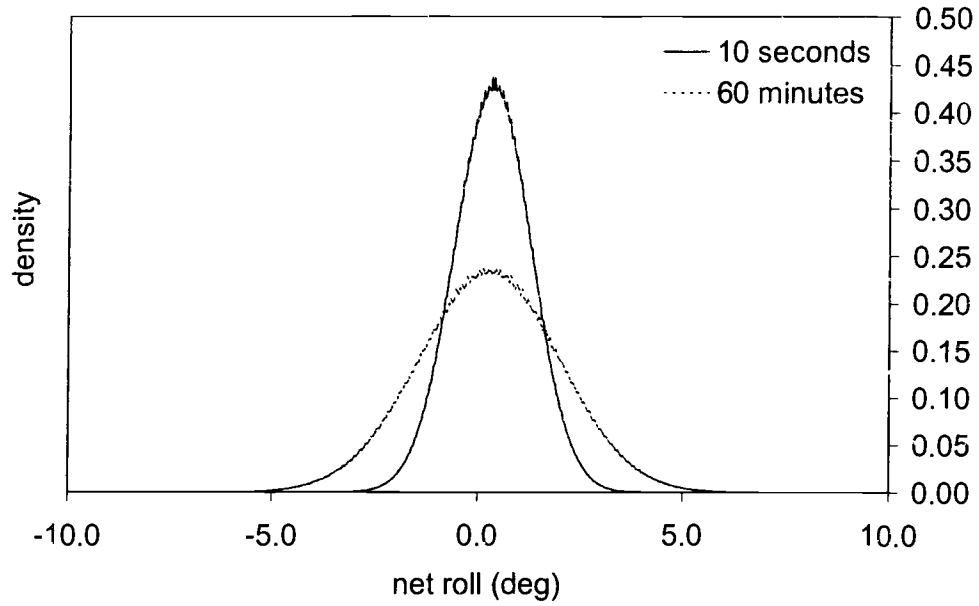

b)

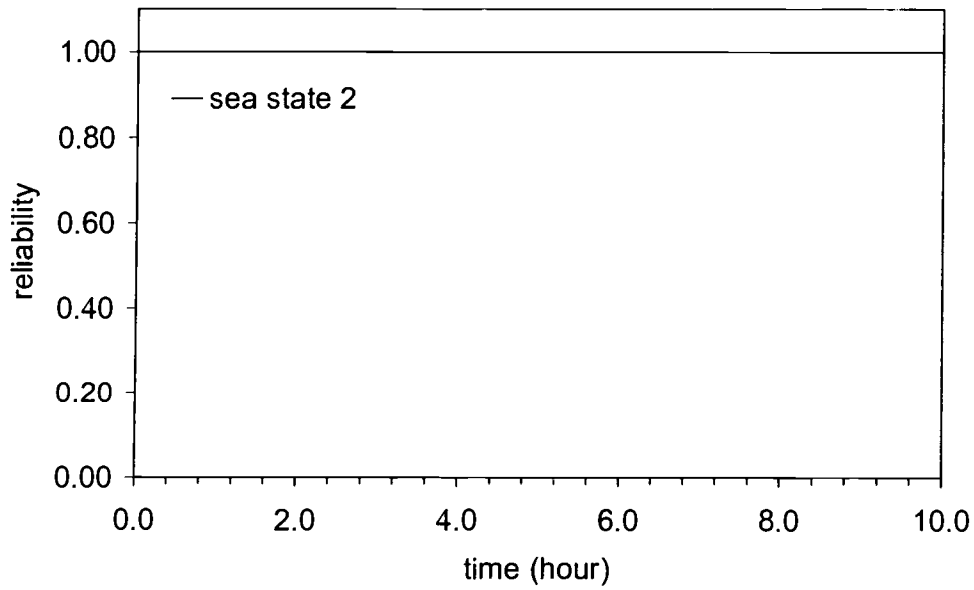

Figure 3.12 (a) Probability density, and (b) reliability against capsizing of barge roll response to sea state 2 random waves.

a)

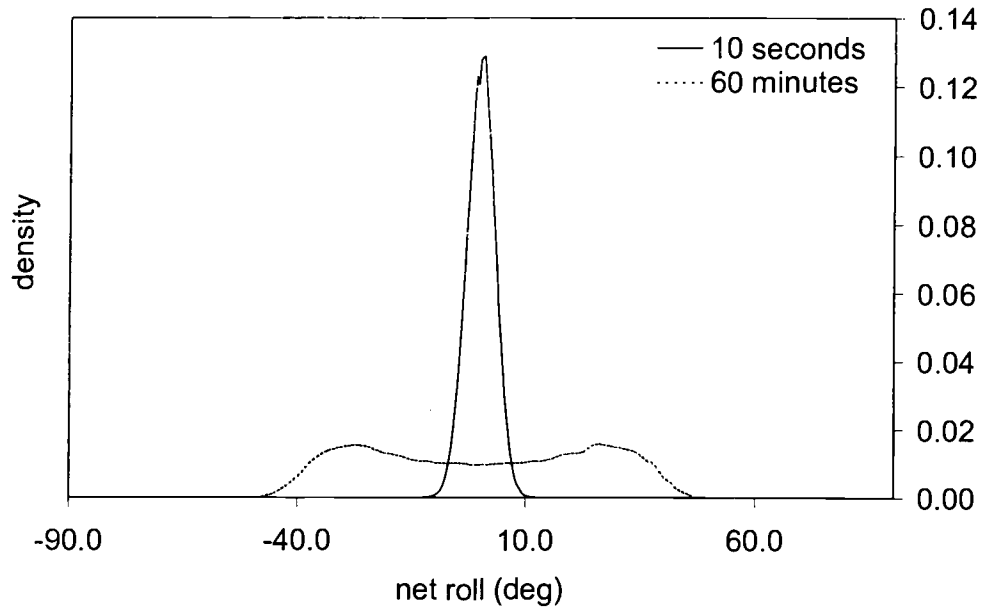

b)

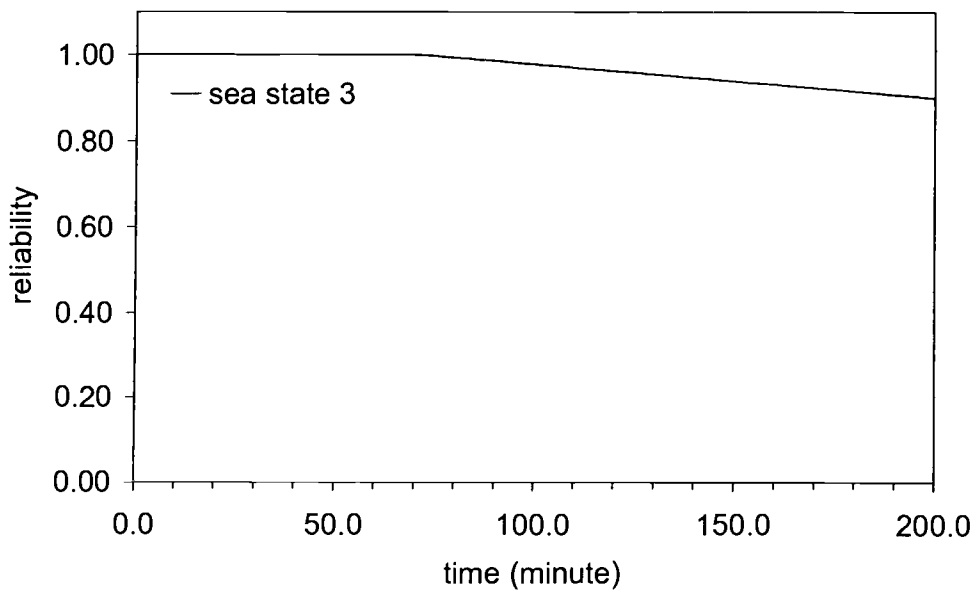

Figure 3.13 (a) Probability density, and (b) reliability against capsizing of barge roll response to sea state 3 random waves.

a)

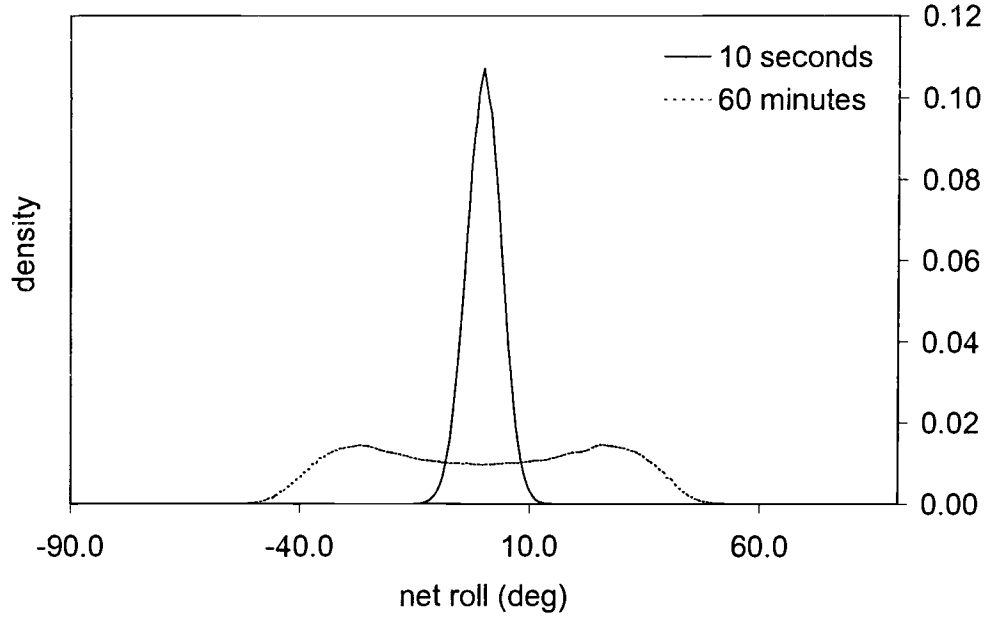

b)

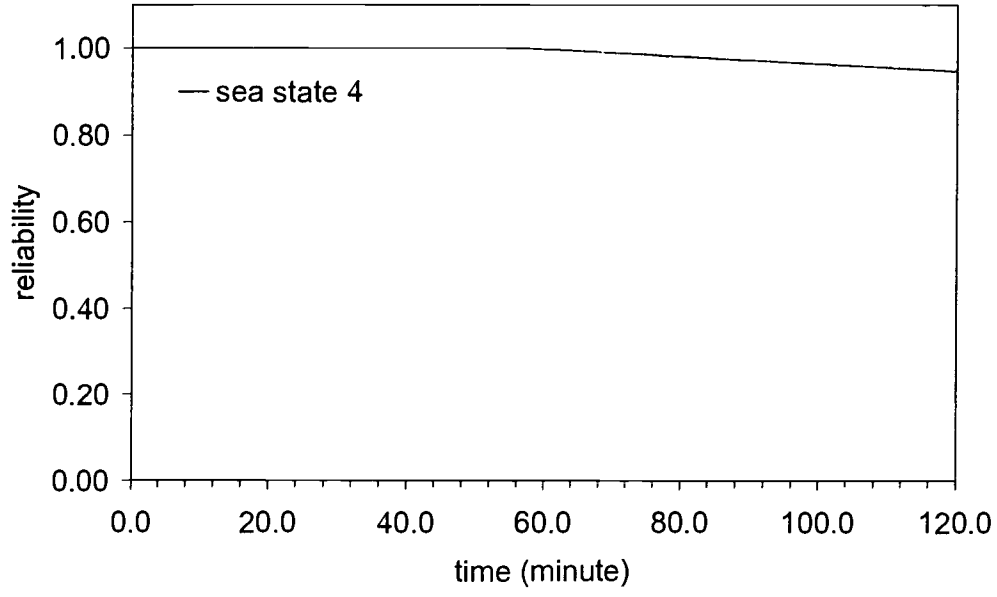

Figure 3.14 (a) Probability density, and (b) reliability against capsizing of barge roll response to sea state 4 random waves.

a)

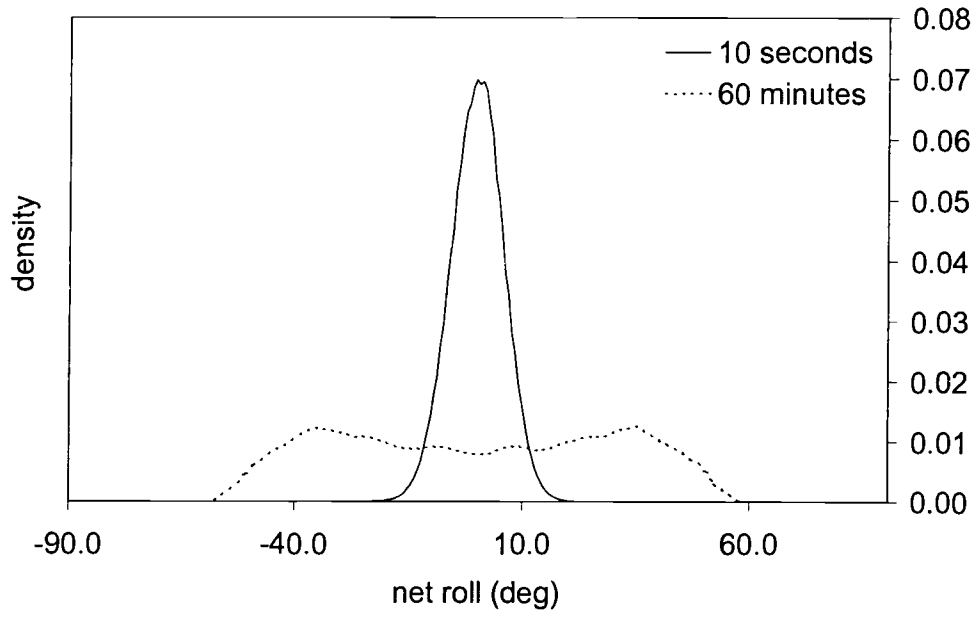

b)

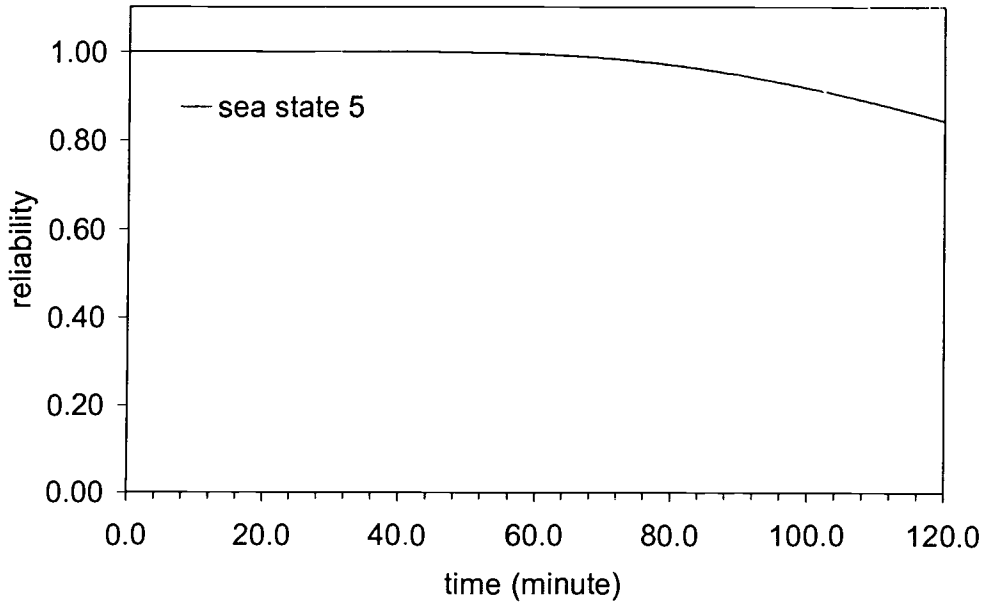

Figure 3.15 (a) Probability density, and (b) reliability against capsizing of barge roll response to sea state 5 random waves.

a)

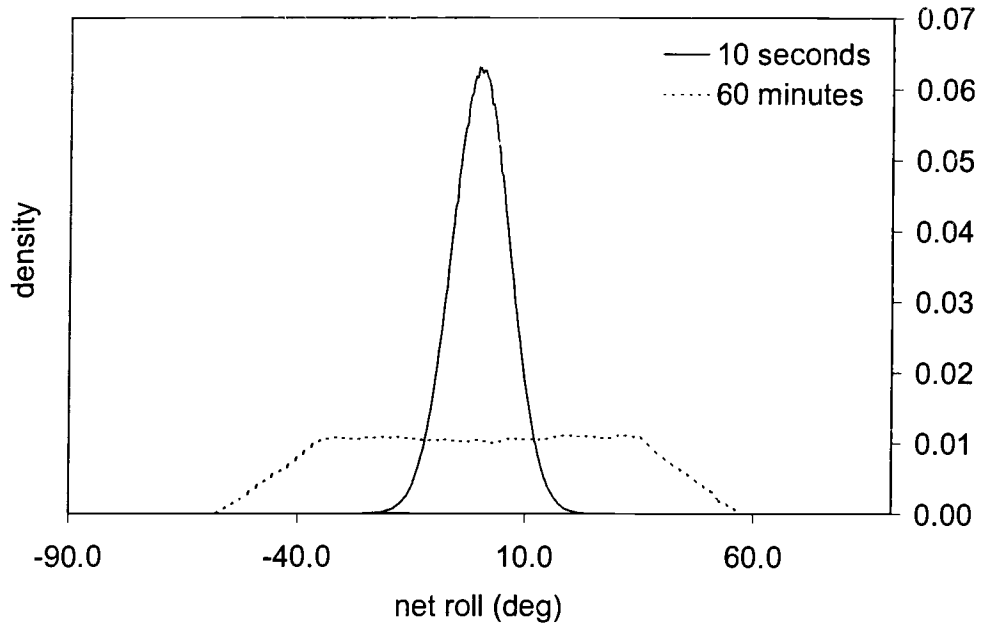

b)

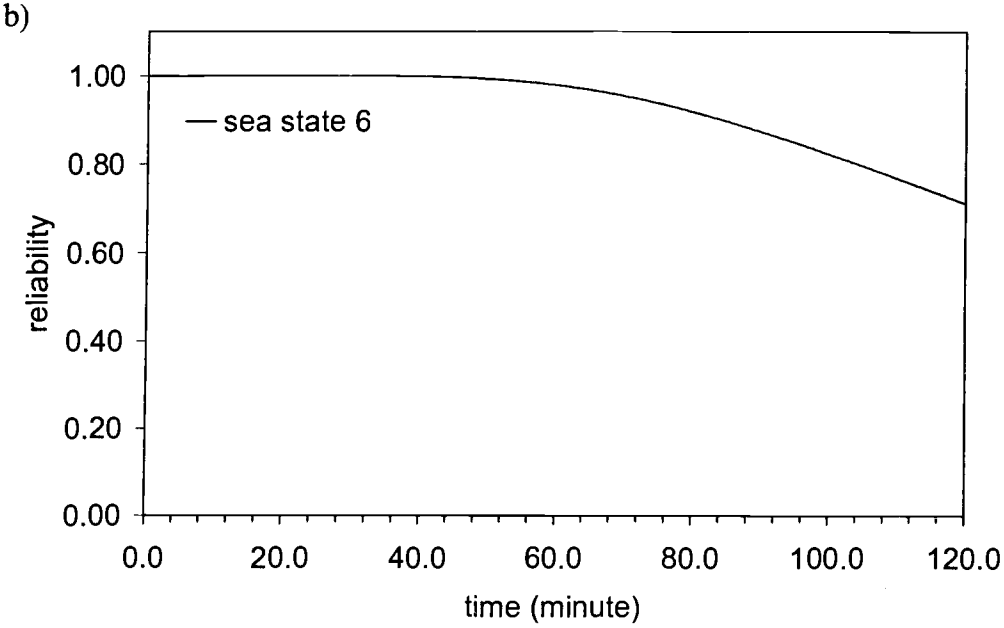

Figure 3.16 (a) Probability density, and (b) reliability against capsizing of barge roll response to sea state 6 random waves.

a)

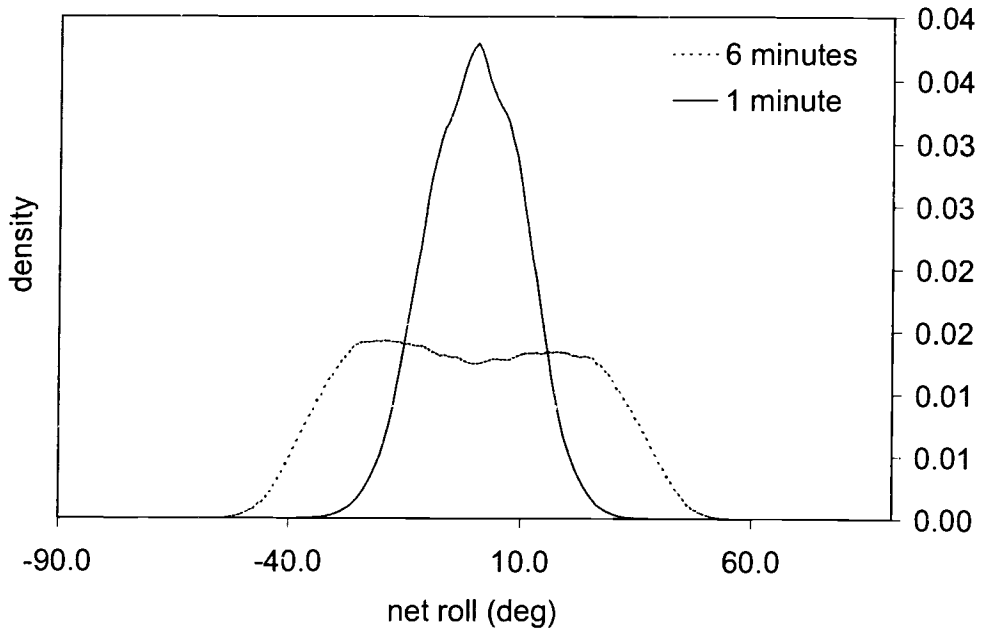

b)

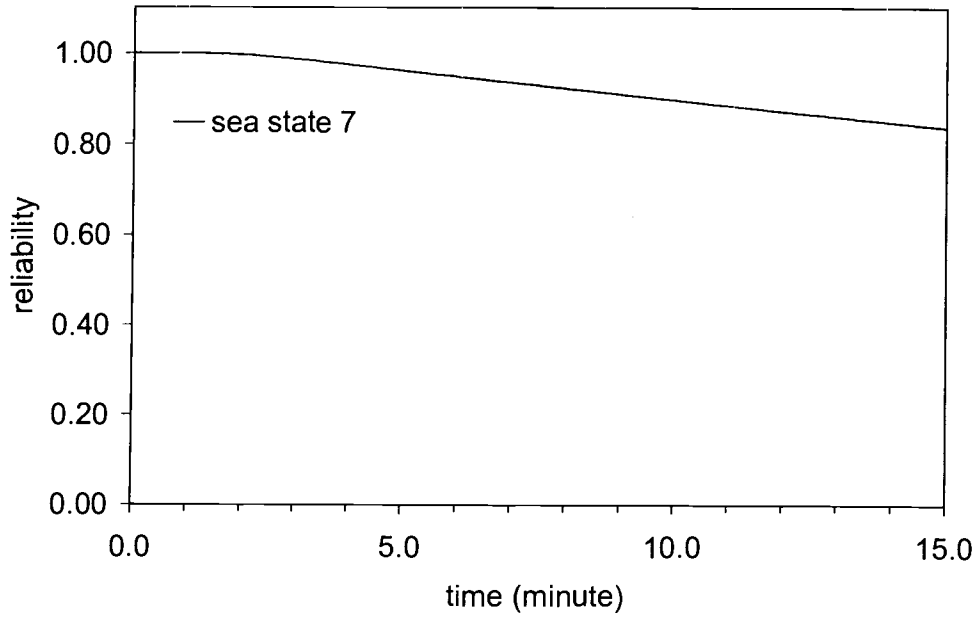

Figure 3.17 (a) Probability density, and (b) reliability against capsizing of barge roll response to sea state 7 random waves.

a)

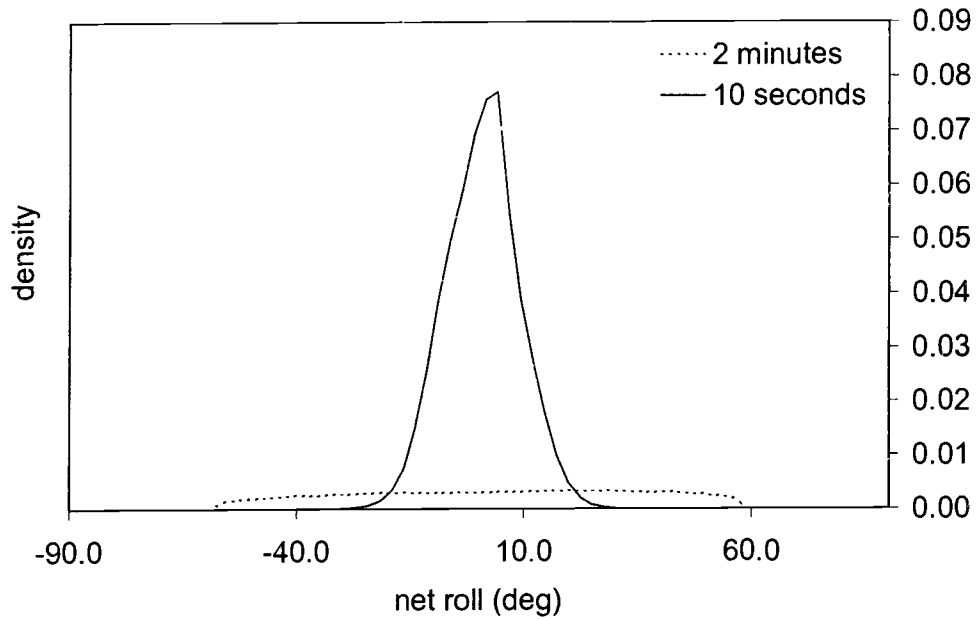

b)

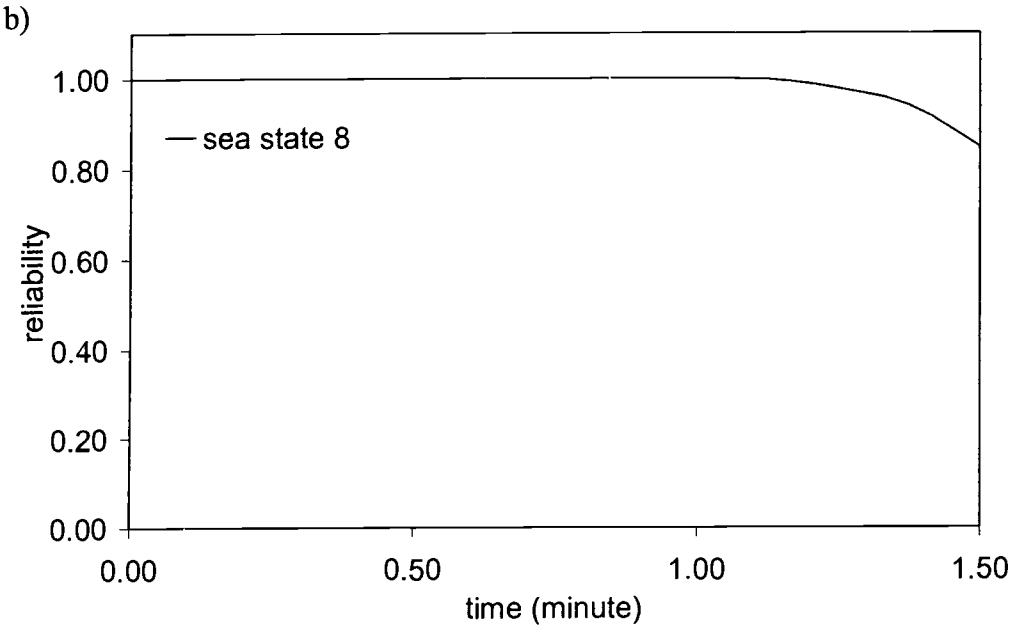

Figure 3.18 (a) Probability density, and (b) reliability against capsizing of barge roll response to sea state 8 random waves.

a)

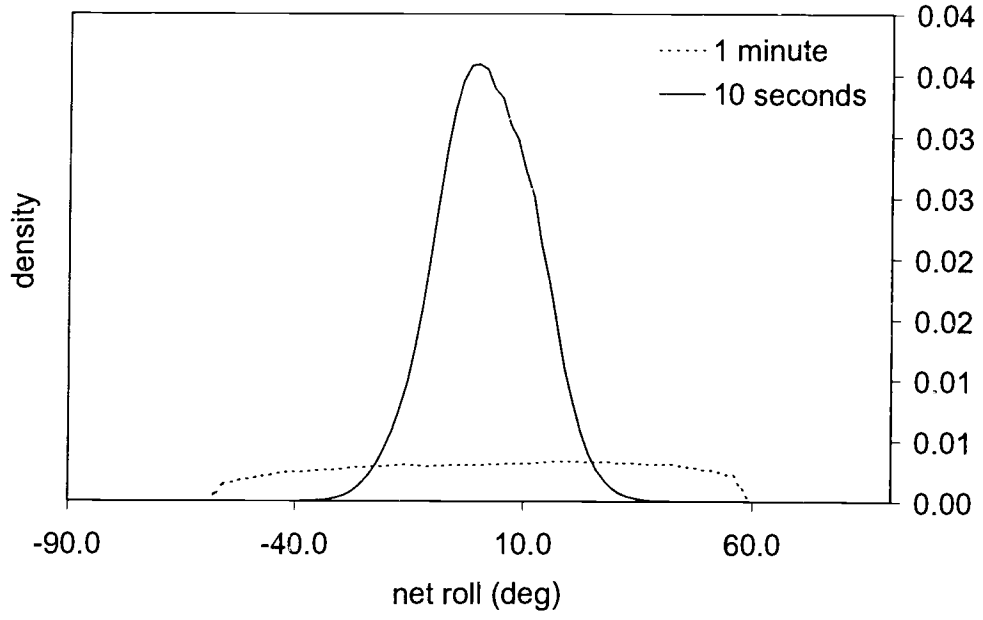

b)

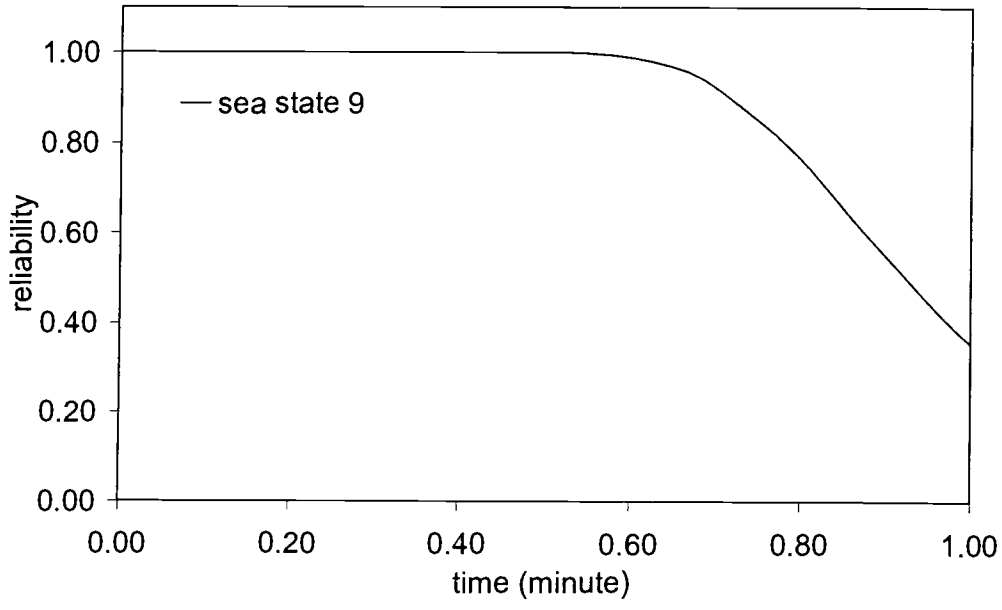

Figure 3.19 (a) Probability density, and (b) reliability against capsizing of barge roll response to sea state 9 random waves.

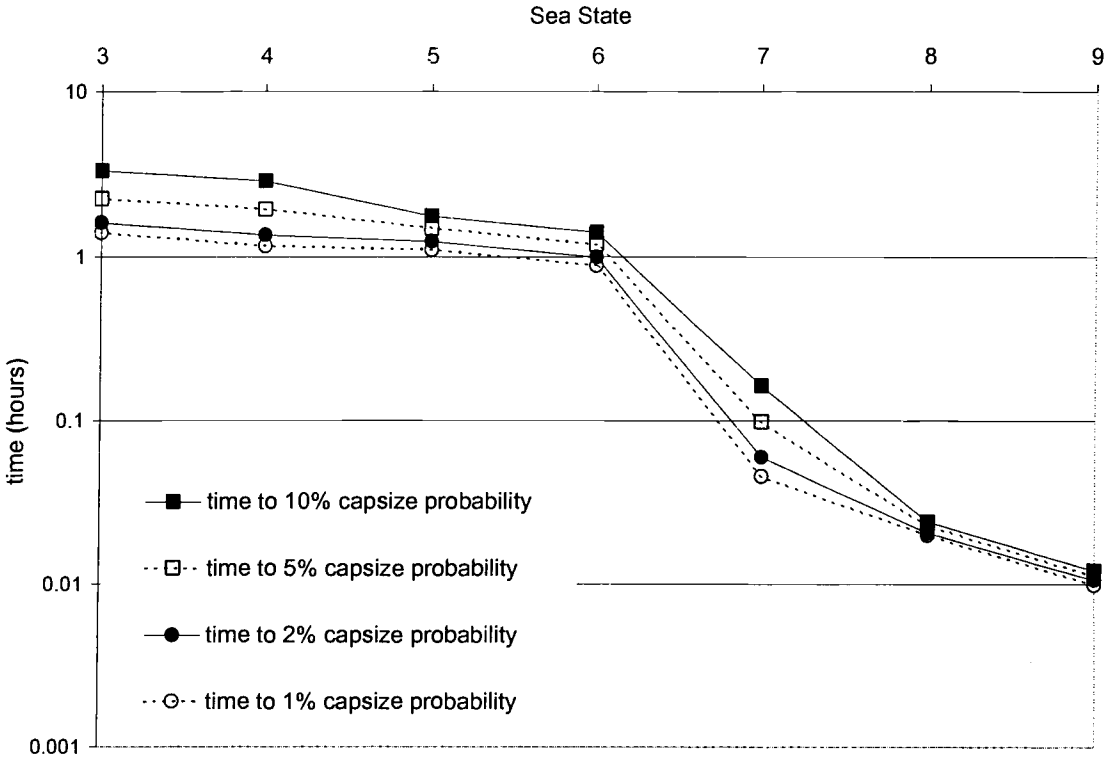

Figure 3.20 Mean time to reach specified capsizing probabilities for a barge operating in sea states 3 through 9 obtained using quasi-2DOF model.

Table 3 .3 Average significant wave height and spectral peak period of sea states 1 through 9

Sea State	Significant wave height H_s (ft)	Spectral peak period T_p (second)
1	0.5	2.4
2	2.0	4.6
3	4.0	6.0
4	6.5	7.5
5	10.0	8.9
6	16.0	10.8
7	30.0	13.6
8	50.0	17.0
9	100.0	22.4

3.9 Conclusions

Stochastic analysis of Roll-Heave (2DOF) and Roll (1DOF) barge motion models is presented here. With the Markov process assumption, the path integral solution is used to obtain barge response probability densities by numerically solving the associated Fokker-Planck equation.

Coupling effects of the heave and roll motions are investigated by comparing barge responses derived from the Roll-Heave and the Roll models. Time and probability domain simulations are employed. With identical excitation, results show that the 2DOF model predicts slightly larger amplitude roll motion than the 1DOF model. The difference becomes more significant when roll motion is large. The governing equations of motion indicate that heave affects roll motion via the hydrostatic roll restoring moment and the initiating inertia moment due to the eccentricity of roll center and KG. Experimental results show that, for the barges

examined, the relative motion between heave and wave elevation is small. Thus, the heave impact on the hydrostatic righting moment is negligible.

A quasi-2DOF model is developed by adding a term that represents the coupling effects of heave on roll motion to the 1DOF model. Heave velocity is approximated by vertical wave velocity to approximate inertia moment caused by heave velocity and the eccentricity of roll center and KG. Time domain and probability domain simulations indicate that the quasi-2DOF model retain the predictive capability of the 2DOF model.

Reliability against capsizing of a barge under various sea conditions is analyzed as a first passage time problem. The quasi-2DOF model is employed to simulate the barge roll motion. The response density evolution is obtained via the path integral solution to the associated Fokker-Planck equation. Random excitations according to each of sea state, 1 through 9, are applied to the stochastic model. Reliability against overturning of a barge (defined as the probability mass that lies within the safe domain at a given time) is examined. Exposure times that create overturning probability of 1, 2, 5 and 10 percent are recorded. Results indicate that the reliability of barge is significantly reduced when operating in sea state 7 or higher sea state conditions. It takes approximately 1 to 5 hours for a barge operating in sea state 3 through 6 to have 1 to 10 percent overturning probability. Barges operating in sea state 1 and 2 are often safe, as its capsizing probability is significantly less than 1 percent after 10 hours of exposure time.

References

Abkowitz, M.A. 1969. Stability and Motion Control of Ocean Vehicles. MIT Press, Cambridge, MA.

Bartel, W.A. 1996. *Modelling, Validation and Simulation of Multi-Degree-of Freedom Nonlinear stochastic barge Motions.* A Thesis submitted to Oregon State University.

Cai, G.Q., Yu, S.J. and Lin, Y.K. 1994. Ship Rolling in Random Sea. *Stochastic Dyanamics and Reliability of Nonlinear Ocean Systems*, ASME DE-Vol. 77: 81-88.

Chakrabarti,S.K. 1994. Hydrodynamics of Offshore Structures, *Computational Mechanics* Publications, Southampton Boston.

Dahle, E. AA., Myhaug, D. and Dahl, S.J. 1988. Probability of Capsizing in Steep and High Waves from the Side in Open Sea and Coastal Waters. *Ocean Engineering*, 15:2:139-151.

Donescu, P. and Virgin, L.N. 1993. Nonlinear Coupled Heave and Roll Oscillations of a Ship in Beam Seas, *Nonlinear Dynamics of Marine Vehicles*, ASME, 51: 21-28.

Dunne, J.F. and Ghanbari, M. 1997. Extreme-Value Prediction for Non-Linear Stochastic Oscillators via Numerical Solution of the FPK Equation. *Journal of Sound and Vibration*, 206:5:697-724.

Falzarano, J.M., Shaw, S.W., and Troesch, A.W. 1992. Application of Global methods for Analyzing Dynamical Systems to Ship Rolling Motion and Capsizing. *International Journal of Bifurcation and Chaos in Applied Sciences and Engineering*, 2:1:101-116.

Kwon, S.H., Kim, D.W. and McGregor, R.C. 1993. A Stochastic Roll Response Analysis of Ships in Irregular Waves. *International Journal of Offshore and Polar Engineering*, 3:1:32-34.

Liaw, C.Y., Bishop, S.R. and Thompson, J.M.T. 1993. Heave-Excited Rolling Motion of a Rectangular Vessel in Head Seas. *International Journal of Offshore and Polar Engineering*, 3:1:26-31.

Liaw, C.Y. 1993. Dynamic Instability of a Parametrically Excited Ship Rolling Model. *Proc. of the Third International Offshore and Polar Engineering Conference*, Singapore.

Lin, H. and Yim, S.C.S. 1995a. Chaotic Roll Motion and Capsizing of Ships Under Periodic Excitation with Random Noise. *Applied Ocean Research*, 17:3:185-204.

Lin, H. and Yim, S.C.S. 1995b. Stochastic Analysis of a Nonlinear Ocean Structural System. Oregon State University Report No. OE-95-04.

Martin, J. P. 1994. Roll Stabilization of Small Ships. *Marine Technology*, 31:4:286-295.

Naess, A., and Johnsen, J.M., Statistics of Nonlinear Dynamic Systems by path integrations. *Nonlinear Stochastic Mechanics*: 401-409.

Naess, A. and Johnsen, J.M., 1993. Response Statistic of Nonlinear, Compliant Offshore Structures by the Path Integral Solution Method. *Probabilistic Engineering Mechanics*, 8:91-106.

Naess, A. 1995. Prediction of Extreme Response of Nonlinear Structures by Extended Stochastic Linearization. *Probabilistic Engineering Mechanics*, 10:153-160.

Nayfeh, A.H., and Mook, D.T. 1979. Nonlinear Oscillations. New York: John Wiley & son.

Newland, D.E. 1993. *An Introduction to Random Vibrations, Spectral & Wavelet Analysis*. Longman Scientific and Technical, Essex England.

Ochi, M.C. 1990. *Applied Probability & Stochastic Processes: in Engineering and Physical Sciences*. New York: John Wiley & son.

Paulling, J.R. 1961. The Transverse Stability of a Ship in a Longitudinal Seaway. *Journal of Ship Research*. March:37-49.

Press W.H., Flannery, B.P, Teukolsky, S.A. and Vetterling, W.T. 1986. *Numerical Recipes*, Cambridge University Press.

Roberts, J.B. 1982a. A Stochastic Theory for Nonlinear Ship Rolling in Irregular Seas. *Journal of Ship Research*, 26:4:229-245.

Roberts, J.B. 1982b. Effect of Parametric Excitation on Ship Rolling Motion in Random Waves. *Journal of Ship Research*, 26:4:246-253.

Robert, J.B.,Dunne J.F., and Debonos A. 1994. Stochastic Estimation Methods for Non-Linear Ship Roll Motion. *Probabilistic Engineering Mechanics* 9:83-93.

Thompson, J.M.T., Rainey, R.C.T. and Soliman, M.S. 1992. Mechanics of Ship Capsize Under Direct and Parametric Wave Excitation," *Phil. Trans. R. Soc. Lond, A*:338:471-490.

Thompson, J.M.T., and Stewart, H.B. 1986. *Nonlinear Dynamics and Chaos*. John Wiley & Sons.

Virgin, L.N. 1987. The Nonlinear Rolling Response of a Vessel including Chaotic Motions leading to Capsize in Regular Seas. *Applied Ocean Research*, 9:2:89-95.

Virgin, L.N. and Bishop, S.R. 1988. Catchment Regions of Multiple Dynamic Responses in Nonlinear Problems of Offshore Mechanics. *Proceedings at 7th International Conference on Offshore Mechanics and Arctic Engineering*, Houston, TX. 15-22.

Virgin, L.N. and Erickson, B.K. 1994. A New Approach to the Overturning Stability of Floating Structures. *Ocean Engineering*, 21:1:67-80.

Wehner, M.F., and Wolfer, W.G. 1983. Numerical Evaluation of Path-Integral Solutions to Fokker-Planck Equations, *Physical Review A*, 27:2663-2670.

Wissel, C. 1979. Manifolds of Equivalent Path Integral Solutions of the Fokker-Planck Equation. *Zeitschrift fur physiks B*, 35:185-191.

Yim, S.C.S., Bartel, W.A., Lin, H. and Huang, E. 1995. Nonlinear Roll Motion and Capsizing of Vessels in Random Seas. Naval Facilities Engineering Service Center, Port Hueneme, CA.

CHAPTER 4

General Conclusions

Summary

Barge motions in beam-sea condition are approximated by coupled three-degree-of-freedom (3DOF, Roll-Heave-Sway) model and lower order ones (2DOF, Roll-Heave and 1DOF, Roll). The models engage rigid body Roll-Heave-Sway relations, coupled nonlinear hydrostatic restoring force-moment and relative motion hydrodynamic force-moment. The hydrostatic force-moment includes effects of barge's sharp edge and effect of combined roll-heave states. The hydrodynamic terms are represented in a 'Morison' type quadratic form. The 3DOF model uses a linear spring in the sway direction to represent mooring cables present in the experiment.

Time domain simulations are employed to examine the predictive capability of the 3DOF and the 2DOF models. System parameters of the 3DOF and the 2DOF models are identified by matching numerical predictions with experimental results for several regular wave test cases. Initial estimates of the system parameters are obtained from potential flow theory. General characteristics of Roll-Heave-Sway barge motions are observed. Predicted barge motions under random waves are obtained from time domain solution of the 3DOF and the 2DOF models. Measured random waves and filtered white noise simulated random waves are applied to both

the 3DOF and 2DOF models. Their accuracy is confirmed by comparing numerical predictions with experimental results. Coupling effects of sway on roll and heave barge motions are examined and found to be negligible. Preliminary parametric studies of excitation for both the 3DOF and the 2DOF models are conducted. A wide range of regular wave heights and wave periods is applied to both models to examine complex nonlinear behaviors.

Stochastic analyses of barge response are conducted using the Markov process approach. The corresponding Fokker-Plank equations of the 2DOF and the 1DOF models are derived based on the Markov assumption. The equations are semi-analytically solved using the path integral solution procedure. Random waves based on the Bretschneider spectrum with specified significant wave height and spectral peak wave period are used to obtain barge response densities for specific exposure times. Resulting probability densities of roll motions based on the 2DOF and 1DOF models are compared. The corresponding time domain analyses are employed to examine heave effects on roll motion.

A quasi-2DOF model is developed by including an additional term to approximate the heave-induced inertia moment. This model retains the characteristic of Roll-Heave motion but can be numerically analyzed as a 1DOF model. Reliability against overturning of a barge under a variety of sea conditions is examined using numerical results based on stochastic analyses of the simplified model. The net roll response densities with various random wave excitations are obtained. The evolutions of net roll response densities are considered. The response

behavior is analyzed as a first passage time problem. The reliability of the response motion is defined as the probability mass the lies within the safe domain at a given time. Time to reach a certain level of capsizing probability is determined. Reliabilities of the barge in sea states 1 through 9 are examined. Stochastic analyses of the 2DOF barge motion model are also employed to calibrate the accuracy of the quasi-2DOF model.

Concluding Remarks

The study of barge motion in beam-sea condition via multi-degree-of-freedom barge motion models results in the following conclusions:

1) A 3DOF Roll-Heave-Sway barge motion model and corresponding lower order ones are derived by considering coupled rigid body roll-heave-sway relations, then including the effect of coupled hydrostatic restoring force-moment and relative motion hydrodynamic force-moment. System parameters of the 3DOF and 2DOF models are identified by deterministic experimental results of several regular wave test cases. The same set of parameter for roll and heave is found to be applicable for both models. The values of all parameters do not deviate much from original values based on the potential theory. This set of fixed system parameters can be effectively applied to regular wave of various wave heights and wave periods.
2) Time domain simulation of barge motion under random waves is employed. Predictive capability of the 3DOF and the 2DOF models under random waves are

examined. It is found that both models provide accurate predictions, little or no significant difference is observed between their numerical results.

3) Time domain simulations indicate that sway does not have significant effects on coupled Roll-Heave-Sway barge motion. Both the 3DOF and the 2DOF models predict similar nonlinear behaviors. Both have the same predictive accuracy and able to capture nonlinear behaviors such as subharmonic, superharmonic and transient complex nonlinear response behaviors (see appendix A).

4) Stochastic analysis with Markov process assumption is applied to the 2DOF and 1DOF models. Associated Fokker Plank equations of both models are derived. Resulting probability densities obtained by the path integral solution indicate significant differences between two models especially at larger roll amplitude, as the 2DOF models produce greater probability densities at larger roll. Time domain analyses also confirm this trend.

5) Several time and probability domain simulations are conducted to examine the coupling effects of heave on the barge roll motion. Numerical results show that the 2DOF produces larger roll amplitude due to coupling effect from heave. The coupling effect increases with larger roll motion. Experimental results from both regular and random wave cases indicate that relative motion between heave and wave elevation is always small. Thus, the coupling effect of heave on hydrostatic roll righting moment is negligible. This implies that coupling effects of heave on roll is caused by introducing inertia moment due to eccentricity of KG and roll center, and the effect is more significant at larger roll angle.

6) The quasi-2DOF model is developed by including an additional term that represents heave-induced inertia moment to the 1DOF model. This additional term features an approximation of heave velocity as vertical wave velocity. Numerical results from both deterministic and stochastic analyses indicate identical accuracy of the quasi-2DOF model compared to the original 2DOF model.

7) A reliability analysis of barge motion under beam-sea condition is conducted. Resulting roll probability densities at a period of exposure time are obtained using the quasi-2DOF model. Random wave densities applied to the model simulate Sea States 1 through 9 via Bretschneider spectrum. Exposure periods of time to reach a specific capsizing probability of 1, 2, 5 and 10 percent are recorded. Results indicate high probability of capsizing in a short period of exposure time in sea state 7 and more severe conditions.

Suggestions for Future Research

This study introduces coupled multi-degree-of-freedom models for barge motion in beam seas. Deterministic and stochastic analysis procedures are presented. Improvements on models and analyses beyond this present work are suggested in this section.

Modeling and Analysis

- Perform extensive parametric study on all system parameters
- Compare model estimates with additional experimental results including capsizing cases
- Provide a matrix of values of system parameters for different barge parameters (e.g. Location of KG, draft, length and width)
- Compare results to other time and probability domain ship motion models
- Study effects of wind and shift of cargo in the model
- Include modeling capabilities for trapped-water-on-deck
- Using parallel computer system to perform extensive probability domain analyses

Analysis Tools

- Add animation graphics to show the motions of the barge for faster interpretation of results
- Make program more "user friendy" with window based "pop up" or "pull down" menu
- Prepare a user manual for the program.

BIBLIOGRAPHY

Abkowitz, M.A. 1969. Stability and Motion Control of Ocean Vehicles. MIT Press, Cambridge, MA.

Bartel, W.A. 1996. *Modelling, Validation and Simulation of Multi-Degree-of Freedom Nonlinear stochastic barge Motions.* A Thesis submitted to Oregon State University.

Cai, G.Q., Yu, S.J. and Lin, Y.K. 1994. Ship Rolling in Random Sea. *Stochastic Dyanamics and Reliability of Nonlinear Ocean Systems*, ASME DE-Vol. 77, 81-88.

Chakrabarti,S.K. 1994. Hydrodynamics of Offshore Structures, *Computational Mechanics* Publications, Southampton Boston.

Dahle, E. AA., Myhaug, D. and Dahl, S.J. 1988. Probability of Capsizing in Steep and High Waves from the Side in Open Sea and Coastal Waters. *Ocean Engineering*, 15(2),139-151.

Donescu, P. and Virgin, L.N. 1993. Nonlinear Coupled Heave and Roll Oscillations of a Ship in Beam Seas, *Nonlinear Dynamics of Marine Vehicles*, ASME, 51, 21-28.

Dunne, J.F. and Ghanbari, M. 1997. Extreme-Value Prediction for Non-Linear Stochastic Oscillators via Numerical Solution of the FPK Equation. *Journal of Sound and Vibration*, 206(5), 697-724.

Falzarano,J. and Taz Ul Mulk, M. 1994. Large Amplitude Rolling Motion of an Ocean Survey Vessel. *Marine Technology*, 31(4), 278-285.

Falzarano, J.M., Shaw, S.W., and Troesch, A.W. 1992. Application of Global methods for Analyzing Dynamical Systems to Ship Rolling Motion and Capsizing. *International Journal of Bifurcation and Chaos in Applied Sciences and Engineering*, 2(1), 101-116.

Kwon, S.H., Kim, D.W. and McGregor, R.C. 1993. A Stochastic Roll Response Analysis of Ships in Irregular Waves. *International Journal of Offshore and Polar Engineering*, 3(1), 32-34.

Liaw, C.Y., Bishop, S.R. and Thompson, J.M.T. 1993. Heave-Excited Rolling Motion of a Rectangular Vessel in Head Seas. *International Journal of Offshore and Polar Engineering*, 3(1), 26-31.

Liaw, C.Y. 1993. Dynamic Instability of a Parametrically Excited Ship Rolling Model. *Proc. of the Third International Offshore and Polar Engineering Conference*, Singapore.

Lin, H. and Yim, S.C.S. 1995a. Chaotic Roll Motion and Capsizing of Ships Under Periodic Excitation with Random Noise. *Applied Ocean Research*, 17(3), 185-204.

Lin, H. and Yim, S.C.S. 1995b. Stochastic Analysis of a Nonlinear Ocean Structural System. Oregon State University Report No. OE-95-04.

Martin, J. P. 1994. Roll Stabilization of Small Ships. *Marine Technology*, 31(4), 286-295.

Naess, A., and Johnsen, J.M., Statistics of Nonlinear Dynamic Systems by path integrations. *Nonlinear Stochastic Mechanics*: 401-409.

Naess, A. and Johnsen, J.M., 1993. Response Statistic of Nonlinear, Compliant Offshore Structures by the Path Integral Solution Method. *Probabilistic Engineering Mechanics*, 8, 91-106.

Naess, A. 1995. Prediction of Extreme Response of Nonlinear Structures by Extended Stochastic Linearization. *Probabilistic Engineering Mechanics*, 10, 153-160.

Nayfeh, A.H., and Mook, D.T. 1979. Nonlinear Oscillations. New York: John Wiley & son.

Newland, D.E. 1993. *An Introduction to Random Vibrations, Spectral & Wavelet Analysis*. Longman Scientific and Technical, Essex England.

Ochi, M.C. 1990. *Applied Probability & Stochastic Processes: in Engineering and Physical Sciences*. New York: John Wiley & son.

Paulling, J.R. 1990. Inclusion of Theoretical Achievements in the Field of Stability in the Ship Design Process. *STAB '90, Fourth International Conference on Stability of Ships and Ocean Vehicles*, Naples, Italy.

Paulling, J.R. 1961. The Transverse Stability of a Ship in a Longitudinal Seaway. *Journal of Ship Research*. March:37-49.

Paulling, J.R. and Rosenberg, R.M. 1959. On Unstable Ship Motions Resulting from Nonlinear Coupling. *Journal of Ship Research*, 3, 36.

Press W.H., Flannery, B.P, Teukolsky, S.A. and Vetterling, W.T. 1986. *Numerical Recipes*, Cambridge University Press.

Roberts, J.B. 1982a. A Stochastic Theory for Nonlinear Ship Rolling in Irregular Seas. *Journal of Ship Research*, 26(4), 229-245.

Roberts, J.B. 1982b. Effect of Parametric Excitation on Ship Rolling Motion in Random Waves. *Journal of Ship Research*, 26(4), 246-253.

Roberts, J.B.,Dunne J.F., and Debonos A. 1994. Stochastic Estimation Methods for Non-Linear Ship Roll Motion. *Probabilistic Engineering Mechanics* 9, 83-93.

Thompson, J.M.T., Rainey, R.C.T. and Soliman, M.S. 1992. Mechanics of Ship Capsize Under Direct and Parametric Wave Excitation," *Phil. Trans. R. Soc. Lond, A*:338, 471-490.

Thompson, J.M.T., and Stewart, H.B. 1986. *Nonlinear Dynamics and Chaos*. John Wiley & Sons.

Virgin, L.N. 1987. The Nonlinear Rolling Response of a Vessel including Chaotic Motions leading to Capsize in Regular Seas. *Applied Ocean Research*, 9(2), 89-95.

Virgin, L.N. and Bishop, S.R. 1988. Catchment Regions of Multiple Dynamic Responses in Nonlinear Problems of Offshore Mechanics. *Proceedings at 7th International Conference on Offshore Mechanics and Arctic Engineering*, Houston, TX. 15-22.

Virgin, L.N. and Erickson, B.K. 1994. A New Approach to the Overturning Stability of Floating Structures. *Ocean Engineering*, 21(1), 67-80.

Wehner, M.F., and Wolfer, W.G. 1983. Numerical Evaluation of Path-Integral Solutions to Fokker-Planck Equations, *Physical Review A*, 27, 2663-2670.

Wissel, C. 1979. Manifolds of Equivalent Path Integral Solutions of the Fokker-Planck Equation. *Zeitschrift fur physiks B*, 35, 185-191.

Yim, S.C.S., Bartel, W.A., Lin, H. and Huang, E. 1995. Nonlinear Roll Motion and Capsizing of Vessels in Random Seas. Naval Facilities Engineering Service Center, Port Hueneme, CA.

APPENDIX

Appendix A

Sensitivity Study of Barge Responses to Regular Waves

ABSTRACT

The nonlinear roll motion in beam-sea condition of ship-to-shore cargo barges is investigated by examining numerical results from two multi-degree-of-freedom nonlinear barge motion models, coupled Roll-Heave-Sway and Roll-Heave. The barges are excited by periodic waves of various wave heights and periods. Subharmonic and superharmonic roll responses are observed. To search for possible complex nonlinear responses, damping of the systems is varied over a wide range of values. Excitation amplitudes are also varied gradually in identified sensitive regions.

INTRODUCTION

This study numerically examines the stability of ship-to-shore cargo barges subjected to regular waves in beam-sea condition. Two multi-degree-of-freedom barge motion models (Roll-Heave-Sway and Roll-Heave) are developed by considering roll, heave and sway parts of the 6DOF system in Abkowitz (1969) and adding hydrostatics and hydrodynamics effects. These models include linear and nonlinear static and kinematic coupling between roll, heave and sway. This study utilizes both models to investigate possible complex nonlinear behaviors of the barge

subjected to simple periodic wave excitations of various heights and periods. The investigation focuses on the roll motion, which is directly related to the stability of the barge. Differences in numerical results of both the Roll-Heave-Sway and the Roll-Heave model are examined. Findings obtained here may be used for the development of a probability-based design and operational methodology.

EQUATIONS OF MOTION

A mathematical model representative of the fluid-structure interaction of the barge in ocean waves is derived. The coupled rigid body relation of the barge in the air is first obtained by considering the roll, heave and sway part of the six-degree-of-freedom rigid body relation (Abkowitz, 1969). The hydrostatic and hydrodynamic terms are then included when placing the barge in water. The physical assumptions employed in the model are as follow. The wave free surface elevation is assumed linear across the beam of the barge (i.e., wavelength is significantly longer than the barge beam). Wave forces and moments act at the center of gravity and are based on momentum theory. The effect of water on deck is treated statically, being modeled only in the hydrostatic restoring moment. Coefficients of added inertia, added mass and damping are assumed constant. The longitudinal center of gravity (LCG) is amidships. The barge is symmetric longitudinally and laterally. The resulting coupled equations of motion for Roll-Heave-Sway motion are

$$
\begin{aligned}
&m\ddot{y} + m_{a_{22}}\cos(\frac{\partial\eta}{\partial y})(\ddot{y}-\dot{v}) + m_{a_{33}}\sin(\left|\frac{\partial\eta}{\partial y}\right|)(\dot{y}-v) + C_{22_L}\dot{y} + C_{22_N}\dot{y}\left|\dot{y}\right| - m\dot{\phi}\dot{z} \\
&\quad -m(z_g\cos\phi)\ddot{\phi} + R_{33}(\phi, z, \eta, \frac{\partial\eta}{\partial y})\sin(\frac{\partial\eta}{\partial y}) + K_{moor}y \quad = \quad 0
\end{aligned}
$$

$$
\begin{aligned}
&m\ddot{z} + m_{a_{33}}\cos(\frac{\partial\eta}{\partial y})(\ddot{z}-\dot{w}) + m_{a_{22}}\sin(\left|\frac{\partial\eta}{\partial y}\right|)(\dot{z}-w) + C_{33_L}\dot{z} + C_{33_N}\dot{z}\left|\dot{z}\right| + m\dot{\phi}\dot{y} \qquad (1) \\
&\quad -m(z_g\cos\phi)\dot{\phi}^2 + mg + R_{33}(\phi, z, \eta, \frac{\partial\eta}{\partial y})\cos(\frac{\partial\eta}{\partial y}) \quad = \quad 0
\end{aligned}
$$

$$
\begin{aligned}
&I_{44}\ddot{\phi} + I_{a_{44}}(\ddot{\phi} - \frac{\partial\ddot{\eta}}{\partial y}) + C_{44_L}(\dot{\phi} - \frac{\partial\dot{\eta}}{\partial y}) + C_{44_N}(\dot{\phi} - \frac{\partial\dot{\eta}}{\partial y})\left|\dot{\phi} - \frac{\partial\dot{\eta}}{\partial y}\right| + m(z_g\cos\phi)\dot{\phi}\dot{z} \\
&\quad -m(z_g\cos\phi)\ddot{y} + R_{44}(\phi, z, \eta, \frac{\partial\eta}{\partial y})\cos(\frac{\partial\eta}{\partial y}) - mgz_g\sin\phi \quad = \quad 0
\end{aligned}
$$

The Roll-Heave-Sway (3DOF) model for the barge motions in beam seas may be further reduced by assuming the effects of sway on roll and heave are negligible, resulting in a 2DOF Roll-Heave model, with corresponding governing equations given by

$$
\begin{aligned}
&m\ddot{z} + m_{a_{33}}(\ddot{z}-\dot{w}) + C_{33_L}\dot{z} + C_{33_N}\dot{z}\left|\dot{z}\right| - m(z_g\cos\phi)\dot{\phi}^2 + mg + R_{33}(z, \phi, \eta, \frac{\partial\eta}{\partial y}) \quad = \quad 0 \\
&I_{44}\ddot{\phi} + I_{a_{44}}(\ddot{\phi} - \frac{\partial\ddot{\eta}}{\partial y}) + C_{44_L}(\dot{\phi} - \frac{\partial\dot{\eta}}{\partial y})\left|\dot{\phi} - \frac{\partial\dot{\eta}}{\partial y}\right| + m(z_g\cos\phi)\dot{\phi}\dot{z} \qquad (2) \\
&\quad + R_{44}(\phi, z, \eta, \frac{\partial\eta}{\partial y}) - mgz_g\sin\phi \quad = \quad 0
\end{aligned}
$$

The wave field is defined by linear regular waves. The numerical solutions to the equations of motion are obtained by recasting the equations into first order ordinary differential equations and solved in the time domain. A 4^{th} order Runge-Kutta method is selected to solve the equations of motion.

APPROACH

Several regular wave excitations with different heights and periods are first applied to both the Roll-Heave-Sway and the Roll-Heave models. The wave heights vary approximately from 4 to 16 ft, and the corresponding wave periods vary from 4 to 12 seconds, which cover the roll natural period of 5.25 seconds. The time histories of wave, roll, heave and sway are observed. The relationship between roll amplitude and wave period is examined.

The system coefficients used in the models have been identified in earlier research by matching numerical model results with experimental data. Once identified, the same set of system coefficients is applied to all models. For the Roll-Heave-Sway model, appropriate high mooring cable stiffness is applied to the model to prevent possible numerical errors caused by excessive sway drift. The study of complex nonlinear responses is conducted by varying roll damping and wave amplitude gradually in the sensitive region.

PRELIMINARY OBSERVED ROLL MOTION CHARACTERISTICS

The relationship between roll amplitude and excitation wave period is examined in this section. Regular waves of various wave heights and periods are employed as input to the 3DOF and the 2DOF models. Specifically, barge motion responses due to excitation wave heights of 6 ft., 8 ft., and 10 ft. are considered. Wave periods are gradually varied from 4 to 9 seconds. The behaviors of the coupled roll, heave and sway motions are observed. The corresponding responses are shown in Figure A1. It is observed that in all cases the peak of the roll amplitude versus wave period is around 5.2 –5.5 seconds, which is near the roll natural period of the barge (5.25 second). The 3DOF model always produce approximate 5 to 10 percent smaller roll magnitudes than the 2DOF model. Figure A2 shows the barge roll response amplitude for a fixed wave period of 6 seconds over a range of wave height between 4 and 16 ft. In this particular case the barge capsized when roll amplitude exceed 30 degree approximately. As observed, both models provide comparable results.

SUBHARMONIC AND SUPERHARMONIC ROLL RESPONSES

The barge is observed to experience subharmonic roll response when excitation wave period is around 3 seconds. The time histories of wave and roll response of such response is shown in Figure A3. The results indicate that the barge rolls at the excitation period as well as its own natural period. Relations between roll versus roll velocity and roll versus wave are shown in the corresponding Phase

diagrams in Figure A4. Wave and roll response spectra shown in Figure A5 also show that the roll response power spectrum occurs at both the excitation and roll natural frequency.

Superharmonic roll response is observed when the excitation wave period is around 10.5 seconds. The time history of wave and roll response for the superharmonic case is shown in Figure A6. The barge rolls at the excitation period and also at its own natural period, which is approximately half of the excitation period. The corresponding phase diagrams for roll-roll velocity and roll-wave are shown in Figure A7. Wave and roll response spectra are shown in Figure A8. As expected, the roll response spectrum has a component at both the excitation frequency and its own natural frequency.

TRANSIENT COMPLEX NONLINEAR ROLL RESPONSES

To examine the nonlinear complex response characteristics, the roll linear and nonlinear damping coefficients are reduced to 0.005 and 0.0008 percent of critical damping respectively (c.f., original values 5 and 0.8 percent). Wave height is gradually varied, as small as 0.001 ft increment, in the range of wave period of 5.6 to 5.7 seconds. Some transient complex nonlinear motions are observed. Figures A9 and A10 demonstrate cases of transient nonlinear behavior before capsizing. Regular waves with H = 12.84 ft and T = 5.70 seconds are applied to the 3DOF model. The barge experiences transient nonlinear behavior for a few hundred seconds and then capsizes as shown in Figure A9. Regular waves with H = 14.50 ft

and T = 5.65 seconds are applied to the 2DOF model. The barge capsizes after having a short period of transient nonlinear behavior. Figures A11 and A12 demonstrate cases of transient nonlinear behavior before settling into periodic motions. Also, regular waves with H = 12.86 ft and T = 5.70 seconds are applied to the 3DOF model. The barge experiences a short period of transient nonlinear motion then settles into periodic motion as shown in Figure A11. Similar behavior is found using the 2DOF model. With regular waves of H = 17.0 ft and T = 5.65 seconds applied to the 2DOF model, the barge experiences nonlinear transients for approximately 100 seconds before settling into periodic motion.

SUMMARY

Nonlinear barge response due to regular wave excitation is examined here extensively. The Roll-Heave-Sway and the Roll-Heave model are employed in the time domain simulation. Subharmonic and superharmonic roll responses are identified. In addition, some transient complex nonlinear behaviors are identified near the region of primary resonance.

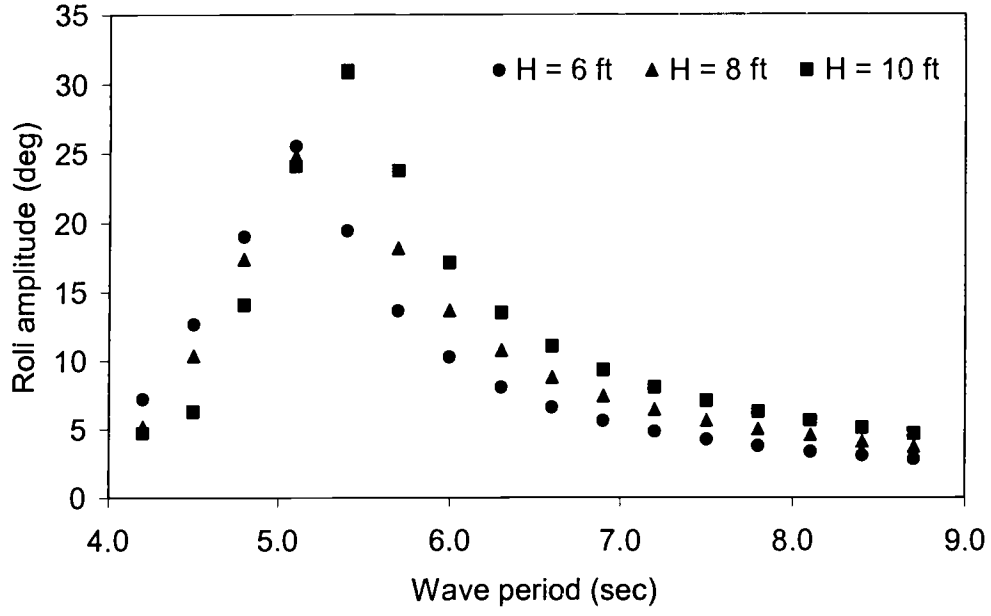

Figure A1 3DOF model predicted periodic roll response amplitude vs. regular wave period (wave heights H = 6, 8, and 10 ft.)

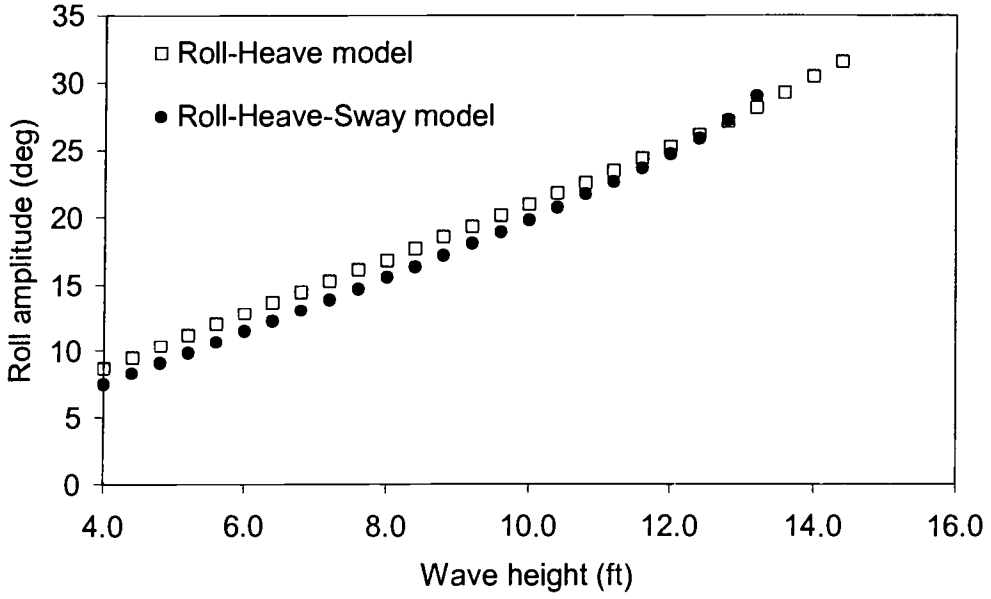

Figure A2 3DOF and 2DOF model predicted periodic roll response amplitude vs. Regular wave height (wave period T = 6 seconds)

a)

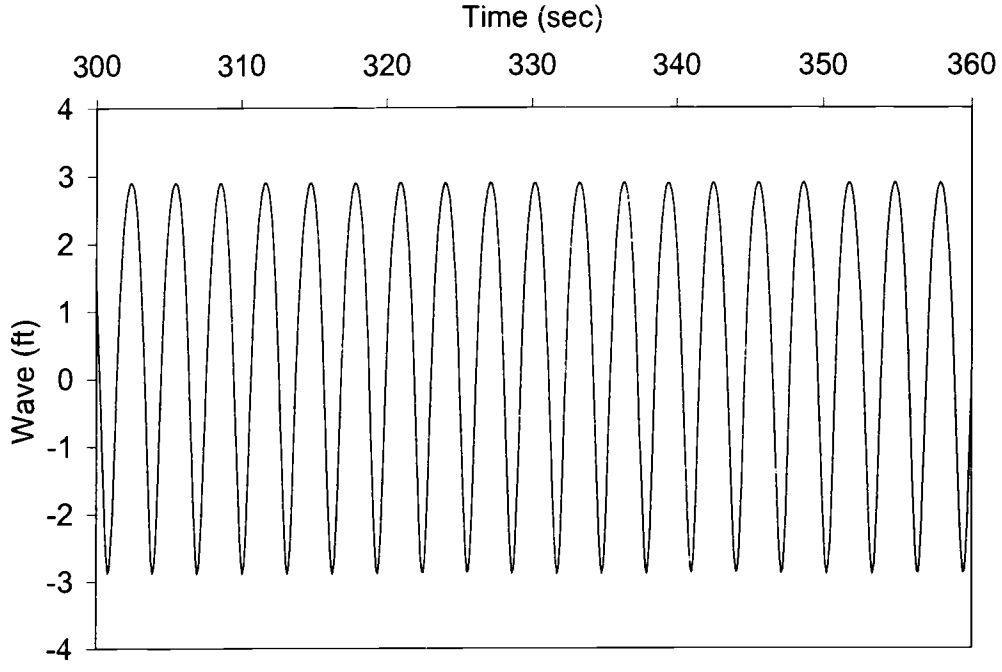

b)

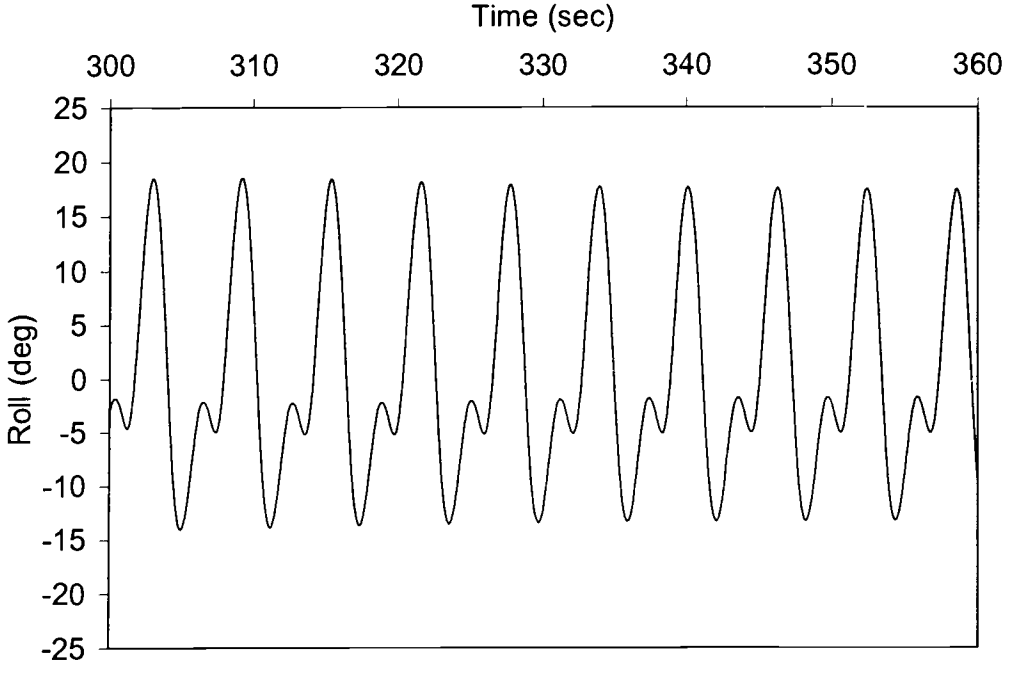

Figure A3 3DOF model predicted subharmonic roll response to regular waves with H = 5.8 ft and T = 3 seconds, (a) wave time history, and (b) roll response time history.

a)

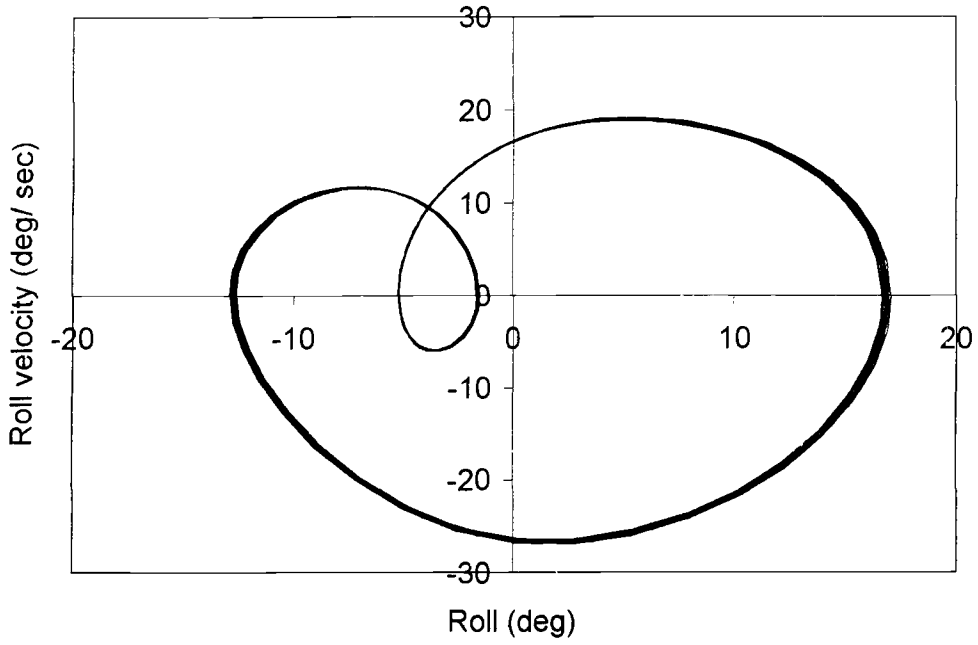

b)

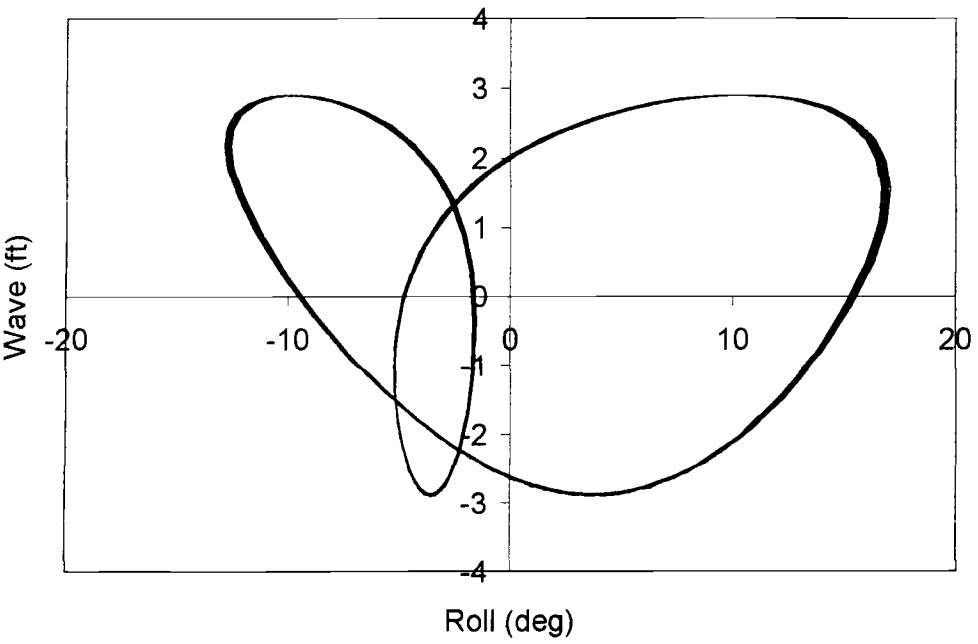

Figure A4 3DOF model predicted subharmonic roll response to regular waves with H = 5.8 ft and T = 3 seconds, (a) phase diagram of roll and roll velocity, and (b) phase diagram of roll and wave.

a)

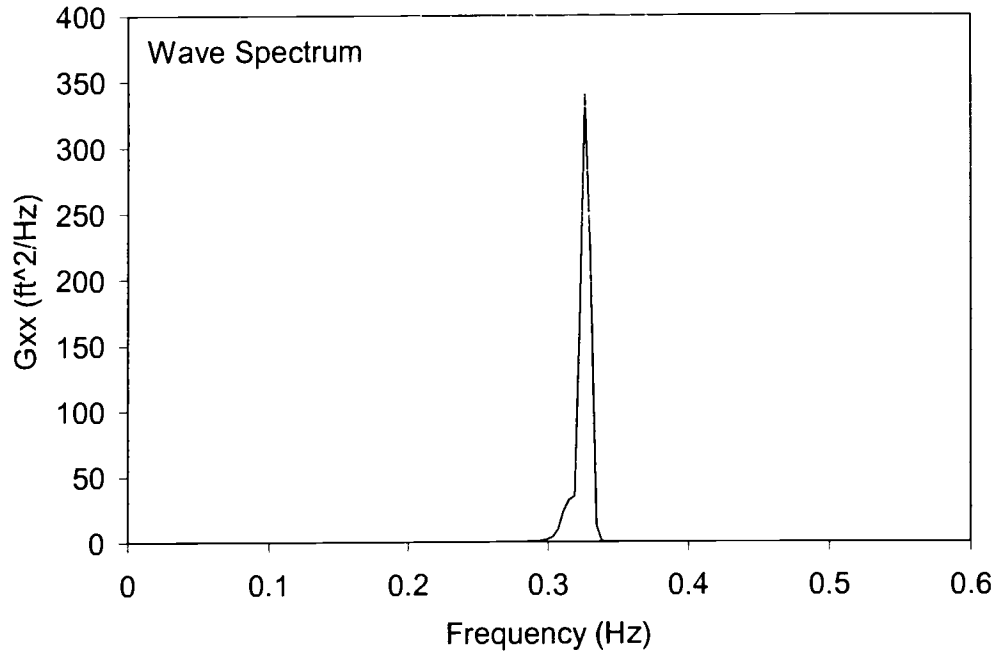

b)

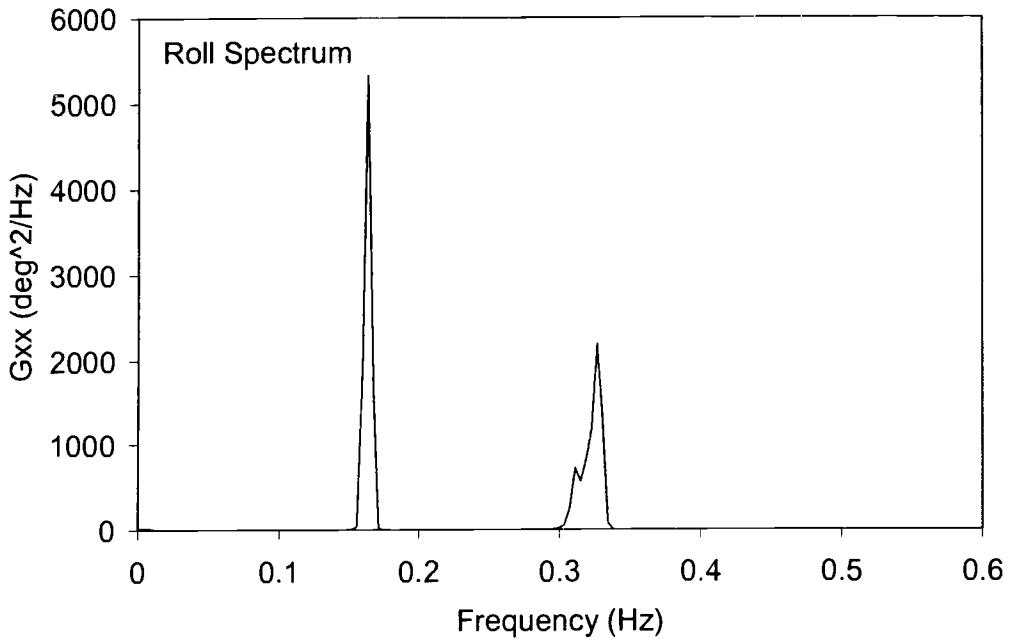

Figure A5 3DOF model predicted subharmonic roll response to regular waves with H = 5.8 ft and T = 3 seconds, (a) wave spectrum, and (b) roll response spectrum.

a)

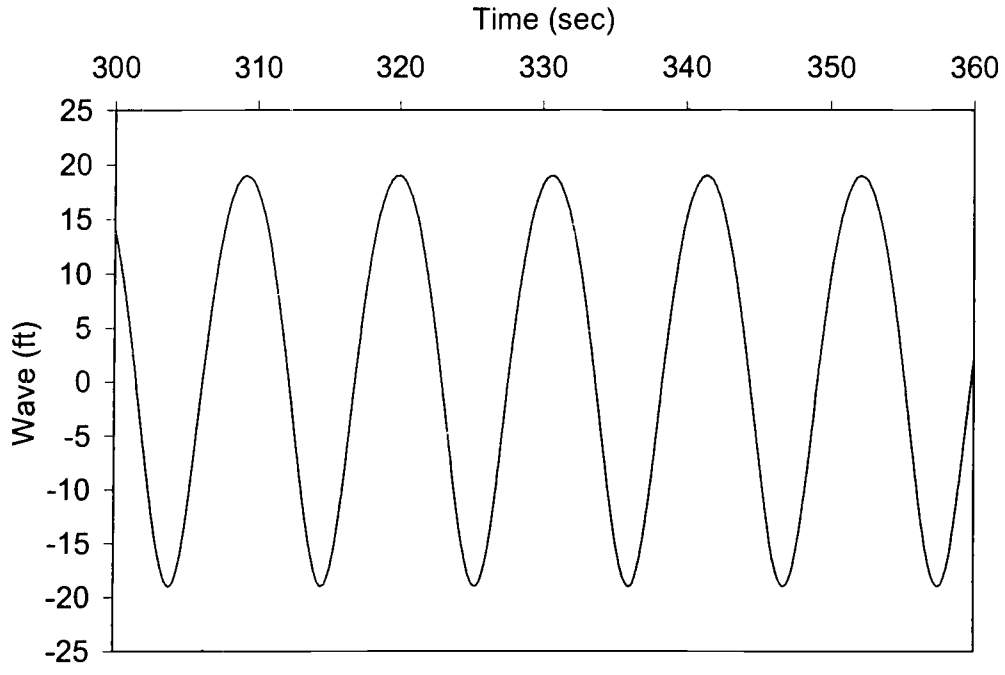

b)

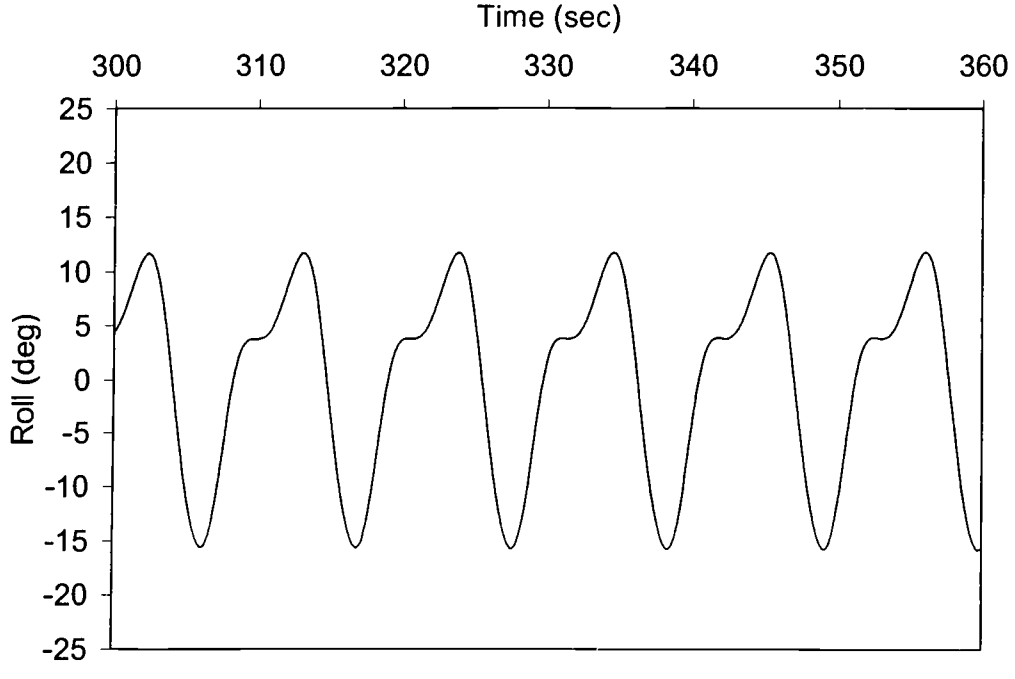

Figure A6 3DOF model predicted superharmonic roll response to regular waves with H = 38 ft and T = 10.65 seconds, (a) wave time history, and (b) roll response time history.

a)

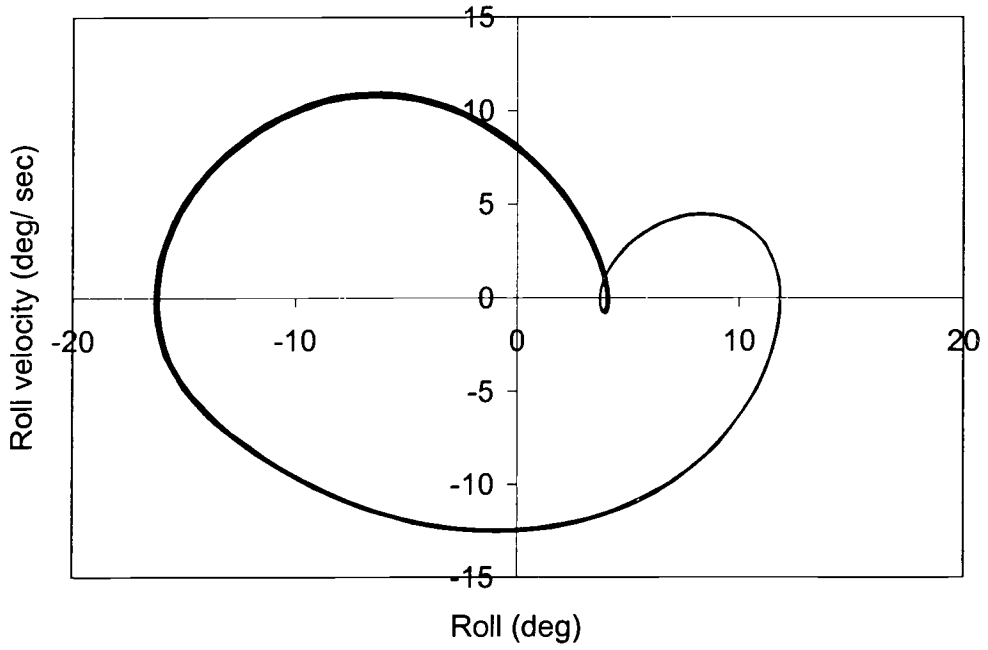

b)

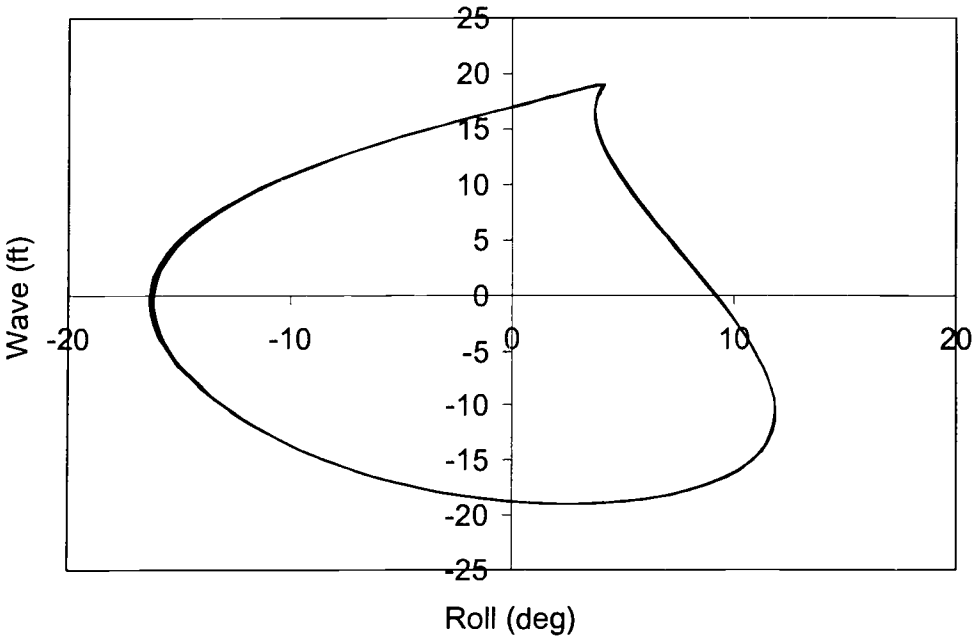

Figure A7 3DOF model predicted superharmonic roll response to regular waves with H = 38 ft and T = 10.65 seconds, (a) phase diagram of roll and roll velocity, and (b) phase diagram of roll and wave.

a)

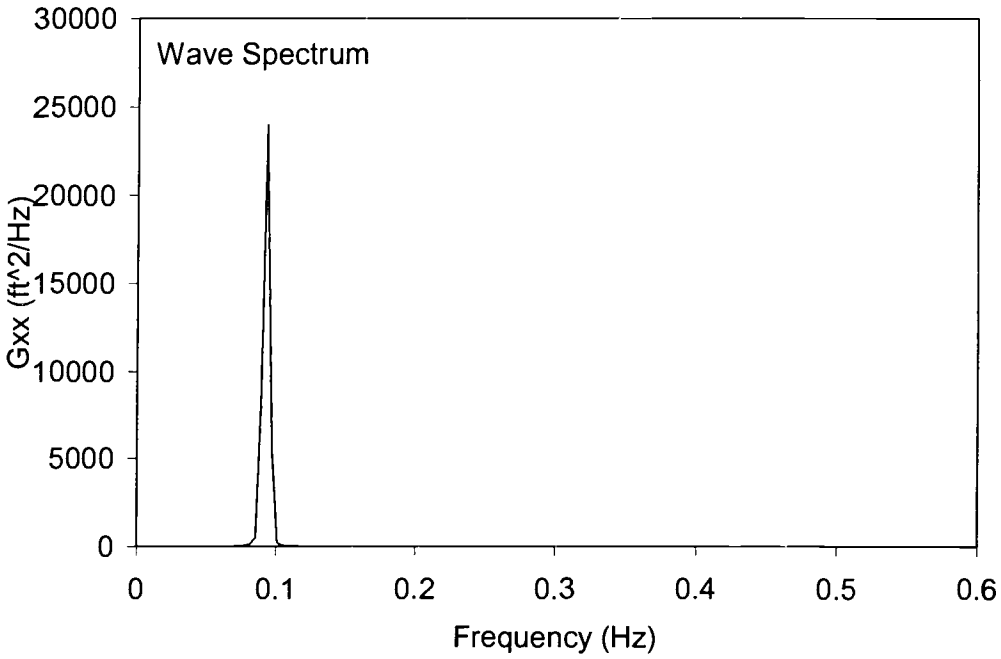

b)

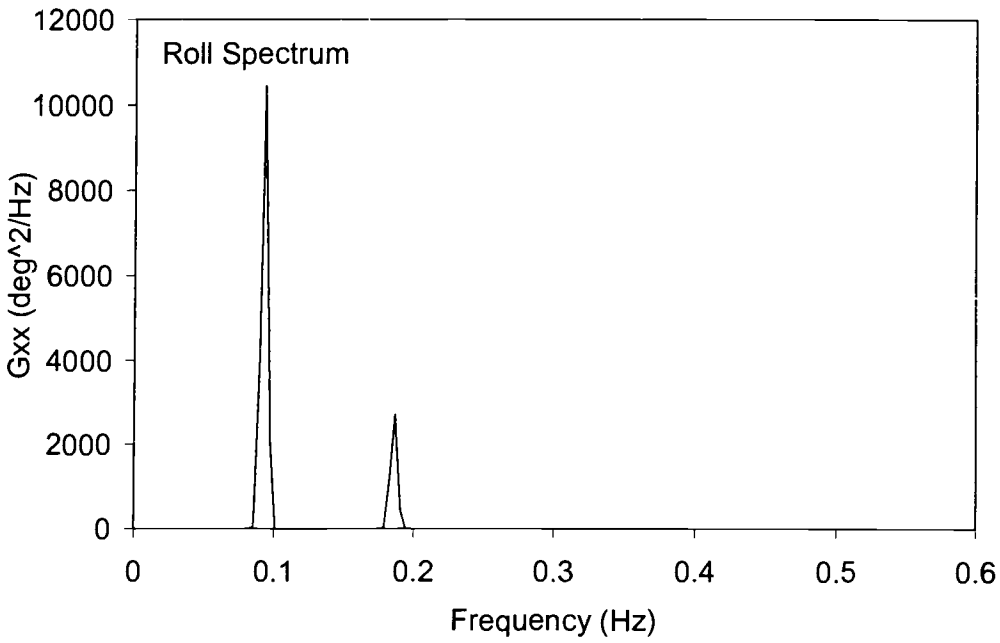

Figure A8 3DOF model predicted superharmonic roll response to regular waves with H = 38 ft and T = 10.65 seconds, (a) wave spectrum, and (b) roll response spectrum.

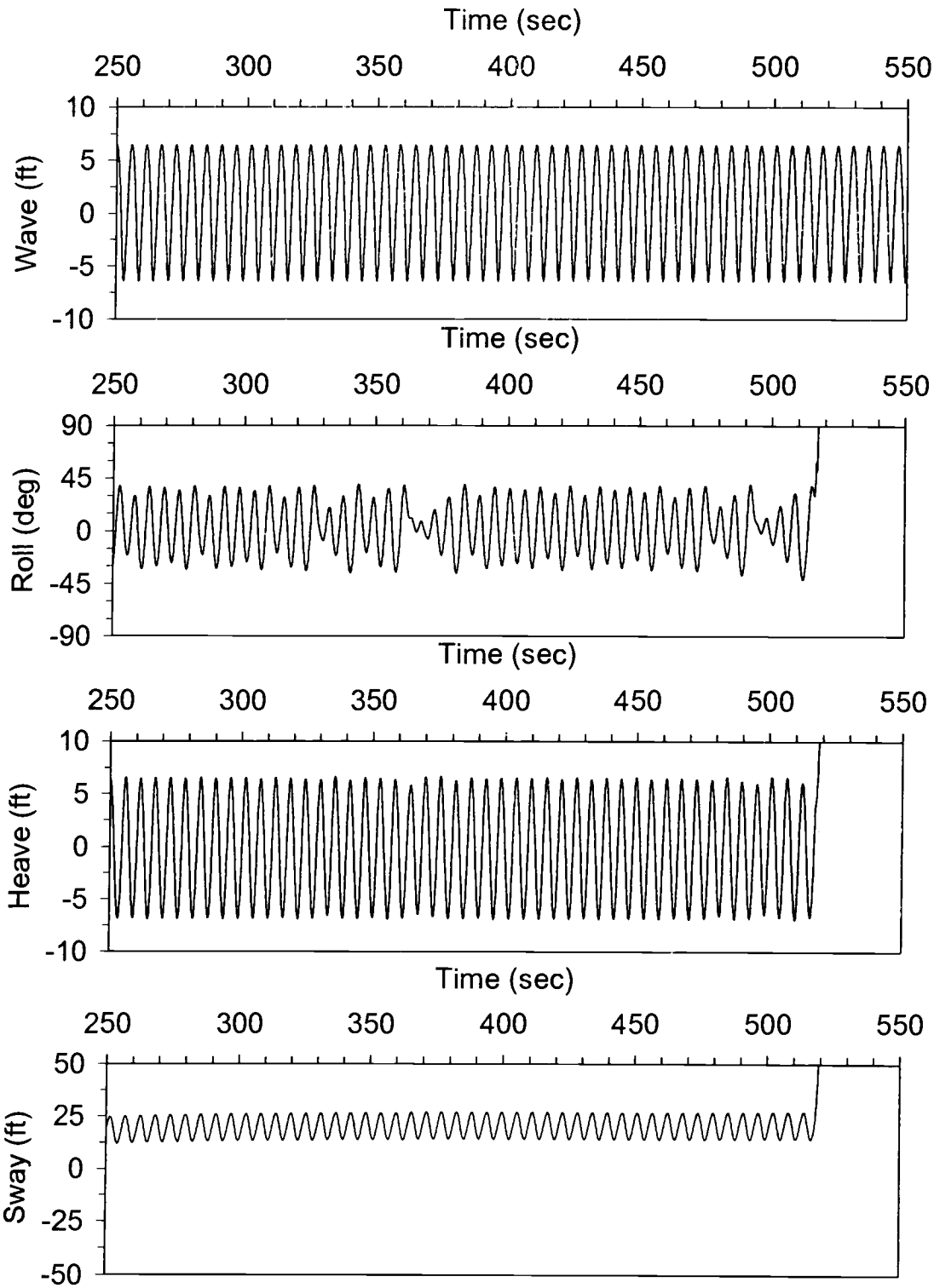

Figure A9 3DOF model predicted transient complex nonlinear roll response to regular waves with H = 12.84 ft and T = 5.70 seconds.

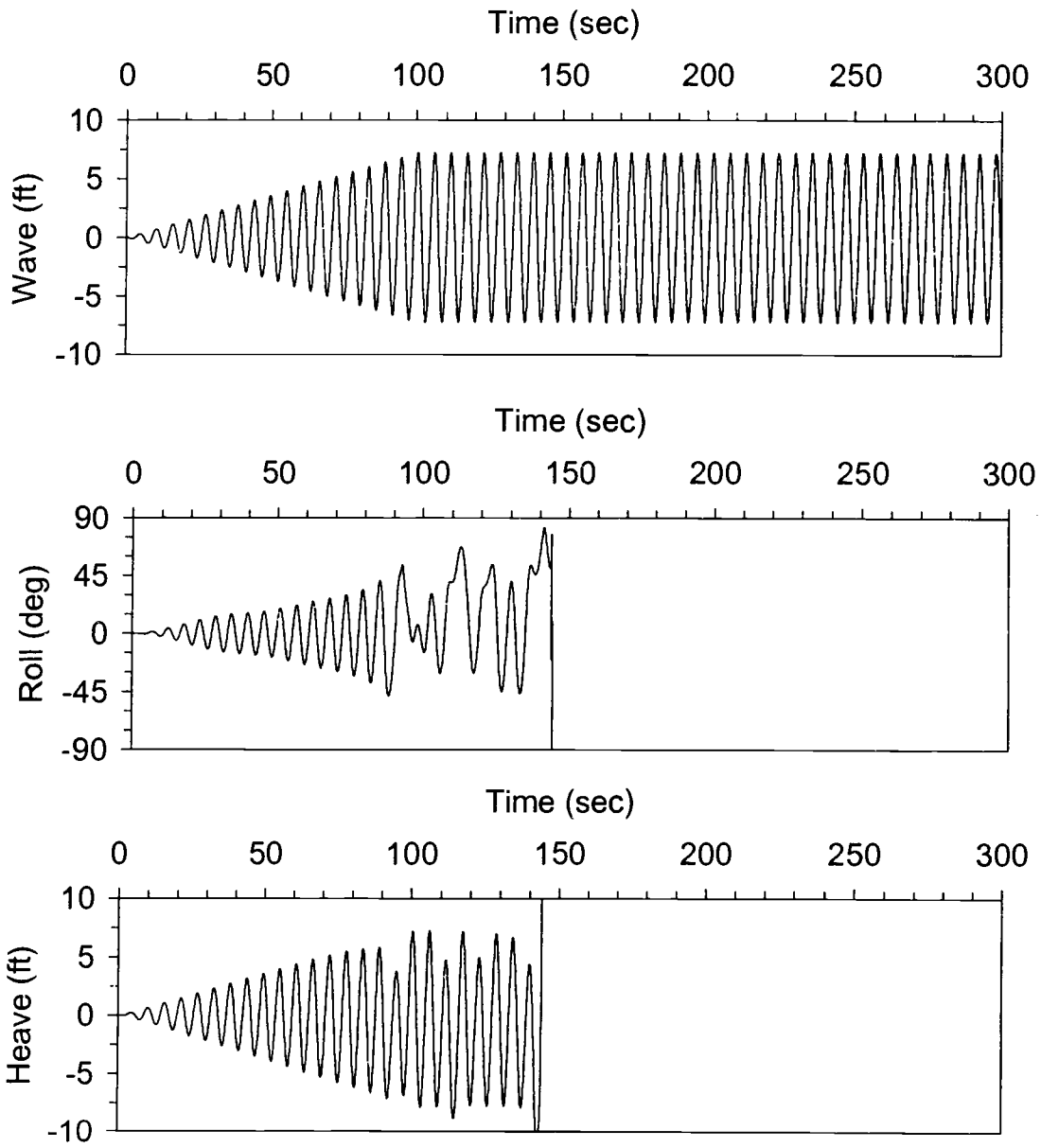

Figure A10 2DOF model predicted transient complex nonlinear roll response to regular waves with H = 14.50 ft and T = 5.65 seconds.

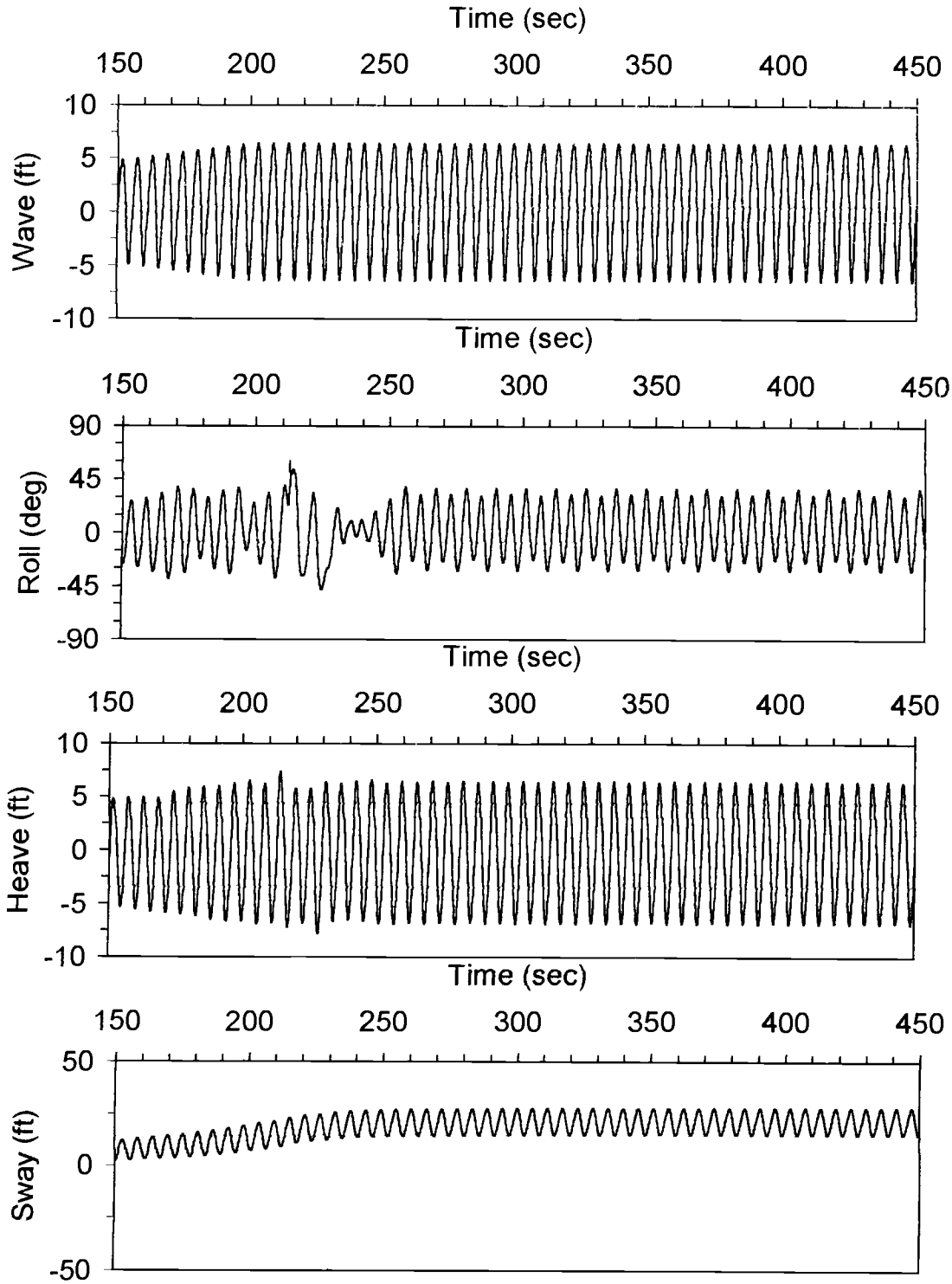

Figure A11 3DOF model predicted transient complex nonlinear roll response to regular waves with H = 12.86 ft and T = 5.70 seconds.

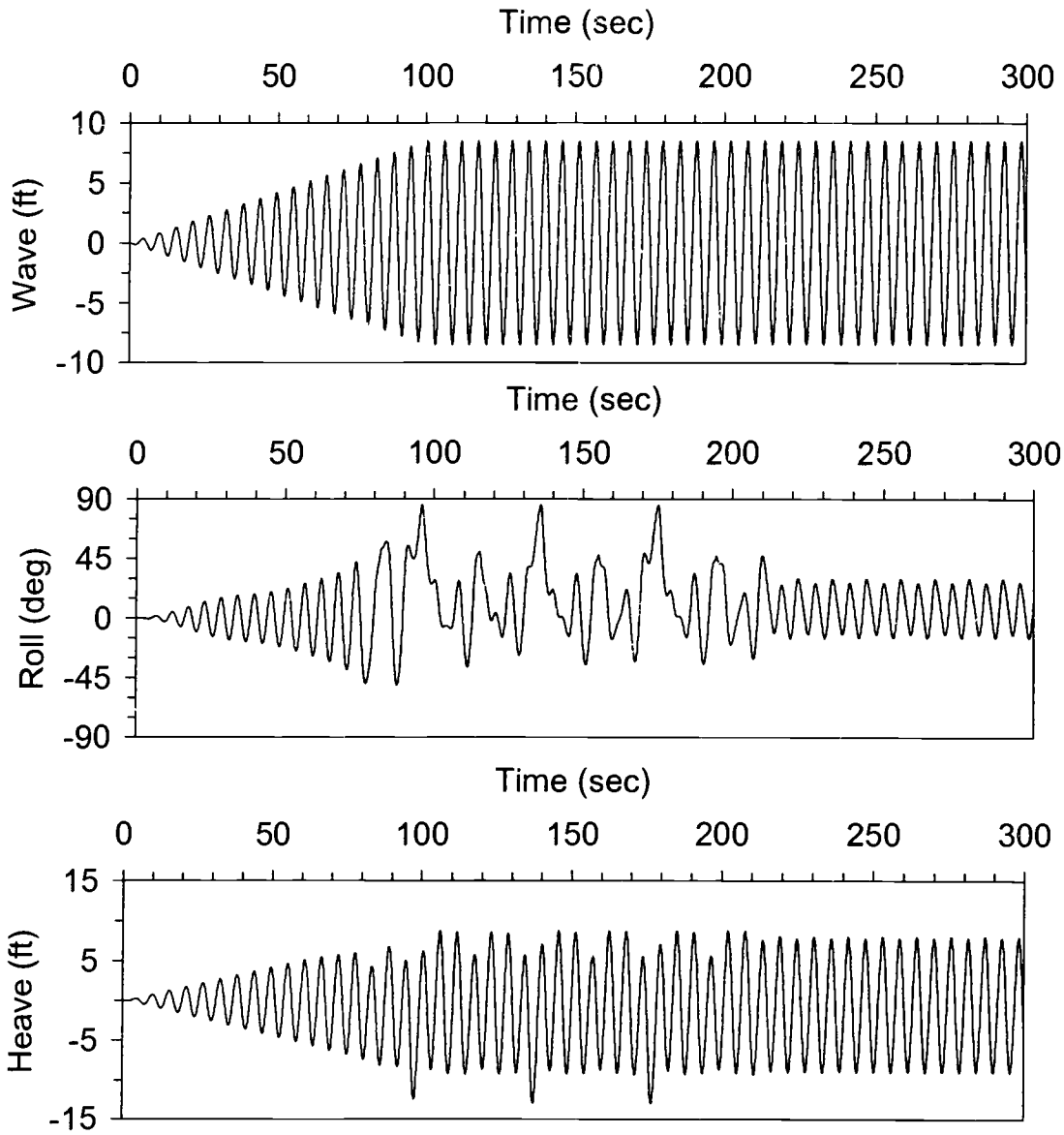

Figure A12 2DOF model predicted transient complex nonlinear roll response to regular waves with H = 17.00 ft and T = 5.65 seconds.